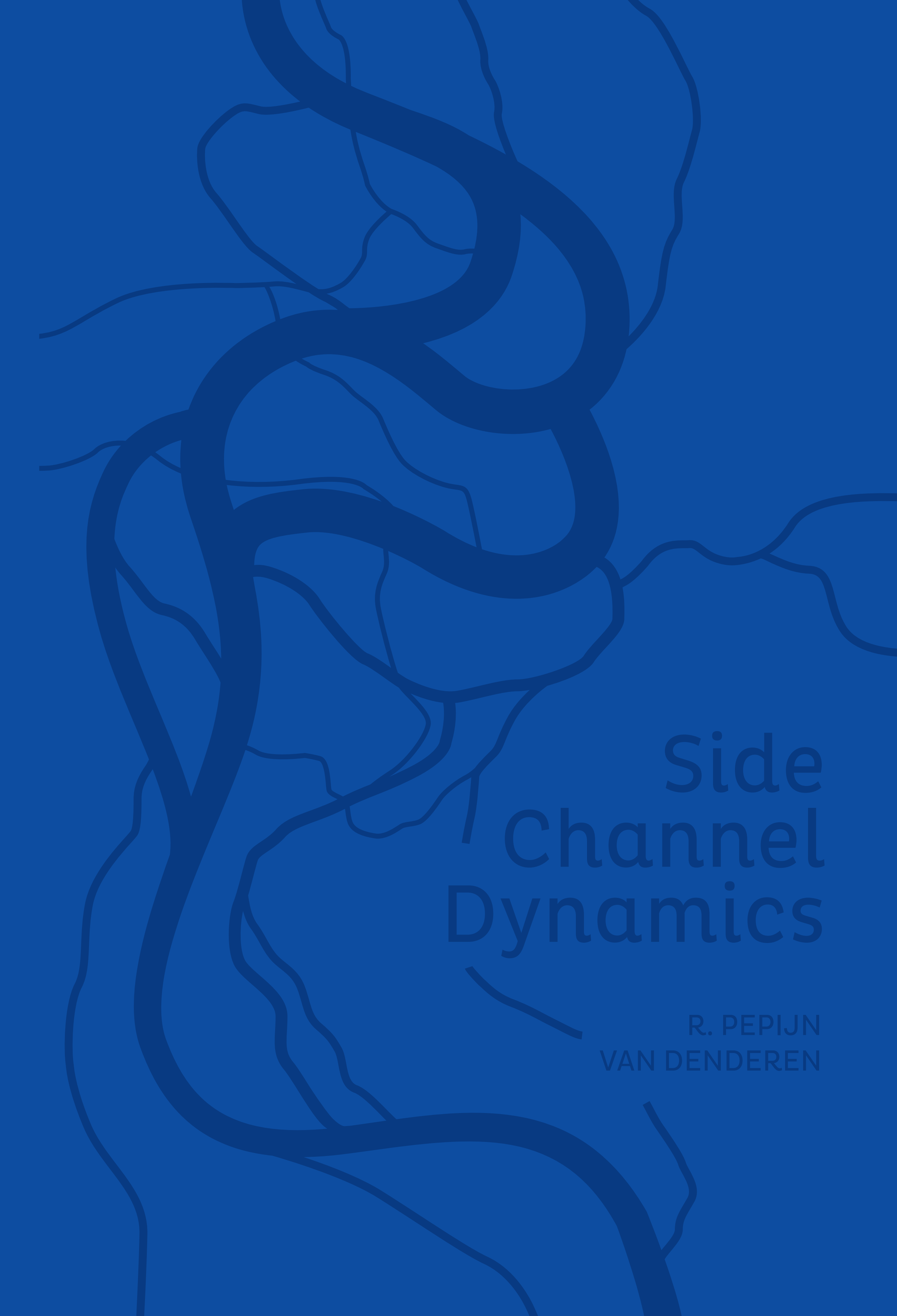

Side Channel Dynamics

R. PEPIJN VAN DENDEREN

Side Channel Dynamics

R. PEPIJN VAN DENDEREN

GRADUATION COMMITTEE:

prof.dr.ir. G.P.M.R. Dewulf	University of Twente, chairman and secretary
prof.dr S.J.M.H. Hulscher	University of Twente, supervisor
dr. R.M.J. Schielen	University of Twente, co-supervisor
dr. M.M. Busnelli	Royal Haskoning DHV
prof.dr. M.H. Garcia	Illinois University
prof.dr.ir. A.J.F. Hoitink	Wageningen University & Research
prof.dr.ir. W.S.J. Uijttewaal	Delft University of Technology
prof.dr. K.M. Wijnberg	University of Twente
dr.ir. D.C.M. Augustijn	University of Twente

The presented research was carried out at the Department of Water Engineering and Management, Faculty of Engineering Technology, University of Twente. This research is supported by the Netherlands Organisation for Scientific Research (NWO), which is partly funded by the Ministry of Economic affairs, under grant number P12-P14 (RiverCare Perspective Programme) project number 13516. This research has benefited from cooperation within the network of the Netherlands Centre for River studies.

ISBN: 978-90-365-4743-7
doi: 10.3990/1.9789036547437
Design: Tessa van der Eem – www.tessavandereem.nl
Printed by: Gildeprint – www.gildeprint.nl

Copyright © 2019 R.P. van Denderen, The Netherlands.
All rights reserved. No parts of this thesis may be reproduced, stored in a retrieval system or transmitted in any form or by any means without permission of the author.

Side Channel Dynamics

DISSERTATION

to obtain
the degree of doctor at the University of Twente,
on the authority of the Rector Magnificus,
prof.dr. T.T.M. Palstra,
on account of the decision of the Doctorate Board,
to be publicly defended
on Thursday the 11^{th} of April 2019 at 14.45 hours

by

Robert Pepijn van Denderen
born on the 7^{th} of February 1991
in Heemstede, the Netherlands

THIS DISSERTATION HAS BEEN APPROVED BY:

prof.dr. S.J.M.H. Hulscher   Supervisor
dr. R.M.J. Schielen   Co-supervisor

CONTENTS

Photo: Bureau Beeldtaal Filmmakers

Preface

After four years of research I present to you my thesis. Many people helped me along the way and I would like to express my gratitude here.

Ralph, thank you for your intensive support and supervision. Our discussions that regularly lasted longer than intended helped us to better understand bifurcations and side channels. Your extensive comments on the various manuscripts significantly improved them and led to the chapters presented here. Many questions and ideas remain, and I look forward to continuing working on them.

Suzanne, even though we did not have very regular meetings, you always gave me good suggestions and sharp comments. This significantly improved the thesis and helped me to look at my research from a different point of view. Your organizational skills allowed me to finish this thesis in a reasonable amount of time. Thank you for your help and your support.

Many thanks to all my coauthors. Astrid and Maarten, you helped me to set up the research plan and to write my first paper. Although our collaboration was less intensive afterwards, your comments and suggestions were much appreciated. Sam and Susanne, together we carried out measurements at Gameren. Thank you for your help and the analysis of the samples; they are an important part of this thesis. Menno and Maarten, thank you for your input on the characterization of side channels.

Tessa, thank you for designing the cover and the layout of my thesis. Many of my figures have improved significantly.

I would like to thank everyone involved in the RiverCare research program. The unofficial 'morphology group' with Gonzalo, Jasper, Liselot, Tjitske, Timo and Victor with whom we regularly met at various conferences. I would like to thank the RiverCare researchers in Twente: Juliette, Koen, Laura, Robert-Jan and Valesca. A special thanks to you, Juliette, for your endless enthusiasm and your dedication in creating the storyline on side channels, and your suggestions for this thesis.

Many thanks to my colleagues at the WEM department which gave me a warm welcome in Twente. I enjoyed the WEM-outings, the Christmas lunches and the many birthday cakes. Thanks to Zhuo La, Hero, Alejandro, Anouk, and Paran for being my (former) office-mates and making the worktime more enjoyable. I also want to thank all my other colleagues for the "daghappen", coffee breaks and cycling tours.

My gratitude goes to my parents, brothers and sister for their support and care for me and my family. Un très grand merci à ma Fanny qui m'a toujours épaulé. Tu es la plus importante dans ma vie et sans toi je ne serai pas arrivé jusqu'ici. Notre petit Alexander a apporté une nouvelle dimension dans notre vie que j'ai hâte de continuer avec vous !

Summary

Side channels are small secondary channels that convey much less discharge than the main channel. Side channels are commonly constructed to increase the discharge capacity of a river during peak flow conditions or to increase the ecological value of the river. The aggradation of side channels that are constructed to increase the discharge capacity of a river should be limited. In the last 20 years, more than 20 side channels have been constructed in the Rhine branches. Observations show that large aggradation occurs in the side channels. Therefore, such channels require regular and costly maintenance. The aim of this research is to better understand the mechanisms that drive the morphodynamic development of side channels and thereby, improve the design of side channels and reduce their maintenance needs.

We first look at natural occurring side channels that can be found in, for example, meandering and anabranching rivers. Using a one-dimensional (1D) bifurcation model, we assess the conditions under which side channels generally aggrade or degrade and we estimate the time scale of their morphodynamic development. We apply the model for a wide range of conditions and compare the results to multitemporal aerial images of four side channel systems. There are limitations to using the 1D model to study the development of side channels, but the model can reproduce the general behavior of the side channel development until the sediment that is transported in the main channel as bed load is no longer responsible for the further aggradation of the channel.

We study the development of side channels in more detail by looking at the development of three side channels at Gameren in the river Waal (the Netherlands). Since the construction of the side channels in 1996 and 1999, bed level measurements have been regularly collected. In addition, we took grain size samples of the sediment deposited in the channels and carried out hydrodynamic computations. We relate the bed level changes, the grain size and the hydrodynamic parameters with each other. In two of the three channels primarily sediment is deposited that in the main channel is transported as suspended bed-material load. In the third channel, wash load is deposited in addition to the suspended bed-material load. The bed level measurements show that the largest aggradation can be expected in years during which the side channel conveys a minimal amount of discharge. With increasing flow frequency of the side channel, the aggradation rate decreases or even degradation can occur. The variation in the hydrodynamic regime and the sediment sorting at the bifurcation of the side channels are therefore both important mechanisms that should be taken into account in estimating the development of a side channel.

We investigate the effect of the hydrodynamic regime and sediment sorting in more detail using a two-dimensional (2D) mixed-sediment morphodynamic model with varying hydrodynamic conditions. We find that the aggradation rate and the sediment size that is deposited in the side channel is related to the discharge in the upstream channel. The lower discharges are responsible for the fining of the side channel bed. The largest aggradation rate occurs during the peak discharges and at the same time the bed coarsens. We find that the results are affected by the transverse bed slope effect, the grain size of the sediment supply in the upstream main channel, the bed roughness, the active layer thickness, the initial bed level in the side channel and structures at the bifurcation.

Based on the measurements and the modeling work, we define three categories of side channels. Our categorization is based on how the sediment that is deposited in a side channel is transported in the main channel. This results in (1) bed load supplied, (2) suspended bed-material load supplied and (3) wash load supplied side channels. For each of the categories different mechanisms are important for estimating the development of a side channel. Based on the characterization, we propose a method to estimate the development for each side channel category. Our characterization can therefore support river managers in the design, operation and maintenance of side channels.

Samenvatting

Nevengeulen zijn kleine secundaire geulen van een rivier. De afvoer in deze geulen is heel gering in vergelijking met de hoofdgeul. Nevengeulen kunnen worden aangelegd om de afvoercapaciteit van een rivier te vergroten tijdens hoogwatercondities of om de ecologische waarde van een rivier te verhogen. In de nevengeulen, die zijn aangelegd om de afvoercapaciteit van de rivier te vergroten, moet de sedimentatie minimaal zijn. In de laatste 20 jaar zijn er meer dan 20 nevengeulen aangelegd in de Rijntakken. De sedimentatiesnelheid is in veel van de nevengeulen hoog. Daardoor zijn er regelmatig dure onderhoudswerkzaamheden nodig om de geulen open te houden. Het doel van dit onderzoek is om beter te begrijpen hoe verschillende mechanismen de ontwikkeling van een nevengeul beïnvloeden en om daarmee het ontwerp en de onderhoudsbehoeften te optimaliseren.

We bestuderen eerst natuurlijk voorkomende nevengeulen die onder andere te vinden zijn in meanderende en anastomoserende rivieren. Met behulp van een eendimensionaal (1D) model berekenen we de condities waarbij nevengeulen in het algemeen sedimenteren en eroderen en maken we een schatting van de bijbehorende tijdschaal. We passen het model toe op een reeks van condities en vergelijken het resultaat met luchtfoto's die de morfologische ontwikkeling van vier nevengeulsystemen weergeven. De toepasbaarheid van het 1D model is beperkt, maar het model kan de ontwikkeling van de nevengeulen nabootsen zolang de geul wordt opgevuld met sediment dat in de hoofdgeul als bodemtransport beweegt.

Om meer over de Nederlandse nevengeulen te weten te komen kijken we in detail naar de drie nevengeulen van de rivier de Waal bij Gameren. Sinds de aanleg van deze nevengeulen, tussen 1996 en 1999, is de bodemhoogte regelmatig gemeten. Daarnaast hebben wij sedimentmonsters genomen en de hydrodynamische condities in de geulen berekend met een tweedimensionaal model. We correleren de bodemhoogteveranderingen, de korrelgrootte van het sediment dat wordt neergelegd in de geulen en de hydrodynamische condities om de processen die de sedimentatie veroorzaken beter te begrijpen. In twee van de drie geulen wordt voornamelijk fijn zand neergelegd dat in de hoofdgeul als zwevend transport beweegt. In de derde geul wordt ook slib en klei neergelegd. De bodemmetingen laten zien dat, afgezien van een initieel effect, de grootste bodemhoogtetoename optreedt in de jaren dat de nevengeul het minste stroomt. Met een toenemende meestroomfrequentie van de nevengeul neemt de sedimentatiesnelheid af en kan zelfs erosie optreden. De variaties in de afvoer van de rivier en de sortering van het sediment bij de bifurcatie zijn dus belangrijke mechanismen in de ontwikkeling van de nevengeulen.

Om het effect van de afvoer en de sortering beter te begrijpen passen we een tweedimensionaal morfologisch model toe waarin ook de sorteringsprocessen worden meegenomen. De resultaten laten een relatie zien tussen de sedimentatiesnelheid en de korrelgrootte van het sediment dat in de nevengeul wordt neergelegd. Tijdens lagere afvoeren is het sediment, dat in de nevengeul wordt neergelegd, fijner dan tijdens hogere debieten. Initieel is de sedimentatiesnelheid het hoogst tijdens lagere debieten, maar met een toenemende bodemhoogte worden de hogere debieten belangrijker voor de sedimentatie in de nevengeul. De resultaten worden beïnvloed door de dwarshellingseffecten bij de bifurcatie, de korrelgrootte van de sedimenttoevoer, de bodemruwheid, de dikte van de actieve laag, de initiële bodemhoogte en constructies bij de bifurcatie.

Op basis van de metingen en de modelresultaten definiëren we drie categorieën van nevengeulen. Onze categorisatie is gebaseerd op hoe het sediment, dat in de nevengeul wordt neergelegd, wordt getransporteerd in de hoofdgeul. Dit resulteert in (1) een met bodemtransport gevulde nevengeul, (2) een met zwevend transport gevulde nevengeul en (3) een met sediment in suspensie gevulde nevengeul. De mechanismen die belangrijk zijn voor het schatten van een nevengeul zijn voor elke categorie anders. Op basis van de categorisatie kunnen we met een 1D model de tijdschaal van de geulontwikkeling schatten voor verschillende condities. Deze karakterisering kan riviermanagers ondersteunen in het ontwerp, beheer en onderhoud van nevengeulen.

Photo: beeldbank.rws.nl, Rijkswaterstaat / Con Mönnich

CHAPTER 1

Introduction

Rivers are intensively managed around the world to reduce the risk of flooding, to keep the river navigable, to have a stable water supply and to increase the ecological value of the river. In the past this led to the construction of structures such as levees, groynes and dams. More recently, more natural interventions or interventions that help to restore the river are constructed. Such Nature Based Solutions (NBS) or Natural and Nature Based Features (NNBF) provide solutions that are inspired or supported by nature in a sustainable way (Nesshöver et al., 2017; Raymond et al., 2017). It is unknown how such interventions develop and affect the river over time. This an important objective of the RiverCare Programme in which we evaluate the development of interventions at intermediate and longer time scales, and their consequences on various river functions (Hulscher et al., 2014; Augustijn et al., 2018). This includes evaluating the development of interventions (e.g., longitudinal dams (Collas et al., 2018; De Ruijsscher et al., 2018), the construction of side channels, the removal of bank protection (Duró et al., 2018a; 2018b), re-meandering of streams (Candel et al., 2018), creating new methods for evaluating such interventions (e.g., Berends et al., 2018; Chavarrías et al., 2018), and communicating the results to a wider audience (e.g., Cortes Arevalo et al., 2018; Den Haan et al., 2018). It is unknown how these interventions develop and affect the river and its functions over time. If we are able to predict the development caused by these interventions more accurately, we can develop a more natural and a more self-sustaining river. This reduces the required maintenance efforts and thereby the maintenance costs. In this thesis, we focus on a single intervention within the scope of NBS and NNBF: the construction of side channels. We study the morphodynamic development of side channel systems using both observations and numerical computations to better estimate the development of side channel systems.

Side channels are secondary channels that convey much less discharge compared to the main channel. In addition, side channels are generally connected at the upstream and downstream end to the main channel. Naturally formed side channels have been disappearing from many regulated rivers due to human interference (e.g., Hohensinner et al., 2014). Artificial side channels are (re)constructed to reduce the flood risk of the river (Simons et al., 2001; Nabet, 2014), to increase the ecological value of the river (Schiemer et al., 1999; Buijse et al., 2002; Formann et al., 2007; Riquier et al., 2015; Van Dyke, 2016), to reduce the degradation of the main channel (Tockner et al., 1998; Formann et al., 2007) and to restore old river branches (Henry et al., 1995; Helfield et al., 2012). In the Netherlands, side channels were created to increase the discharge capacity of the river, i.e. as part of the Room for the River programme (e.g., Van Stokkom et al., 2005), and to increase the habitat diversity of the river (e.g., Nienhuis et al., 2002). This has resulted in more than 20 side channels in the Rhine branches that are connected to the main channel at both their upstream and downstream end (Figure 1.1). It is found that almost all constructed side channels aggrade (Simons et al., 2001; Formann et al., 2007; Riquier et al., 2017). A better understanding of the mechanisms that cause aggradation may lead to a more optimal design of side channels and a reduction of the maintenance costs.

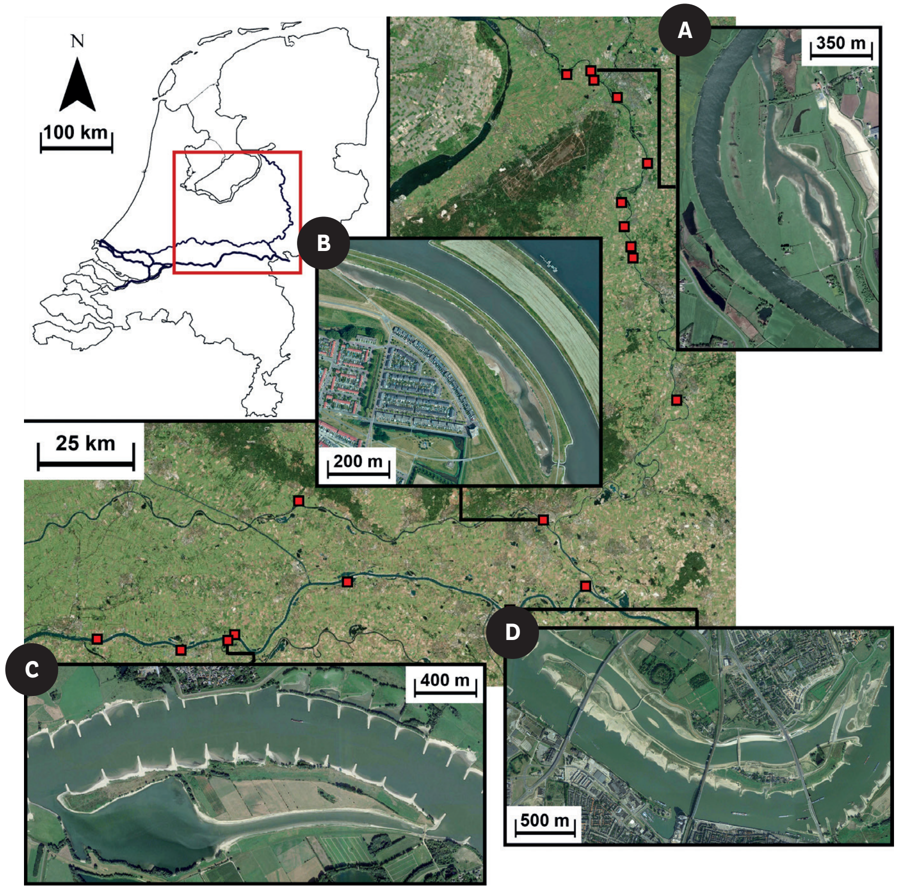

FIGURE 1.1 Locations of side channels in the Rhine branches in the Netherlands that are connected with the main channel at both the upstream and the downstream end. Examples of such channels are **(A)** Vreugderijkerwaard in the river IJssel. **(B)** Bakenhof in the river Nederrijn. **(C)** Opijnen and Hurwenen in the river Waal. **(D)** Nijmegen-Lent in the river Waal. *(after images of Rijkswaterstaat and Google Earth)*

1.1 BACKGROUND

Bed level changes in rivers are a result of an imbalance between the sediment supply and the transport capacity of the channel (Lane, 1955). In a single channel system with fixed channel banks, this leads to a single solution to the morphodynamic equilibrium state for both uni-size and mixed-size sediment conditions (Blom et al., 2016; Blom et al., 2017). In a bifurcating river, the development of the downstream channels is determined by the partitioning of discharge and sediment. The partitioning of sediment depends on many factors and therefore the development of a bifurcation is not straightforward to estimate. In contrast to large river bifurcations, the sediment partitioning at the bifurcation point of a side channel system and the transport capacity in the side channel and in the main channel are strongly asymmetric. The transport capacity in the side channel is generally much lower and therefore, other mechanisms, such as the deposition of wash load (Riquier et al., 2015), can become important.

1.1.1 DEVELOPMENT OF SIDE CHANNELS

Naturally-formed side channels occur, for example, in meandering, braiding and anabranching rivers (Figure 1.2). Artificial side channels are expected to develop similarly to such naturally-formed secondary channels. The development of a meander, just after a cutoff channel is formed, is similar to a side channel system. The cutoff channel is generally shorter than the meander channel resulting in a larger water level gradient over this branch. The larger water level gradient results in a larger conveyance by the cutoff channel relative to the meander channel (Mendoza et al., 2016) and therefore the transport capacity is relatively larger compared to the meander channel (Van Dijk et al., 2014). A cutoff channel generally degrades and becomes the dominant channel. An artificial side channel that is shorter than the main channel is expected to show the same behavior. To prevent such a cutoff of the main channel by the side channel, a side channel is generally constructed longer than the main channel.

The meander generally aggrades due to the decreased transport capacity. If the sediment supply to the meander is relatively coarse compared to the transport capacity, it is likely that a plug bar forms (Constantine et al., 2010; Toonen et al., 2012; Dieras et al., 2013). A large bifurcation angle can result in the formation of a flow separation zone at the entrance of the meander. The flow separation zone captures sediment at the entrance of the channel which in case of a limited transport capacity can enhance the growth of a plug bar (Constantine et al., 2010; Dieras et al., 2013). After the formation of a plug bar, sediment can still enter the channel at the confluence and during water level variations this can lead to the deposition of fines in the channel (Citterio and Piégay, 2009; Riquier et al., 2017). From the moment that the meander is disconnected from the main channel, the filling-in of the channel occurs with fine material during overbank flow

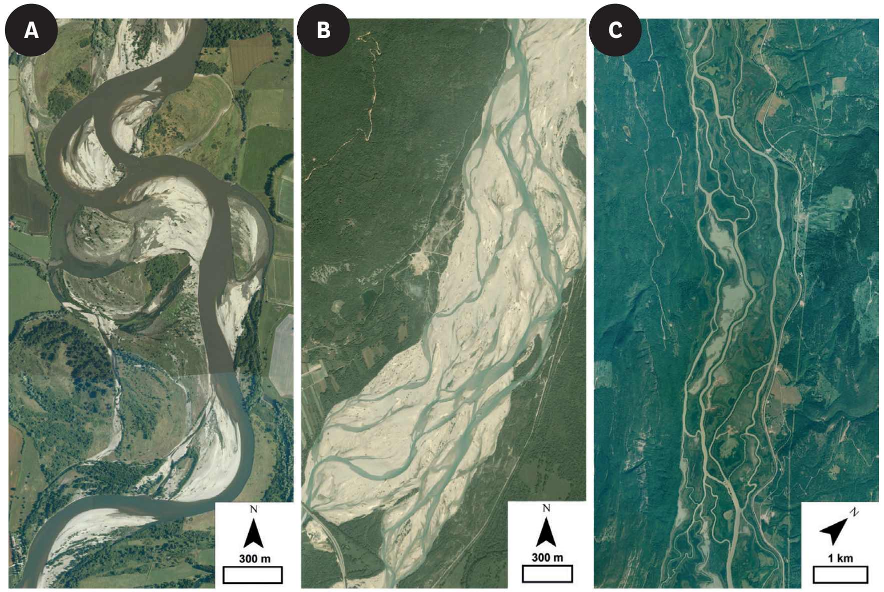

FIGURE 1.2 Examples of **(A)** a meandering river (river Allier, France), **(B)** a braiding river (river Tagliamento, Italy) and **(C)** an anabranching river (Colombia River, Canada). *(Images Google Earth)*

conditions (Makaske et al., 2002; Constantine et al., 2010; Toonen et al., 2012). If the transport capacity in the meander is high compared to the grain size of the sediment supply, then the aggradation is likely more spread over the channel (Toonen et al., 2012; Dieras et al., 2013). This results in faster aggradation of the channel with coarser material compared to the channel closed with a plug bar (Makaske et al., 2002; Dieras et al., 2013). The aggradation continues until the channel is sufficiently shallow such that vegetation is able to colonize and deposition of fines occurs (Makaske et al., 2002). Similar processes occur in artificial side channels (Riquier et al., 2015; 2017).

1.1.2 BIFURCATION DEVELOPMENT

The sediment partitioning at a bifurcation is determined by the flow patterns and the morphodynamic features at the bifurcation. Therefore, the sediment partitioning is a function of the bifurcation geometry, morphodynamic features in the upstream channel and the characteristics of the sediment transport. In this section we give a short overview on how such mechanisms affect the development of a bifurcation.

The bifurcation angle is the angle between the side channel and the main channel at the bifurcation and is generally considered to be an important parameter in estimating the development of a bifurcation. A side channel with a large bifurcation angle seems to be more likely to close (Mosselman et al., 1995). This can be caused by a spiral flow just upstream of the bifurcation (Bulle, 1926) or by a flow separation zone in the side channel (Constantine et al., 2010). The spiral flow at the bifurcation is caused by the curvature of the streamlines in which the velocity near the bed is directed towards the side channel (Bulle, 1926; Riad, 1961; Van der Mark and Mosselman, 2013; Dutta et al., 2017). This effect generally increases with increasing bifurcation angle and hence, increases the sediment supply towards the side channel (Bulle, 1926; De Heer and Mosselman, 2004; Van der Mark and Mosselman, 2013; Dutta et al., 2017). If the bifurcation angle is large or if the angle is sharp-edged, a flow separation zone can form (Bulle, 1926; Riad, 1961; Constantine et al., 2010; Zinger et al., 2013; Dutta et al., 2017). The flow velocities in the flow separation zone are generally low resulting in the formation of a bar at the entrance of the channel. If the side channel attracts sufficient amount of discharge, the narrowing of the entrance of the channel can lead to scour and bank erosion (Kleinhans et al., 2013; Zinger et al., 2013). If the side channel attracts a limited amount of discharge, the deposition of sediment in the flow separation zone promotes the formation of a plug bar (Constantine et al., 2010; Kleinhans et al., 2013).

Morphodynamic features of the river, such as river bends or bars upstream of the bifurcation, can affect the development of a side channel system. River bends just upstream of the bifurcation can affect the sediment partitioning (Habermaas, 1935; Kleinhans et al., 2008; Hardy et al., 2011). In the river bend secondary flow creates a transverse flow velocity that near the bed is directed towards the inner bend (Dietrich and Smith, 1984). If the bifurcation is located just downstream of the river bend, the secondary flow increases the sediment supply to the channel in the inner bend (Kleinhans et al., 2008; Van Dijk et al., 2014). Sediment sorting in the river bend generally also affects the sediment partitioning at the downstream bifurcation leading to a coarser sediment supply to the channel in the outer bend compared to the one in the inner bend (Sloff et al., 2003; Frings and Kleinhans, 2008; Sloff and Mosselman, 2012). A second morphodynamic feature that affects the development of bifurcations is the presence of alternating bars (Bertoldi and Tubino, 2007; Bertoldi et al., 2009). The development of the bifurcation is a function of the position of the bifurcation relative to the bar (Le et al., 2018a; 2018b). Therefore, free alternating bars can lead to an oscillatory discharge partitioning to the downstream channels (Bertoldi et al., 2009).

From experimental and numerical work it was found that the development of a bifurcation towards an equilibrium state is a function of the Shields parameter (Bolla Pittaluga et al., 2003; Federici and Paola, 2003; Bertoldi and Tubino, 2007; Edmonds and Slingerland, 2008; Bolla Pittaluga et al., 2015). It was found that for low Shields stresses in the upstream channel, the bifurcation likely develops towards an equilibrium state with both branches open in which the discharge partitioning is asymmetrical. With increasing Shields stress, the equilibrium discharge partitioning becomes more stable. This mainly holds for bifurcations in gravel-bed rivers in which bed load sediment transport is partitioned at the bifurcations. For higher Shields stresses in sand-bed rivers in which sediment is also transported in suspension, the equilibrium discharge partitioning is more likely to be asymmetrical (Edmonds and Slingerland, 2008; Bolla Pittaluga et al., 2015). This depends, for example, on the distribution of the sediment concentration over the water column (Slingerland and Smith, 1998).

1.1.3 BIFURCATION MODELS

The development of a bifurcation can be described using mathematical models. The development of the downstream branches is a balance between the sediment supply and transport capacity. After proposing a more complex relation, Wang et al. (1995) propose the following simplified relation for the sediment supply:

$$\frac{Q_{s1}}{Q_{s2}} = \left(\frac{Q_1}{Q_2}\right)^k \left(\frac{W_1}{W_2}\right)^{1-k} \tag{1.1}$$

in which Q_{si} is the sediment supply in branch i, Q_i is the discharge in branch i and W_i is the channel width of branch i. Using a linear stability analysis, Wang et al. (1995) find that both branches remain open if $k > n/3$ in which n is the non-linearity of the sediment transport relation ($Q_S \propto u^n$), and that one branch closes if $k < n/3$. The value of k determines the sediment supply to the downstream branches and varies as function of, for example, the downstream bed level and the Shields parameter (Bolla Pittaluga et al., 2003; Kleinhans et al., 2008; Van Dijk et al., 2014). However, a model for k does not exist yet.

A more physical based model was developed by Bolla Pittaluga et al. (2003). This model assumes that just upstream of the bifurcation sediment is directed towards one of the branches by bed slope effects or transverse flow velocities. Using this model, the sediment supply is not fully based on a single empirical parameter, but on several more physically-based relations. Both branches remain generally open in the resulting equilibrium state (Bolla Pittaluga et al., 2003). However, the stability of two similar downstream branches with the same discharge conveyance varies as function of the Shields stress and the width-depth ratio (Bolla Pittaluga et al., 2003). Based on the relations by Wang et al. (1995) and Bolla Pittaluga et al. (2003), other mechanisms that affect the equilibrium state of bifurcations were studied such as spiral flow due to a river bend upstream of a bifurcation (Kleinhans et al., 2008), adaptation of the channel width (Miori et al., 2006; Kleinhans et al., 2011; Mosselman, 2017), migration of alternating bars (Bertoldi et al., 2009) and spiral flow due to a large bifurcation angle (Van der Mark and Mosselman, 2013).

In case of side channel system, the side channel is often filled with finer material than found on the bed of the main channel (Riquier et al., 2015). Therefore, sediment sorting occurs at the bifurcation and suspended bed-material load and wash load transport become important. The effect of sediment sorting at the bifurcation of the side channel leads to new equilibrium states of a bifurcation (Schielen and Blom, 2018). The estimation of side channel development using a bifurcation model requires therefore further research.

1.2 KNOWLEDGE GAPS

Side channels have been constructed in many rivers. The design of such channels is often based on simple guidelines or determined by the fact that an old channel is present that was disconnected or silted up. Constructed channels generally aggrade, but only a limited amount of morphodynamic measurements are available. This makes it difficult to predict the morphodynamic development of side channels. Large aggradation or degradation in the channels can therefore occur. A better understanding of the mechanisms that play a role in the development of side channels aids in estimating their development and thereby optimizing their design and the required maintenance.

1.3 RESEARCH AIM AND QUESTIONS

The aim of this thesis is to better understand the mechanisms that drive the morphodynamic development of side channels to enable estimating their development. This results in the following research questions:

Q1 *Which mechanisms make side channels aggrade or degrade and at which rate?*

Q2 *How is the aggradation rate and the deposited sediment size in Dutch side channels related the hydrodynamic conditions?*

Q3 *How is the aggradation rate of a side channel, in which primarily fine sand is deposited, related to varying hydrodynamic conditions and its design conditions?*

Q4 *How can we characterize the side channel development and how can we use this characterization to estimate the development of side channels?*

1.4 METHODOLOGY

We study the development of side channels with a combination of methods consisting of observations and numerical models. We discuss the methodology for each research question separately. Our approach is as follows:

Q1 The development of artificial side channels is similar to the development of more natural secondary channels in meandering and anabranching rivers. Using aerial images in combination with descriptions of such systems from literature, we can identify the main mechanisms that affect the development of secondary channels. We use a simple one-dimensional bifurcation model to reproduce the development of such systems. In addition, we use the model to estimate the equilibrium state and the time scale of development in a more generalized way, which allows us to optimize the design of such side channel systems.

Q2 Literature shows that in many cases the sediment deposited in side channels is much finer than sediment on the bed of the main channel. We carry out measurements to study the morphodynamic development of the side channel system at Gameren in the river Waal (The Netherlands). We use bed level data to study the temporal variation in the aggradation rate and collect sediment samples in the channels that help us to characterize the side channel development. In addition, we use a hydrodynamic numerical model to estimate the hydrodynamic conditions in the channels. Based on the data and the hydrodynamic model we draw conclusions on the morphodynamic behaviour of the side channel system.

Q3 We use a mixed-sediment depth-averaged morphodynamic model to study the development of a two-channel system. We apply the model to an idealized side channel system and study the effect of variations in the hydrodynamic regime in the main channel and the characteristics of the side channel on the aggradation rate in the side channel and the fining of the side channel bed. Furthermore, we vary parameters such as the sediment supply and the bed roughness to study their effect on the morphodynamic development of a side channel system.

Q4 Based on the literature and our experiences from the previous questions, we propose a characterization of side channel development. We base this characterization on the type of sediment deposited and the transport mode of this sediment in the main channel. With this characterization, we set up an initial framework that can be used in estimating the development of side channel systems. This aids the future design and the operation and maintenance of side channels.

1.5 OUTLINE OF THE THESIS

The structure of this thesis is as follows (Figure 1.3). In Chapter 2, we address **Q1** by studying the development of side channels using aerial images and a simple numerical model. In Chapter 3, we discuss the development of the side channel system at Gameren in the river Waal **(Q2)**. Next, in Chapter 4, we propose a more complex numerical model that we apply to a side channel system **(Q3)**. In Chapter 5, we propose a characterization and a method to estimate the development of side channel systems **(Q4)**. Finally, Chapters 6 and 7 contain the discussion and conclusion, respectively.

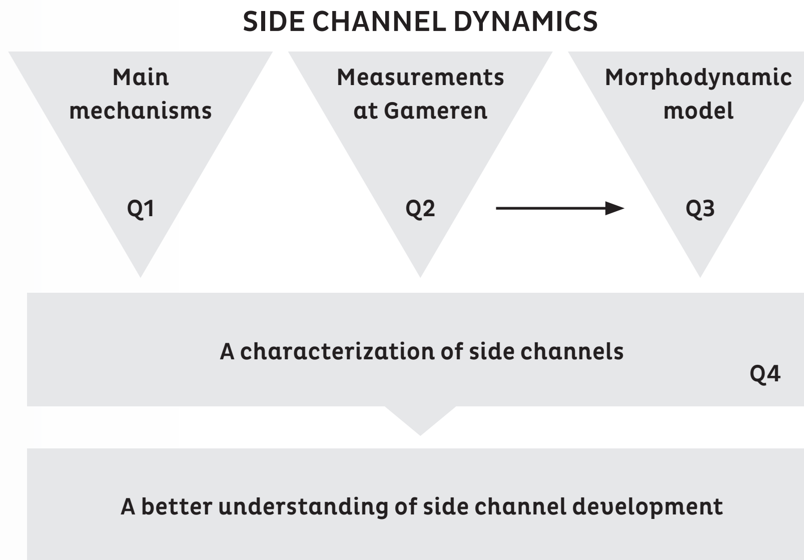

FIGURE 1.3 An overview of the research approach.

Photo: Bureau Beeldtaal Filmmakers

CHAPTER 2

Morphodynamic assessment of side channel systems using a simple one-dimensional bifurcation model and a comparison with aerial images

This chapter is published as Van Denderen, R.P., R.M.J. Schielen, A. Blom, S.J.M.H. Hulscher, and M.G. Kleinhans, 2018: Morphodynamic assessment of side channel systems using a simple one-dimensional bifurcation model and a comparison with aerial images. *Earth Surface Processes and Landforms*, 43, 1169–1182, DOI:10.1002/esp.4267.

Side channel construction is a common intervention applied to increase the river's conveyance capacity and to increase its ecological value. Past modelling efforts suggest two mechanisms affecting the morphodynamic change of a side channel: 1) a difference in channel slope between the side channel and the main channel and 2) bend flow just upstream of the bifurcation. The objective of this paper is to assess the conditions under which side channels generally aggrade or degrade and to assess the characteristic time scales of the associated morphological change. We use a one-dimensional bifurcation model to predict the development of side channel systems and the characteristic time scale for a wide range of conditions. We then compare these results to multitemporal aerial images of four side channel systems. We consider the following mechanisms at the bifurcation to be important for side channel development: sediment diversion due to the bifurcation angle, sediment diversion due to the transverse bed slope, partitioning of suspended load, mixed sediment processes such as sorting at the bifurcation, bank erosion, deposition due to vegetation, and floodplain sedimentation. There are limitations to using a one-dimensional numerical model as it can only account for these mechanisms in a parameterized manner, but the model reproduces general behavior of the natural side channels until floodplain forming processes become important. The main result is a set of stability diagrams with key model parameters that can be used to assess the development of a side channel system and the associated time scale, which will aid in the future design and maintenance of side channel systems.

02

2.1 INTRODUCTION

A side channel system is a term for a two-channel system that is connected to each other at both ends in which the side channel conveys much less discharge than the main channel. In the past many side channel systems disappeared due to human interference, which resulted in a loss of habitat diversity and a decrease in the conveyance capacity of the river. In several rivers in Europe and North America, restoration projects aim to restore the river to a more natural state and such stream restoration may include the construction of side channels. The main objectives of side channel construction are to improve flood safety (Simons et al., 2001; Nabet, 2014), to increase ecological value (Schiemer et al., 1999; Formann et al., 2007), to restore river branches, and to reduce degradation in the main channel (Tockner et al., 1998; Formann et al., 2007). However, side channels often suffer from aggradation or degradation, which results in the need for regular maintenance. This is both expensive and can deteriorate the targeted ecosystem, and therefore a side channel without the need for intensive maintenance is desirable. However, it is unclear whether such a maintenance-free side channel system can exist. A better understanding of the mechanisms that influence morphodynamic changes of side channel systems is therefore needed.

Side channels also occur in natural rivers in the form of, for example, cutoff channels and chute channels. After the initiation of such a new channel, various mechanisms determine the discharge and sediment partitioning at the bifurcation which in turn determine the development of the two-channel system (Slingerland and Smith, 1998, 2004; Van Dijk et al., 2012). A cutoff channel that becomes the dominant channel reduces the transport capacity in the main channel, leading to aggradation in the main channel (Constantine et al., 2010; Van Dijk et al., 2012). This aggradation can be distributed over the channel (Dieras et al., 2013) or if, for example, the bifurcation angle is large, local deposition at the entrance of the channel may lead to the formation of a plug bar. After the main channel is closed due to a plug bar, it slowly silts up through deposition of fine sediment due to overbank flow (Constantine et al., 2010; Toonen et al., 2012). From the moment that the discharge in the closing channel is limited, a return current in the side channel can form due to water level variations at the confluence. This can increase the aggradation rate of the closing channel (Citterio and Piégay, 2009; Le Coz et al., 2010).

The stability of a bifurcation is determined by the sediment supply to the downstream branches and their sediment transport capacity (Wang et al., 1995). There are several mechanisms that affect the sediment supply and the transport capacity of the downstream branches: a difference in slope between the side channel and the main channel (Bolla Pittaluga et al., 2003), sediment diversion due to bend flow (Kleinhans et al., 2008; Van Dijk et al., 2014), sediment diversion due to a transverse bed slope at the bifurcation (Bolla Pittaluga et al., 2003; Kleinhans et al., 2008), sediment diversion due to the bifurcation angle (Bulle, 1926; Van der Mark and Mosselman, 2013; Dutta et al., 2017), partitioning of suspended load (Slingerland and Smith, 1998, 2004; Van Dijk et al., 2012; Gaweesh and Meselhe, 2016) mixed sediment processes (Sloff et al., 2003; Frings and Kleinhans, 2008; Sloff and Mosselman, 2012; Kästner et al., 2017), bank erosion (Miori et al., 2006; Kleinhans et al., 2011), deposition due to vegetation (Rodrigues et al., 2006), and floodplain sedimentation (Toonen et al., 2012). The discharge partitioning at the bifurcation is proportional to the water surface slope in the downstream channels and is therefore related to the length of the channels (Mendoza et al., 2016). The sediment partitioning at the bifurcation is related to the discharge partitioning and is among other things affected by a transverse bed slope (Bolla Pittaluga et al., 2003) and bend flow (Kleinhans et al., 2008). Bend flow creates a secondary flow that at the water surface is directed toward the outer bend and at the bed towards the inner bend (Dietrich and Smith, 1984; Struiksma et al., 1985). If a bifurcation is located just downstream of a bend (Figure 2.1), the sediment transport is slightly directed towards the channel in the inner bend (Kleinhans et al., 2008; Hardy et al., 2011; Van Dijk et al., 2014). The transverse bed slope results from a difference in bed level between the downstream branches that influences the bed level up to a certain distance upstream of the bifurcation. This transverse slope deflects sediment into the deeper channel due to the gravity effect (Bolla Pittaluga et al., 2003; Kleinhans et al., 2008). Both bend flow and the transverse bed slope affect the partitioning of bed load at the bifurcation. Suspended bed-material load is less affected by slope effects and the sediment concentration varies less with vertical distance from the bed than bed load (Church, 2006), which means that vertical differences in flow direction also have a smaller influence on the partitioning of suspended bed-material load. Wash load is almost uniformly distributed over the depth (Bridge, 2003). The partitioning of wash load is therefore expected to be about the same as the discharge partitioning.

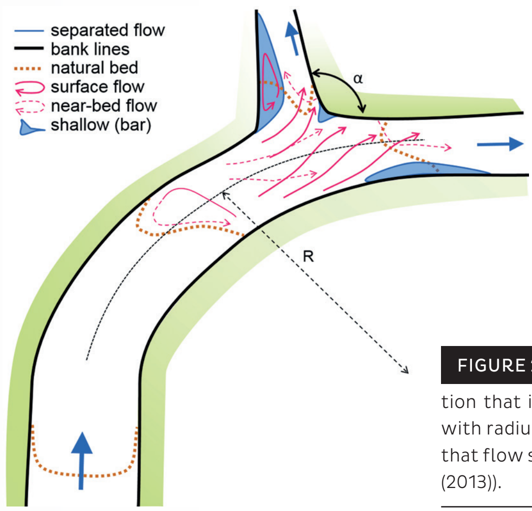

FIGURE 2.1 The flow patterns at a bifurcation that is located downstream of a river bend with radius R and the bifurcation angle (∝) is such that flow separation occurs (After Kleinhans et al. (2013)).

The bifurcation angle is the angle between the side channel and main channel (Figure 2.1) and is defined at the intersection between the center lines of the downstream channels. The diversion of the flow towards the side channel is associated with a spiral flow upstream of the bifurcation in which the velocity near the bed is directed towards the side channel. This increases the sediment load towards the side channel, which is also known as the Bulle effect (Bulle, 1926; Riad, 1961; Van der Mark and Mosselman, 2013). It is expected that the Bulle effect increases with an increasing bifurcation angle (De Heer and Mosselman, 2004; Van der Mark and Mosselman, 2013; Dutta et al., 2017). However, for large bifurcation angles a flow separation zone may develop (Figure 2.1) (Bulle, 1926; Riad, 1961; Constantine et al., 2010; Dutta et al., 2017). If flow separation occurs, the influence of the Bulle effect on the sediment partitioning seems small compared to the influence of the flow separation zone (De Heer and Mosselman, 2004; Van der Mark and Mosselman, 2013). Due to the smaller flow velocities and the circulation inside the flow separation zone, a bar forms inside this zone (Constantine et al., 2010; Zinger et al., 2013). The reduced effective width increases the flow velocities at the entrance of the side channel (Figure 2.1), causing large scour and, potentially, bank erosion (Kleinhans et al., 2013; Zinger et al., 2013). However, if the side channel attracts only a limited amount of discharge, large deposition in the separation zone may lead to a plug bar (Constantine et al., 2010; Kleinhans et al., 2013).

Bank erosion and accretion influence the time scale of bifurcation development (Kleinhans et al., 2011). Width adaptation allows for a larger difference in discharge between the downstream branches than without width adaptation (Miori et al., 2006). In a degrading channel, bank erosion adds more sediment to the channel, thus reducing the amount of sediment that is picked up from the bed (Kleinhans et al., 2011). On the other hand, in the case of bank accretion sediment is deposited on the sides of the channel reducing the amount of sediment deposited in the middle of the channel. This means that the time after which an equilibrium flow depth is reached, increases.

The dynamics of bifurcations have been studied using various models. One-dimensional modelling of bifurcation behavior requires a relation for the sediment partitioning that accounts for two-dimensional (2D) and three-dimensional (3D) effects on the sediment partitioning in a parametrized way. The sediment partitioning is expected to be related to the characteristics of the downstream channels (Riad, 1961; Wang et al., 1995). After introducing a more extended nodal point relation, Wang et al. (1995) introduce a strongly simplified relation and use this in a linear stability analysis:

$$\frac{Q_{s2}}{Q_{s3}} = \left(\frac{Q_2}{Q_3}\right)^k \left(\frac{W_2}{W_3}\right)^{1-k} \quad (2.1)$$

where Q_{si} is the sediment load delivered to the downstream branch i (where $i \in [2,3]$ indicates each of the downstream branches), Q_i is the water discharge in branch i, W_i is the width in branch i and k is an empirical parameter. It was found that for $k > n/3$ the bifurcation is stable and for $k < n/3$ the bifurcation is unstable (Wang et al., 1995), which implies that one of the downstream branches closes. The parameter n is the degree of non-linearity of the sediment transport relation ($Q_S \propto u^n$ and $n = 5$ for Engelund and Hansen (1967)). A case with $k < n/3$ implies that a small increase of the discharge in branch i leads to a small increase of the sediment supply to branch i and at the same time a relatively large increase of the transport capacity, which results in degradation. This increases the discharge even more, which implies that the bifurcation is unstable. A case with $k > n/3$ implies that a small increase of the discharge in branch i leads to an increase of the sediment supply that is larger than the increase of the sediment transport capacity, which results in aggradation. The aggradation decreases the discharge to this branch and leads to a stable bifurcation. A model for k is still lacking, which complicates the application of Equation 2.1 to natural cases.

A second model to study bifurcation dynamics is proposed by Bolla Pittaluga et al. (2003). The model is based on a mass balance over two computational cells upstream of the bifurcation between which a transverse sediment flux occurs. This flux occurs due to: (A) the fact that the discharge partitioning generally differs from the width ratio (Q_y in Equation 2.12); (B) the transverse bed slope associated with a difference in bed level between the downstream branches (Bolla Pittaluga et al., 2003); (C) the presence of bend flow upstream of the bifurcation (Kleinhans et al., 2008). A degrading deeper channel leads to a larger transverse bed slope and therefore a larger sediment supply. This continues until an equilibrium is reached and results in an asymmetric stable bifurcation in which neither branch is forced to close. The transverse bed slope therefore has a stabilizing effect. The magnitude of the transverse bed slope effect is a function of the Shields parameter, the width to depth ratio and the bed level difference between the downstream channels (Bolla Pittaluga et al., 2003; 2015). Several laboratory experiments and field cases show that such stable asymmetric bifurcations can occur in cases that are dominated by bed load (Bertoldi and Tubino, 2007; Kleinhans et al., 2008; Bolla Pittaluga et al., 2015). If the transverse bed slope and the bend flow are ignored the nodal point relation of Bolla Pittaluga et al. (2003) reduces to Equation 2.1 with $k = 1$.

The objective of this paper is to assess the conditions under which side channels generally aggrade or degrade and to assess the characteristic time scales of the associated morphological change. We use a one-dimensional bifurcation model to predict the development of side channel systems and the associated time scale for a range of conditions, and generalize these in the form of stability diagrams with the most important model parameters. We then compare these results with aerial images that show the development of four side channel systems to test whether the model reproduces these configurations. First we introduce the model (Section 2.2) and explain how we use it (Section 2.3). In the results section we first show the predicted side channel development (Section 2.4.1) and then we compare these results to the observed development of the four side channel systems (Section 2.4.2).

2.2 MODEL DESCRIPTION

We use the one-dimensional numerical bifurcation model developed by Kleinhans et al. (2011). The model consists of four branches: the upstream channel, the main channel, the side channel parallel to the main channel and the recombined downstream channel. The length of each branch is assumed to be constant in the model. A constant bankfull discharge is imposed at the upstream boundary and at the downstream end a constant water level is imposed. Floodplain processes and effects on flow division are excluded and Kleinhans et al. (2008) showed that discharge fluctuations then have a negligible effect on the development of such well-defined bifurcating channels. The discharge partitioning at the bifurcation is computed by numerically solving the flow depth at the bifurcation using the backwater equation (Parker, 2004) under the condition that the water levels at the upstream end as well as the downstream end, where they recombine, of the side channel and main channel are equal. The sediment transport is computed using the sediment transport relation by Engelund and Hansen (1967). The sediment partitions at the bifurcation based on the nodal point relation by Bolla Pittaluga et al. (2003) (Appendix 2.A) with an adjustment of the transverse sediment transport due to a river bend upstream of the bifurcation (Kleinhans et al., 2011). To account for width adaptation of the channels, an empirical equilibrium width is computed based on the discharge in the channel (Equation 2.13). The sediment that is added or removed from the banks is accounted for as a source or sink term in the Exner conservation law (Equation 2.16).

As a constant bankfull discharge overestimates the yearly averaged sediment transport rate of the river, the model underestimates the time scale of the side channel development. We introduce an intermittency factor that corrects for the nonlinear behavior of the sediment supply in relation to the water discharge (Parker, 2004; Kleinhans et al., 2011). We define the intermittency factor as the measured yearly-averaged sediment transport rate of the river divided by the yearly-averaged sediment transport rate as estimated with bankfull discharge.

Two additional mechanisms are accounted for in this paper. Firstly, we assume a fraction μ of the sediment supply that is unaffected by bed slope effects or bend flow. This fraction is therefore related to the limited effect of a transverse bed slope or bend flow at the bifurcation on suspended load. Secondly, we account for the effects of flow separation with a simple parametrization of the reduction of the effective entrance width caused by the separated flow cell. The size of the flow separation zone is estimated by (Constantine et al., 2010):

$$\varepsilon = 1 - 0.94e^{-0.013\alpha} \tag{2.2}$$

where ϵ is a fraction of the channel width that is occupied by the flow separation zone and α is the diversion angle in degrees. This relation is based on model results in which the shape of the bifurcation is abrupt (Constantine et al., 2010). The sediment load that enters the flow separation zone (Q_{sf}) is estimated by:

$$Q_{sf} = \varepsilon Q_{si} \tag{2.3}$$

where Q_{si} is the total amount of sediment supplied to branch *i*. The length of the flow separation zone is unknown, but as a first estimate we assume that the length of the flow separation zone is the same size as the first grid cell (Δx). This leads to:

$$\frac{\partial W_{x0}}{\partial t} = \frac{1}{h}\frac{Q_{sf}}{\Delta x} \tag{2.4}$$

where W_{x0} is the width of the channel entrance and h is the flow depth at the entrance of the channel. From this it follows that the size and the growth rate of the bar at the entrance of the bifurcation is a function of the grid cell size Δx. We recognize that this approach is not appropriate as the discretization may not affect the results. It is a pragmatic choice which will need to be reformulated and improved in future analyses.

2.3 METHOD

We compute the side channel development and the corresponding time scale for a range of side channel characteristics, including three rivers: the river Ain, the Wabash River and the Sacramento River (Table 2.1). We then compare these results with observed development of the side channel systems in these rivers.

Table 2.1 List of side channel systems with their main characteristics. L_{side}/L_{main} is the length of the two channels in which the side channel is the initially smallest channel, Q_{bank} and W_{bank} are the bankfull discharge and width, D_{50} is the median grain size, *k* is the Nikuradse roughness length and $Q_{s,yearly}$ is the average annual sediment load of the river.

River	Location	L_{side}/L_{main} [m/m]	Q_{bank} [m³/s]	W_{bank} [m]	D_{50} [mm]	k [m]	Fr	θ	$Q_{s,yearly}$ [m³/yr]	Reference
Ain, France	**Mollon** (45°56'51.14"N; 5°14'55.36"E)	1600/1800	400	80	30	0.33[1]	0.38	0.06	60,000	Bravard (1986); Rollet (2007); Olivier et al. (2009); Dieras et al. (2013)
	Martinaz (45°56'5.14"N; 5°15'9.72"E)	950/1000	400	80	30	0.33[1]	0.38	0.06	60,000	
Sacramento River, USA	**Colusa** (39°19'31.35"N; 122°1'31.28"W)	1200/1900	1840	259	2	0.7[2]	0.2	0.48	1,500,000	Singer and Dunne (2004); Constantine et al. (2010)
Wabash River, USA	**Mackey Bend** (37°48'57.99"N; 88°2'29.52"W)	2500/11500	2000	300	0.7	0.12[3]	0.2	0.40	1,320,000	Zinger et al. (2011); Zinger et al. (2013); Konsoer (2014); Zinger (2016)

[1] Based on water depth and discharge measurements.
[2] Based on bankfull discharge, width and velocity estimation (Constantine et al., 2010).
[3] The Nikuradse roughness length was estimated using the ripple roughness height relation (Van Rijn, 1993) based on the measured dune height and length in the upstream channel (Zinger, 2016) during a discharge of 1565 m³/s.

2.3.1 ASSESSMENT OF GENERAL SIDE CHANNEL BEHAVIOR

We use the one-dimensional numerical model described in Section 2.2 to study the general development of side channel systems. We compute the development for the three selected rivers (Table 2.1) and we vary five model parameters between reasonable ranges to study the stability of the side channel system. These model parameters are the length of the side channel, bend flow at the bifurcation, bank erosion, the bifurcation angle, and the fraction of suspended bed-material load. We assume the initial water discharge into the side channel to be 10% and into the main channel equal to 90%. The effect of this assumption on the result appears to be limited for small variations of the initial condition. Based on this initial discharge and assuming an equilibrium water depth in each branch, we estimate the initial bed level. We assume that an equilibrium is reached when the discharge changes less than 0.5 m^3/s between subsequent years. The time scale of the side channel development is estimated based on the tangent line at the largest gradient in the time-discharge results of the side channel (Figure 2.2). The time scale is non-dimensionalized using the yearly averaged sediment supply and the initial volume of the side channel ($V_{side} = W_{side}\, L_{side}\, h_{side}$):

$$T_{ref} = \frac{T_{side}}{\left(\dfrac{W_{side} L_{side} h_{side}}{\dfrac{W_{side}}{W_{main} + W_{side}} Q_{s,yearly}}\right)} \tag{2.5}$$

in which $Q_{s,yearly}$ is the yearly averaged sediment supply, W_{side} is the initial width of the side channel, L_{side} is the length of the side channel from the bifurcation to the confluence and h_{side} is the initial flow depth of the side channel.

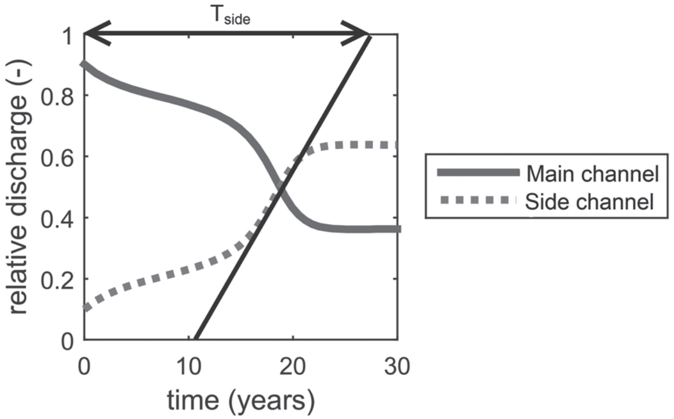

FIGURE 2.2 An example of the calculation method of the time scale of side channel development. A tangent line is drawn at the location where the gradient in the discharge is largest. This time scale is then made dimensionless by Equation 2.5.

2.3.2 USE OF AERIAL IMAGES

We study four side channel systems using aerial image time series (Table 2.1). We selected these four sites because their side channel development is visible from the time series and human influence on their development seems limited. The length of a channel is measured following its center line. Using the aerial images, we study the locations of deposition and scour, the time scale of side channel development and channel migration. We then pose several hypotheses for mechanisms that determine or affect the morphodynamic change in the side channel systems. The results of the one-dimensional (1D) model are used to quantify the effects of the mechanisms on the stability of the side channel system and the time scale of the side channel development.

2.4 RESULTS

2.4.1 GENERAL SIDE CHANNEL DEVELOPMENT

We apply 1D numerical model described in Section 2.2 to estimate the equilibrium state of a side channel system. According to the model the length of the side channel relative to that of the main channel strongly determines the side channel development (Figure 2.3). If the side channel is much shorter than the main channel, the side channel becomes the dominant channel. Neither channel fully closes, because at some point the transverse bed slope is large enough to divert a sufficient amount of sediment from the shallower channel to the deeper channel such that the transport capacity in each downstream channel is equal to its sediment supply. There is an abrupt transition between the dominance of the side channel and the dominance of the main channel. This abrupt transition is caused by the transverse bed slope effect. A situation with an equal discharge in both branches is unstable due to a small transverse bed slope. These results show that the transition between a dominant side channel and a dominant main channel occurs for similar length ratios for a sand-bed river such as the Wabash River, a sand-gravel river such as the Sacramento River and a gravel-bed river such as the river Ain. With increasing discharge asymmetry, the transverse bed slope increases until the sediment supply to the channel matches its sediment transport capacity. The stability of the bifurcation and the location of the transition therefore depends on the magnitude ($\partial\eta/\partial y$) and the intensity ($1/f(\theta)$) of the transverse bed slope effect (Equation 2.8), which agrees with previous studies (Bolla Pittaluga et al., 2003; 2015). This causes the transition to occur at slightly different values for the three rivers. The transition for the Sacramento River occurs at a slightly lower length ratio, because the high Shields parameter reduces the transverse bed slope effect (Table 2.1).

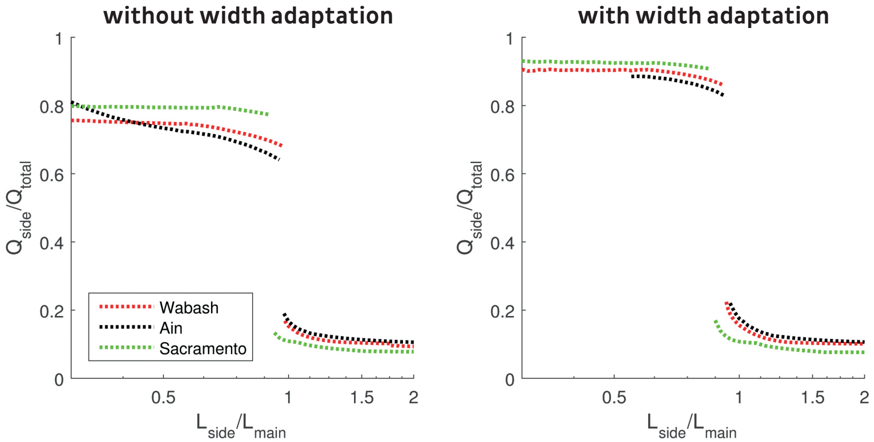

FIGURE 2.3 The equilibrium discharge partitioning for three rivers as a function of the length difference between the side channel and the main channel.

We extend this analysis with the effect of bend flow at the bifurcation (Figure 2.4). If the side channel is located in an inner bend, more sediment is supplied to the side channel compared to a case with a straight upstream channel and therefore it is likely that the main channel becomes dominant (Figure 2.4A). Similarly, when the side channel is located in the outer bend, it receives less sediment and it is more likely that the side channel becomes dominant (Figure 2.4B). The abrupt transition (Figure 2.3) is in these graphs shown as a white line. The smaller transverse bed slope effect in the Sacramento River shifts the transition to lower values of the length ratio. The transition for the river Ain is similar to the Wabash River for gradual bends, but with a decreasing relative radius the intensity of the bend flow increases faster for the river Ain due to a larger depth-width ratio (Equation 2.11).

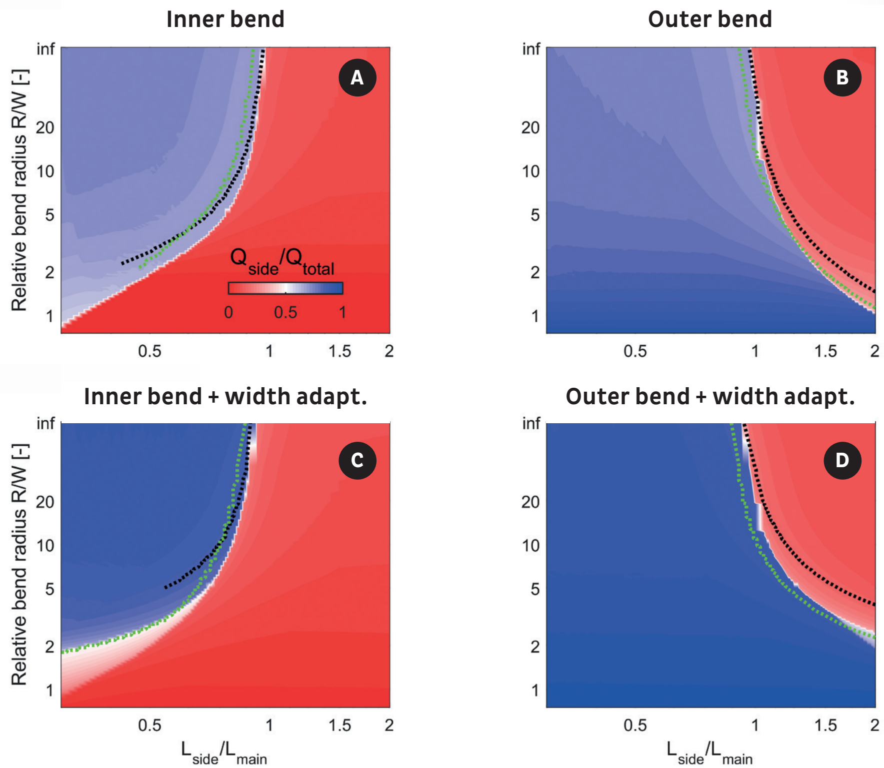

FIGURE 2.4 The equilibrium state of the two-channel system in the Wabash River (Figure 2.9) depending on the length difference between the channels, bend flow and width adaptation. The relative bend radius (y-axis) is defined as the ratio between the radius and the width of the upstream channel. An infinite relative radius corresponds with a straight channel and a smaller relative radius corresponds with a larger bend flow intensity. The x-axis shows the ratio between the side channel length and the main channel length. The blue color means that the side channel becomes dominant and the red color means the main channel remains dominant. The white line that separates the blue and red surfaces is a result of interpolation and represents the abrupt transition. The black and green dotted line represent the abrupt transition for the river Ain and the Sacramento River respectively.

The results slightly change if the width adaptation of the downstream branches is accounted for (Figures 2.4C and D). The width adaptation is assumed a function of the flow rate (Equation 2.13) and a degrading channel will therefore increase in width. This increases the time scale of the side channel development since the eroded sediment acts as source of sediment in the Exner conservation law. The flow depth in a degrading channel increases less with an increase of discharge compared to the case without width adaptation. This also leads to a smaller difference in bed level between the downstream channels and therefore a smaller transverse bed slope. The side channel system stabilizes therefore at a larger discharge asymmetry and it is easier to switch from a dominant main channel to a dominant side channel which results in a shift of the transition zone. This is shown in Figure 2.4D as an upward shift of the transition line at large length ratios. In the case of a side channel in the inner bend and width adaptation (Figure 2.4C), a large transition zone occurs, because due to bend flow the upstream channel supplies sufficient sediment to the side channel to match its increased transport capacity. This does not occur in the case without width adaptation, because the transverse sediment transport due to bend flow increases with a decreasing width difference between the downstream branches (Equation 2.10).

The time scale of side channel development (Equation 2.5) depends on the transport capacity in and the sediment supply to each branch (Figure 2.5). The maximum time scale goes theoretically to infinity because there are conditions under which the supplied sediment matches the transport capacity of the channels. However, the model results are discrete and therefore do not show an infinite time scale. The line with the maximum time scale is shown in Figures 2.5E and F. This is not a stable situation; rather, a minor perturbation would initiate change. Below this line, the gradient in the time scale is much larger than above. This line occurs for similar conditions for each of the three rivers (Figures 2.5E and F). The time scale increases if width adaptation is accounted for and is in that case sensitive to the width adaptation time scale (Kleinhans et al., 2011).

In the model the size of the flow separation zone is related to the bifurcation angle. Depending on the angle between the downstream channels and the upstream channel, a flow separation zone may occur in the main channel (Figure 2.6A) and in the side channel (Figure 2.6B). A large angle means a large flow separation zone that reduces the channel width at the entrance and therefore reduces the discharge in that channel, which results in aggradation. The computations with a flow separation zone in the side channel (Figure 2.6B) show a transition zone between a dominant main channel and a dominant side channel. The large transverse bed slope, which is induced by scour at the entrance of the channel, results in a transverse sediment flux at the bifurcation that is large enough to balance the increased transport capacity of the side channel. The flow separation zone increases the likelihood that the channel in which flow separation occurs closes.

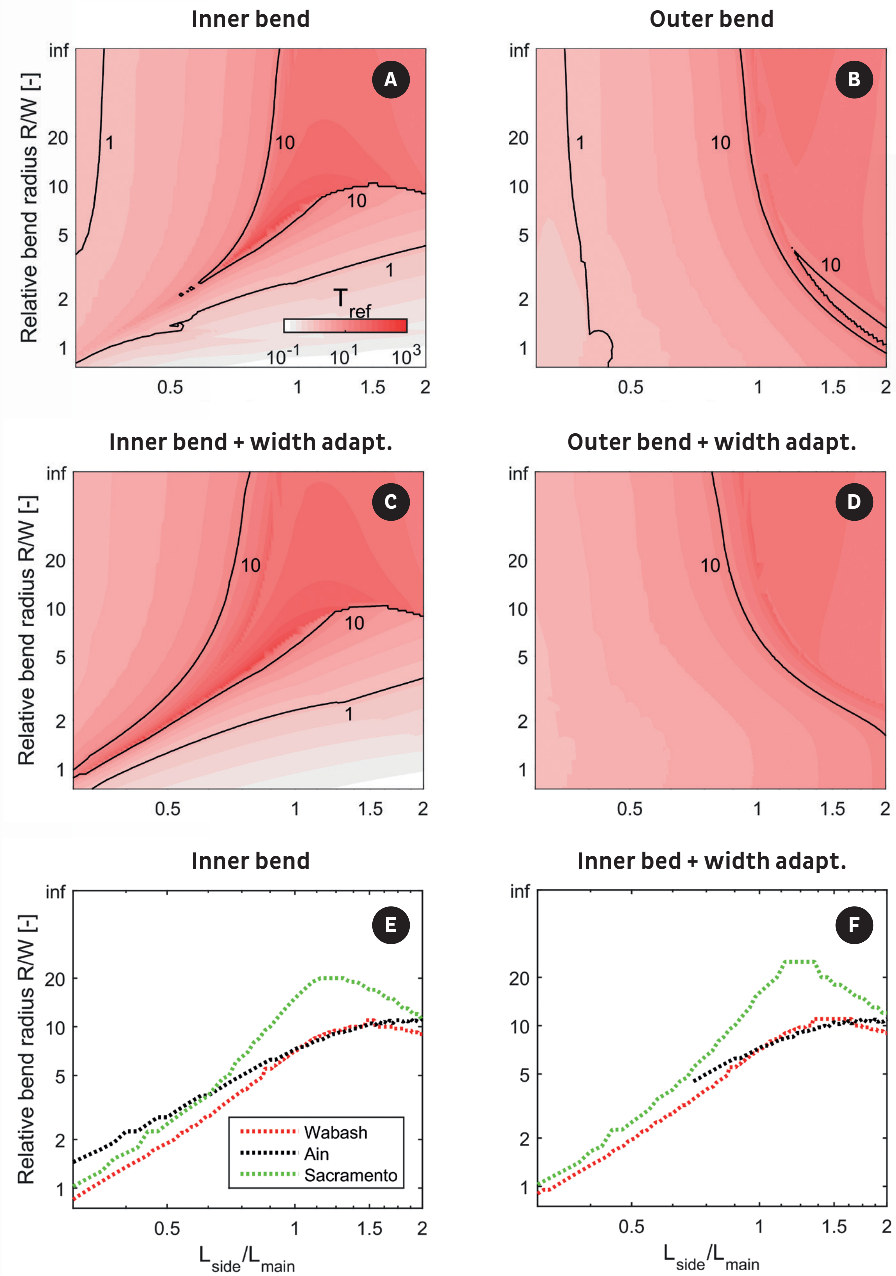

FIGURE 2.5 The time scale of the side channel development as defined in Figure 2.2 corresponding with Figure 2.4. Graphs **E** and **F** show the maximum time scale for three rivers derived from Graphs **A** and **C**.

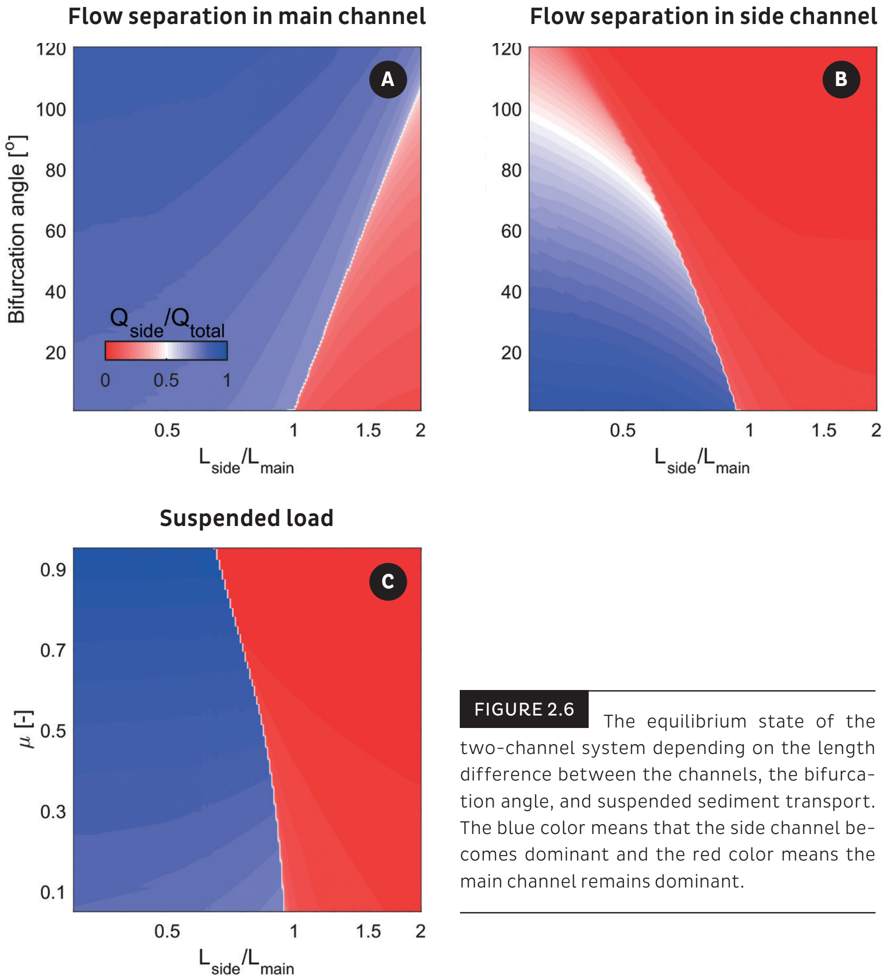

FIGURE 2.6 The equilibrium state of the two-channel system depending on the length difference between the channels, the bifurcation angle, and suspended sediment transport. The blue color means that the side channel becomes dominant and the red color means the main channel remains dominant.

The partitioning of the suspended bed-material load is different from the partitioning of bed load and this affects the equilibrium state (Figure 2.6C). We vary the parameter μ which is the fraction of the sediment that is affected by the transverse bed slope (y-axis). For $\mu = 0$ we deal with bed load only and for $\mu = 1$ the sediment partitioning is independent of the transverse bed slope. In the latter case, the sediment partitioning is similar to the water discharge partitioning and one of the branches fully closes. The transport capacity in the side channel increases with $i_b^{5/2}$, in which i_b is the slope of the side channel, whereas the water discharge increases with $i_b^{1/2}$. This means that if the side channel is steep enough, the transport capacity increases faster than the water discharge leading to erosion of the side channel. In the case of $\mu = 1$ this is the mechanism that can lead to a dominant side channel. For $\mu < 1$ it is easier for the side channel to become dominant, because due to the transverse bed slope more sediment is diverted to the main channel.

2.4.2 FIELD CASES

We apply the presented stability diagrams to four side channel systems. We study the side channel systems using aerial images and compare them with the 1D numerical results.

MOLLON, RIVER AIN (FRANCE)

The river Ain is located in the south-east of France and is a tributary of the river Rhône. The average annual discharge is 120 m^3/s and the 2-year peak flow is 760 m^3/s (Dieras et al., 2013). The surface grain size varies between 15 and 46 mm (Rollet, 2007). Figure 2.7 shows a series of aerial images of a two-channel system in the river Ain near Mollon, France. In 1968 the two-channels have similar lengths. The west channel aggrades over time and a bar forms at the entrance. From 1991 a meander forms in the east channel as is visible in 1996. This meander induces a length difference between the channels. In 1996 the west channel reopens due to a chute incision (Dieras et al., 2013). The water level gradient over the west channel is larger than over the east channel due to their length difference. The west channel attracts therefore relative to its size more discharge, which leads to degradation of the west channel. The discharge in the east channel therefore decreases, which leads to aggradation. From 2003 the conveyance capacity is larger in the west channel than in the east channel and in 2005 the east channel does not convey water during base flow (Dieras et al., 2013). Vegetation growth has likely accelerated aggradation due to increased trapping of sediment (Figure 2.7, 2010). The images show a widening of the west channel, which seems to be due to the unstable and poorly cohesive banks (Piégay et al., 2002).

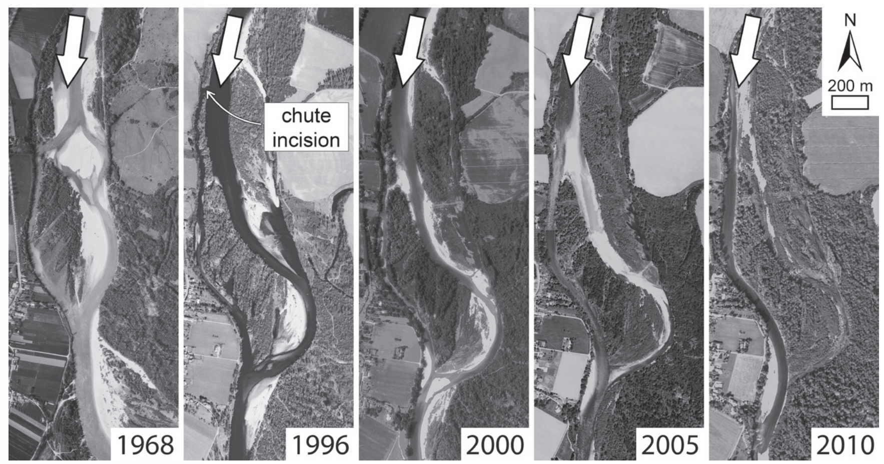

FIGURE 2.7 A series of aerial images of a two-channel system in the river Ain near Mollon, France. In 1995, the west channel is reopened and around 2005, the east channel closes *(IGN-France and Google Earth)*.

Based on the stability diagrams (Figure 2.4), we hypothesize that the length difference between the two channels caused the switch from a dominant main channel to a dominant side channel (Table 2.1). Based on Figure 2.4 we find that the length difference between the west and east channel is sufficient for the west channel to become dominant. The predicted time scale is of the order of 25 or 90 years, depending on whether width adaptation is included (Figure 2.5). The banks in the river Ain are unstable (Piégay et al., 2002) which suggests that the width adaptation time scale might be overestimated leading to an overestimation of the time scale of side channel development. This could be solved by calibrating the time scale of the width adaptation on the basis of data, and would put the modelled timescale between the two present values. We expect that mechanisms that are not accounted for in the model lead to the filling up of the channel, for example, aggradation of finer sediments and the trapping by vegetation.

MARTINAZ, RIVER AIN (FRANCE)

A second two-channel system in the river Ain is found near the village of Martinaz. Between 1954 and 1968 a meander forms (Figure 2.8), which cuts into an already existing channel (Figure 2.8, 1954), forming the side channel system shown in 1968. The bifurcation is located at the downstream end of the bend. Bend flow, i.e. spiral flow that is directed toward the inner bend near the bed, likely increases the sediment load into the west channel. In 1968 and 1970 a cutoff channel is visible in the meander. This cutoff does not become dominant, but may have affected the stability and the time scale of the side channel development. In 1976 another cutoff forms and the west channel aggrades such that it is disconnected from the main channel during base flow.

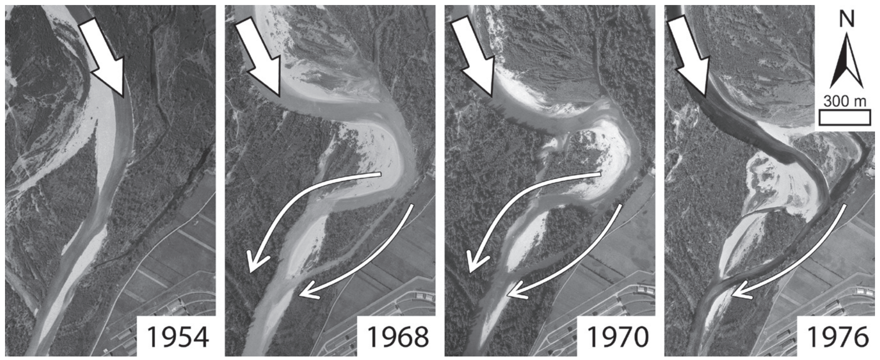

FIGURE 2.8 A series of aerial images of a two-channel system in the river Ain near Martinaz, France. A meander cuts into a former channel which is connected to the main channel in the outer bed (see image of 1968). The west channel starts to aggrade and the east channel becomes the main channel *(IGN-France)*.

The development of the side channel system is likely affected by the bend flow at the bifurcation and the cutoff of the bend in 1968 and 1970. The numerical model results (Figure 2.4) show that the small length difference is sufficient for the east channel to become dominant and that bend flow increases the water discharge conveyed by the east channel. Including these two mechanisms and width adaptation in the numerical model yields a time scale of the order of 10 years to reach its equilibrium which is comparable to the 8 to 10 years after which the west channel seems to have been disconnected (Figure 2.8).

MACKEY BEND, WABASH RIVER (USA)

The Wabash River is located on the border of Illinois and Indiana (USA). The average annual discharge is 825 m^3/s and the 2-year flood is 3795 m^3/s (Zinger et al., 2013). Mackey Bend is located just upstream of the confluence between the Wabash River and the Ohio River (Figure 2.9, 2007A). In June 2008, a large discharge in the Wabash River in combination with a low discharge in the Ohio River leads to the formation of a cutoff channel (Zinger et al., 2013). The bifurcation angle of 82° (Zinger et al., 2013) leads to flow separation at the left bank of the cutoff channel. A bar forms in the flow separation zone (Figure 2.9, 2009). The first cutoff channel is shorter than the meander and therefore the cutoff attracts a relatively large discharge. The large flow velocity in combination with the large flow separation zone, appears to result in bank erosion, allowing the channel to migrate and to reduce the bifurcation angle to about 60° in 2009.

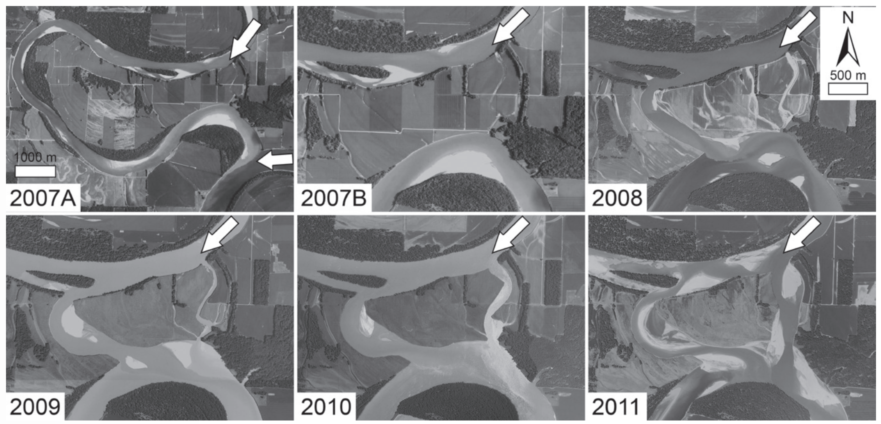

FIGURE 2.9 A series of aerial images of a meander cutoff in the Mackey Bend of the Wabash River, USA. The first image (2007A) shows the full river bend and the confluence with the Ohio River in the bottom right corner. The other images are zoomed in on the location of the cutoffs. The first cutoff occurs in 2008 and the second in 2009. The second cutoff becomes the main channel. The former meander channel and the first cutoff slowly fill with sediment. *(NAIP)*

After several floods, a second cutoff channel forms in June 2009 (Zinger et al., 2011). This new channel has an even larger water surface slope and therefore attracts a large fraction of the upstream water discharge. Measurements show that initially the bar in the flow separation zone remains small and bank migration is limited (Zinger et al., 2013). During a moderate flood in the beginning of July 2010 the width increases rapidly and a bar forms in the flow separation zone as shown in 2011. The two sharp corners in the banks, visible in 2010, possibly hinder the migration of the channel and the growth of the bar at the entrance. It is not clear why these seemingly hard corners in the banks occur. From 2011 the second cutoff channel conveys the larger part of the discharge and measurements show that during a flood event with a return period of 2 years in 2015, about 80% of the total discharge is conveyed by the second cutoff channel (Zinger, 2016).

The length difference and the bifurcation angle likely affected the development of the channels. The numerical model shows that very large bifurcation angles can outweigh the favorably short length of the side channels such that the main channel remains dominant (Figure 2.6B), but this only occurs if bank erosion is limited. The side channel system of the Wabash River shows extensive bank migration, which reduces the bifurcation angle. If we ignore the effect of the bifurcation angle, the time scale of the development of the first cutoff is about 2 years (Figure 2.5), which appears to be an underestimation on the basis of the aerial images. Possibly bar formation and bar-induced channel migration increased the time scale of the side channel development.

COLUSA, SACRAMENTO RIVER (USA)

The Sacramento River is located in California (USA). Its average annual discharge is 350 m^3/s and its 2-year flood is equal to 2100 m^3/s (Constantine et al., 2010). The average suspended load ($1.5 \cdot 10^6$ m^3/yr) is much higher than the average bed load ($7.5 \cdot 10^4$ m^3/yr), and is for a large part transported as wash load (Singer and Dunne, 2004; Constantine et al., 2010). A side channel system exists just upstream of the city of Colusa (Figure 2.10). Between 1964 and 1976 the west channel is connected to the main channel and it is much shorter than the east channel. We therefore expect the west channel to grow, but it only starts to do so after 1998. This may be due to a limited sediment transport in the river, barely erodible banks or the formation of a bar upstream of the bifurcation which from 1993 may induce bend flow at the bifurcation. From 2009 the width of both channels is the same. We therefore expect that the conveyance capacity in the west channel is larger than in the east channel. In 2015 the sedimentation in the downstream part of the east channel almost closes the channel and we expect that the east channel closes in the next few years. This suggests a large difference in time scale between the opening of the west channel (in the order of 30 years) and the closing of the east channel (in the order of 10 years). Suspended bed-material load or even wash load may induce such a difference, as it requires space and time to settle. Suspended bed-material load has a limited effect on the opening of the west channel, but may determine the closing of the east channel. The role of suspended load seems to be confirmed by the 2015 image, which shows that aggradation starts near the downstream end of the east channel. This corresponds with the spatial lag expected for suspended load.

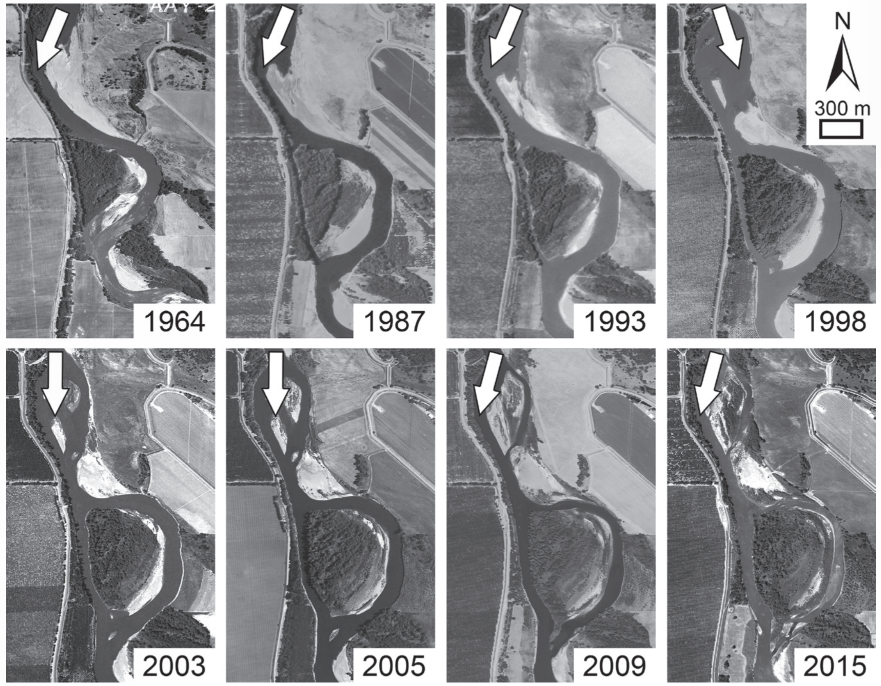

FIGURE 2.10 A series of aerial images of a meander cutoff upstream of Colusa in the Sacramento River, USA. The west channel increases in size and around 2009 the west channel seems to be the dominant channel. In 2015 large aggradation is visible in the east channel. *(Geoportal California, NAPP USGS, NAIP and Google Earth)*

The large difference between bed load and suspended supply in the river likely affects the side channel development. Based on only bed load, the model predicts that the west channel becomes dominant and that the time scale of side channel development is of the order of 70 years (Figures 2.4 and 2.5). This corresponds with a switch of a dominant side channel to a dominant main channel after 35 years (Appendix 2.B). This agrees with the order of 30 years that was observed from the aerial images. However, the observed aggradation in the east channel is much faster than the model predicts. For equal channel slopes, suspended sediment that is less affected by the transverse bed slope than bed load tends to force the shallowest channel to close (Figure 2.6C). When a sufficient amount of water discharge is diverted into the west channel, suspended bed-material load may be able to settle in the east channel, which accelerates the side channel development and this may explain the observed deposition in the downstream part of the east channel. The bend flow due to the bar that forms after 1993 might be an additional mechanism that diverts more sediment towards the east channel. The images show that the relative bend radius varies between 1 and 2.5, which means that the time scale varies between 5 and 40 years.

2.5 DISCUSSION

Our modelling study underlines the importance of a number of mechanisms affecting side channel development. The final stages of channel closure and its conversion to floodplain were not modelled. In this section, we give an overview of the closing mechanisms that were not considered, the limitations of our method, and finally the applicability of the results to designing of side channel systems.

2.5.1. CLOSING MECHANISMS

The four field cases show diverse behavior. The aerial images are taken during base flow conditions and show that in a few cases one of the channels is disconnected from the main channel under base flow conditions, but the model does not reproduce this. We expect that silting up of the channels mainly occurs with fine sediment as in meander cutoff channels (Citterio and Piégay, 2009; Constantine et al., 2010; Toonen et al., 2012; Dieras et al., 2013). Indeed, grain size measurements in the channels of the Wabash River clearly show that the bed of the closing channels consists of much finer sediment than the bed of the dominant channel (measurements from Zinger (2016) and USACE). If the closing channel conveys limited discharge, for example in case of a plug bar at the bifurcation, the connectivity at the confluence becomes important. When the discharge in the main channel varies, flow reversal can occur in the side channel and then new sediment is delivered to the closing channel through the confluence. This can increase the aggradation rate of such channels (Citterio and Piégay, 2009; Le Coz et al., 2010).

A second mechanism that may induce or enhance aggradation in the closing channel is vegetation. Vegetation encroachment and settling is a mechanism that can induce aggradation in the channel. Vegetation increases the hydraulic roughness, creates a zone characterized by a smaller flow velocity and traps sediment (Makaske et al., 2002; Rodrigues et al., 2006; Baptist et al., 2007; Van Oorschot et al., 2016). The growth of vegetation depends, for example, on the flow depth, bed level change and the flow velocity (Van Oorschot et al., 2016). The flow depth and flow velocity in the closing channel may be small enough for vegetation to settle. We expect that in the side channel near Mollon (Figure 2.7) vegetation affects morphodynamic change. In closing channels, conditions generally favor vegetation growth and therefore trapping of sediment.

2.5.2 LIMITATIONS OF THE NUMERICAL MODEL AND THE USE OF AERIAL IMAGES

There are many uncertainties in the use of the 1D numerical model. Some of the relevant mechanisms are not included or strongly simplified. 2D and 3D flow patterns that are important at the bifurcation are parameterized. Significant uncertainty follows from the nodal point relation that is a function of the transverse bed slope relation. Large differences can be found between transverse bed slope relations (Bolla Pittaluga et al., 2015; Baar et al., 2017) and this affects the stability of the bifurcation. A weaker transverse bed slope effect means that the side channel system is less stable and it is more difficult for the side channel to become dominant, because less sediment is diverted into the main channel (similarly to Figure 2.6C). The second source of transverse sediment flux is bend flow. The parameterization of bend flow assumes that spiral flow is fully developed and that flow separation does not occur. This implies that the effect of bend flow may be overestimated especially for small radii (Blanckaert and De Vriend, 2004). Other sources of uncertainties in our model are the bifurcation angle and the width adaptation parameterizations. Regardless of this, the model seem to be able to reproduce the development of side channel systems and previous studies show that the model is able to reproduce the bifurcation development reasonably well (Kleinhans et al., 2008; 2011; Gupta et al., 2014; Van Dijk et al., 2014; Bolla Pittaluga et al., 2015).

The use of aerial images in studying the development of side channels has some limitations. In the case of the Wabash River, measurements were available on the flow velocity and the water discharge partitioning, but for the other cases assumptions were made based on the river geometry and the observed morphodynamic change. In addition, the aerial images do not provide information on the discharge partitioning and the bed level variation. We therefore assume an initial water discharge partitioning and derive the initial bed level from this estimate. The aerial images are taken with irregular frequency which means that processes that occur on short time scales are not visible. In addition, there is no reason to assume that the last recorded image represents the equilibrium state of the side channel system. The 1D numerical model always approaches and reaches an equilibrium, but, for example, temporally variable boundary conditions and meander formation, which are not included in the numerical model, affect the stability and the development of the side channel system and likely lead to a dynamic equilibrium state.

2.5.3 APPLICATION POSSIBILITIES

Our stability diagrams provide a first insight on best practices for the design of a constructed side channel. As an example we consider a case where the required design is such that the main channel remains dominant and that slow side channel development is beneficial. This implies that it is preferable to design the side channel to be longer than the main channel, and preferably downstream of an outer bend or at the inside of a mild bend (Figure 2.4). This leads to the largest time scales of side channel development and the main channel remains dominant. This recommendation is unaffected by flow separation in the side channel or a large influence of suspended bed-material load. Flow separation in the main channel should be avoided, as it tends to form a dominant side channel (Figure 2.6A).

Generally, structures are placed in constructed side channels to control the discharge partitioning. The effect of structures is not included in the current 1D analysis and a better understanding of their influence on morphodynamic change is needed for a more accurate estimation of the time scale of side channel development.

Whether a maintenance-free side channel exists has yet to be determined. The numerical model suggests that a stable bifurcation exists in which the side channel remains open, but we did not account for floodplain-forming processes that may lead to full closure. Conceivably, side channels that gradually transform to floodplain could be ecologically valuable enough to outweigh the costs for maintenance.

2.6 CONCLUSIONS

Several mechanisms determine the equilibrium state of a side channel, development and characteristic time scale. Typically, the length of the side channel is an important parameter: a shorter side channel is more likely to become dominant and decreases the time scale of the side channel development. However, other mechanisms may outbalance or reduce the effect of a length difference. Bend flow increases the sediment load to one of the branches, the transverse bed slope can stabilize the side channel system, the flow separation zone decreases the water discharge to one of the branches and suspended load reduces the effect of the transverse bed slope. Bank erosion hardly affects the equilibrium state, but causes larger time scales of side channel development depending on bank erodibility.

The 1D numerical results reproduce the morphological development and time scale of four side channels observed in multitemporal imagery. Furthermore these cases demonstrate that the mechanisms are quite similar between sand-bed and gravel-bed rivers. Generalized results can therefore be used to assess the development and the corresponding time scale for various side channel designs.

ACKNOWLEDGEMENTS *This research is supported by the Netherlands Organisation for Scientific Research (NWO), which is partly funded by the Ministry of Economic affairs, under grant number P12-P14 (RiverCare Perspective Programme) project number 13516. This research has benefited from cooperation within the network of the Netherlands Centre for River studies. An anonymous reviewer and Bart Makaske are acknowledged for valuable comments that helped to improve the paper.*

APPENDIX

2.A EQUATIONS OF THE 1D NUMERICAL MODEL

Bolla Pittaluga et al. (2003) propose a mass balance over two computational cells upstream of the bifurcation:

$$Q_{s2} = Q_{s1}\frac{W_2}{W_2+W_3} + q_{sy}\alpha_W W_1 \tag{2.6}$$

where q_{sy} is the transverse sediment transport rate and $\alpha_W W_1$ is the distance upstream of the bifurcation over which the transverse sediment flux occurs. The factor α_W is assumed to vary between 2 and 3 based on physical and numerical experiments (Kleinhans et al., 2008; Bolla Pittaluga et al., 2015). The transverse sediment flux is computed by calculating a deflection angle of sediment in longitudinal direction:

$$q_{sy} = \tan\beta_s \frac{Q_{s1}}{W_1} \tag{2.7}$$

where β_s is the deflection angle of the sediment transport flux. This angle is given by (Koch and Flokstra, 1980):

$$\tan\beta_s = \frac{\sin\beta_\tau - \dfrac{1}{f(\theta)}\dfrac{\partial\eta}{\partial y}}{\cos\beta_\tau - \dfrac{1}{f(\theta)}\dfrac{\partial\eta}{\partial x}} \tag{2.8}$$

where β_τ is the angle between the direction of the bed shear stress and the streamwise direction, $\partial\eta/\partial y$ is the transverse bed slope, $\partial\eta/\partial x$ is the longitudinal bed slope and $f(\theta)$ is a ratio between the fluid drag and the gravity forces on a particle (Talmon et al., 1995):

$$f(\theta) = 9\left(\frac{D}{h_1}\right)^{0.3}\sqrt{\theta} \tag{2.9}$$

where D is the sediment diameter, θ is the Shields stress, and h_1 is the water depth in the upstream channel. The angle of the shear stress (β_τ) is given by the transverse velocity and the effect of the spiral flow due to a river bend (Struiksma et al., 1985):

$$\beta_\tau = \tan^{-1}\left(\frac{v}{u}\right) - \tan^{-1}\left(A\frac{W_{min}}{W_{max}}\frac{h_1}{R}\right) \tag{2.10}$$

where v and u are the depth-averaged transverse and longitudinal flow velocity respectively, A is the spiral flow intensity and R is the radius of curvature of the streamlines (Kleinhans et al., 2008). This radius is assumed to be similar to the radius of the centreline of the channel. In case of a large difference in channel width between the downstream channels, a smaller portion of sediment transport rate that is affected by the spiral flow, is transported over the interface between the two computational cells. Therefore, a damping factor (W_{min}/W_{max}) is added (Kleinhans et al., 2011), which is the ratio between the width of the downstream channels. The spiral flow intensity is given by (Struiksma et al., 1985):

$$A = \frac{2\varepsilon}{\kappa^2}\left(1 - \frac{\sqrt{g}}{\kappa C}\right) \tag{2.11}$$

where κ is the Von Kármán constant, C is the Chézy coefficient, and ε is a calibration coefficient ($\varepsilon \approx 1$). It is assumed that the spiral flow is fully developed, the bend is smooth, and the radius so large that flow separation does not occur. The depth-averaged transverse velocity (v) is derived from the transverse discharge (Q_y). This transverse discharge arises from the fact that the discharge partitioning over the bifurcates generally differs from the width ratio of the bifurcates (Bolla Pittaluga et al., 2003).

$$Q_y = \frac{1}{2}\left(Q_2 - Q_3 - Q_1 \frac{W_2 - W_3}{W_2 + W_3}\right) \tag{2.12}$$

The width adaptation is incorporated by assuming an empirical equilibrium width as a function of the water discharge (Kleinhans et al., 2011).

$$W_{eq} = \gamma Q^{\beta_W} \tag{2.13}$$

where W_{eq} is the equilibrium bank full width, γ is estimated based on the upstream channel, and $\beta_W \approx 0.5$ (van den Berg, 1995). The change of the width is given by (Miori et al., 2006; Kleinhans et al., 2011):

$$\frac{\partial W}{\partial t} = \frac{W_{eq} - W}{T_W} \tag{2.14}$$

where W is the actual channel width and T_W represents the time scale over which the width adjustment occurs. The time scale is given by (Kleinhans et al., 2011):

$$T_W = \alpha_{T_W} \frac{Wh}{q_{s,bank}} \tag{2.15}$$

where $q_{s,bank}$ is a fraction of the total streamwise sediment transport per unit width (q_s) that contributes to bank retreat or aggradation, α_{T_W} is a calibration parameter and Wh represents the volume of sediment per unit length of the channel. The sediment transport rate near the bank ($q_{s,bank}$) is assumed to be $q_{s,bank} = q_s h/W$ (Kleinhans et al., 2011). This is an initial estimate of the time scale, in which local characteristics of the banks are not taken into account. The eroded or deposited sediment from the banks is conserved by adding an additional source/sink term to the Exner conservation law

$$(1-p)\frac{\partial \eta}{\partial t} - \frac{\partial q_s}{\partial x} = \frac{\partial W}{\partial t}\frac{h}{W} \tag{2.16}$$

where p is the porosity of the bed sediment and η is the bed level.

2B REPRODUCTION OF THE SIDE CHANNEL CASES

In addition to the generalized side channel development, we reproduced the development of each field case separately with the one-dimensional model. The main input parameters are presented in Table 2.1. For each field case several scenarios were tested (Table 2.2).

Table 2.2 An overview of each scenario that is computed with the 1D numerical model. α_{T_W} is the calibration parameter of the width adaptation time scale (Equation 2.15), R/W is the bend radius divided by the channel width (Equation 2.10), and μ is the fraction of the sediment supply that is not affected by the transverse bed slope or bend flow.

Case	α_{T_W}	Parameter	Value	Parameter	Value	Parameter	Value
MolA	-						
MolB	1						
MolC	0.55						
MarA	-						
MarB	-	R/W	-3				
MarC	1	R/W	-3				
WabA	-						
WabB	1						
WabC	-	Bifurcation angle	60°				
WabD	1	Bifurcation angle	60°				
SacA	-	D_{50}	2 mm	Q_s	75,000 m³/yr		
SacB	1	D_{50}	2 mm	Q_s	75,000 m³/yr		
SacC	-	D_{50}	0.5 mm	Q_s	1,500,000 m³/yr	μ	1
SacD	1	D_{50}	0.5 mm	Q_s	1,500,000 m³/yr	μ	1

02

MOLLON, RIVER AIN (FRANCE)

We try to reproduce the development of the side channel system through assessing three scenarios (Table 2.2). The results are presented as a variation of the discharge partitioning ratio with time (Figure 2.11) in which the discharge in each channel is divided by the discharge at the upstream boundary of the model. The discharge in the west channel slowly increases and the discharge in the east channel decreases due to the length difference (Figure 2.11A). This corresponds with large degradation in the west channel and aggradation in the east channel. The model shows that after 15 years the discharge in the west channel is larger than in the east channel. This lasts longer than expected from the aerial images (Figure 2.7). When width adaptation is accounted for in the model (Figure 2.11B), the time scale of the side channel development increases, as the sediment that is eroded from the banks is a sediment source in the Exner conservation equation (Equation 2.16) reducing the amount of sediment picked up from the bed. The banks in the river Ain are unstable (Piégay et al., 2002) which suggests that the width adaptation time scale might be overestimated based on a simple first estimation (Equation 2.15). This time scale is therefore calibrated by changing α_{TW} to show a similar time scale as the aerial images (Figure 2.11C). The time scale of the side channel development in the 1D model is sensitive to the time scale of the width adaptation, but it does not affect the discharge partitioning at equilibrium. In each of the computations the closing channel remains open as expected from the 1D model. We expect that mechanisms that are not accounted for in the model lead to the filling up of the channel.

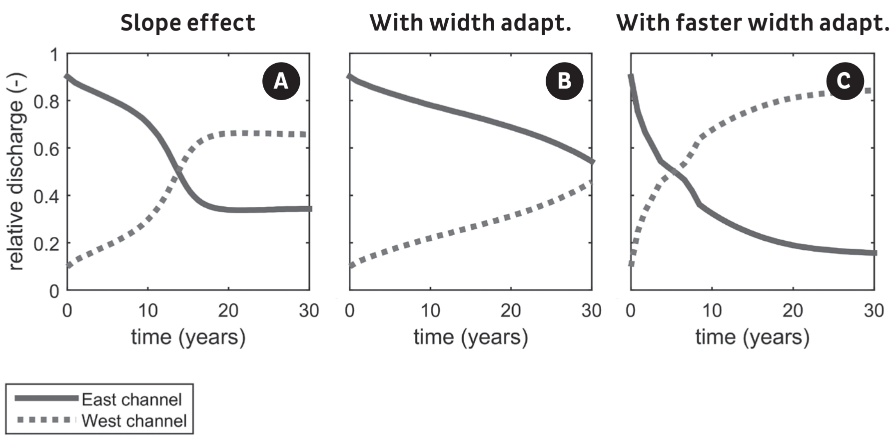

FIGURE 2.11 The temporal change of the discharge partitioning ratio in the two-channel system near Mollon according to the 1D numerical model due to **(A)** a length difference between the downstream channels, **(B)** a length difference between the downstream channels and adaptation of the channel width, **(C)** a length difference between the downstream channels and adaptation of the channel width with a small time scale (T_W).

MARTINAZ, RIVER AIN (FRANCE)

The length difference between the two channels is small, but seems sufficient to cause the west channel to aggrade and the east channel to degrade (Figure 2.12A). Bend flow (Figure 2.12B) increases the sediment load to the west channel. This results in a decrease in the time scale of the side channel development, as the difference between the delivered sediment load and the transport capacity is larger. In addition, the discharge asymmetry increases at the equilibrium state compared to the case without bend flow. Width adaptation allows the channel to widen and increases the discharge difference between the channels at the end of the computation (Figure 2.12C). The aerial images tell us that the west channel closes after 8 to 10 years (Figure 2.8). The model shows that the west channel does not close, but its discharge becomes small after 8 years. The model is unable to reproduce the closure of a channel, because there is a point where the transverse bed slope diverts sufficient sediment to the deeper channel to balance the transport capacity.

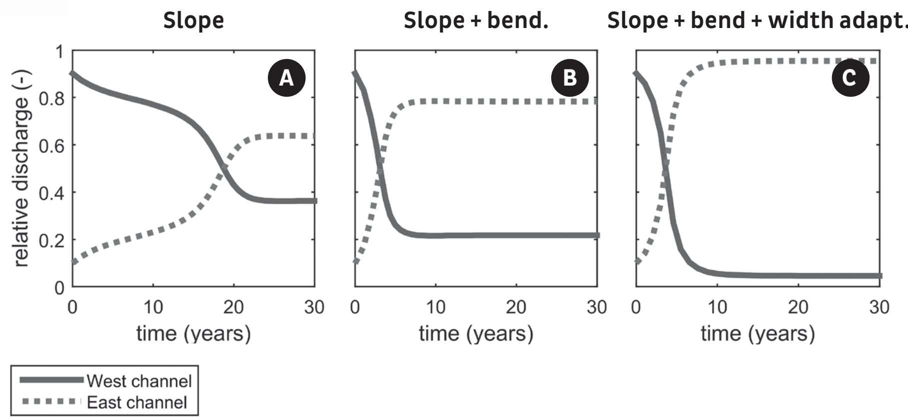

FIGURE 2.12 The temporal change of the discharge partitioning ratio in the two-channel system near Martinaz according to the 1D numerical model due to **(A)** a length difference between the downstream channels, **(B)** a length difference between the downstream channels and bend flow, **(C)** a length difference between the downstream channels, bend flow and adaptation of the channel width.

MACKEY BEND, WABASH RIVER (USA)

This case is simplified in the 1D model by only simulating the development of the first cutoff channel (Figure 2.13). The difference in length between the bend and the first cutoff channel shows the expected development of the side channel system (Figure 2.13A). Including the effect of flow separation due to the large bifurcation angle reduces the width at the entrance of the channel and therefore reduces the discharge in the channel (Figure 2.13C). Bank erosion due to the large bifurcation angle counteracts the effect of the flow separation zone (Figures 2.13B and D). This may imply that the effect of the bifurcation angle is limited if bank erosion occurs. This seems to be confirmed by the aerial images (Figure 2.9), which show that bank erosion reduces the bifurcation angle and therefore the size of the flow separation zone.

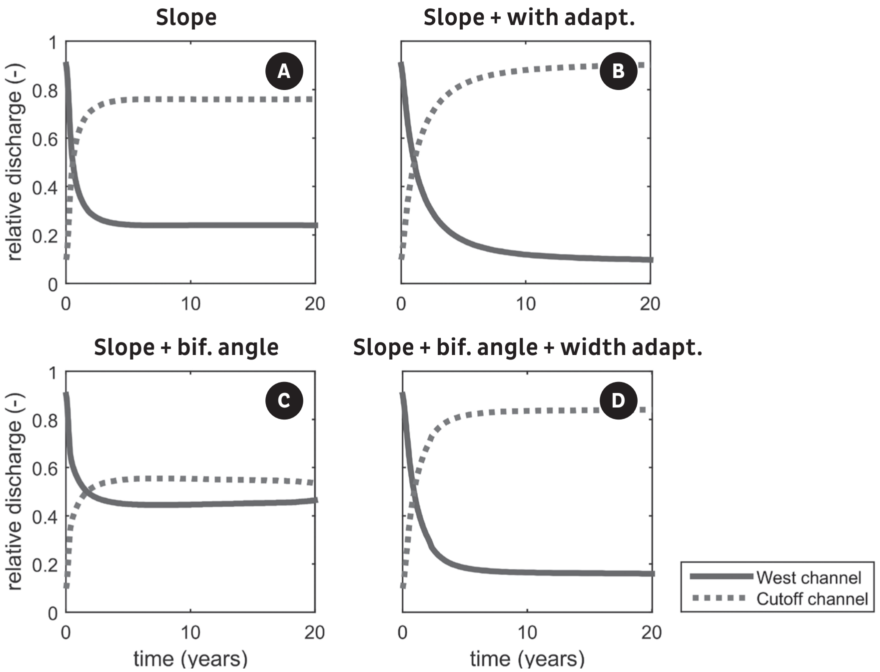

FIGURE 2.13 The temporal change of the discharge partitioning ratio in the two-channel system in the Mackey Bend according to the 1D numerical model due to **(A)** a length difference between the downstream channels, **(B)** a length difference between the downstream channels and adaptation of the channel width, **(C)** a length difference between the downstream channels and the bifurcation angle, **(D)** a length difference between the downstream channels, adaptation of the channel width and the bifurcation angle.

COLUSA, SACRAMENTO RIVER (USA)

We distinguish between bed load and suspended load to reproduce the development of the side channel system near Colusa. We assume the suspended load to be uniformly distributed over the cross-sectional area and therefore the sediment partitioning is only related to the discharge partitioning which corresponds with $k = 1$ in Equation 2.1 (Wang et al., 1995; Bolla Pittaluga et al., 2003). This assumption may underestimate the effect of secondary flow on the suspended load partitioning at the bifurcation, which due to vertical differences in sediment concentration may affect its partitioning. The scenarios with bed load (Figures 2.14A and B) show that the transverse bed slope steers part of the sediment away from the side channel, as the bed level of the side channels is initially higher, and that both branches remain open. In case of only suspended load

(Figures 2.14C and D), one of the branches fully closes as is expected from $k = 1$ (Wang et al., 1995). The case without width adaptation leads to the closure of the west channel, while when including width adaptation the west channel becomes dominant. For equal channel slopes, suspended load seems to tend to force the shallowest channel to close. The time scale of the scenarios with bed load is much larger than for suspended load due to the much smaller annual bed load of the river. The combination of bed load and width adaptation (Figure 2.14B) shows a similar time scale as in the natural case for the opening of the west channel, but the closing of the east channel in the model is much slower than in reality, which may be because suspended load is ignored. The scenarios with suspended load (Figures 2.14C and D) underestimate the time scale compared to reality. Based on the computations, it seems likely that bed load is dominant in the opening of the west channel and suspended load is dominant in the closing of the east channel.

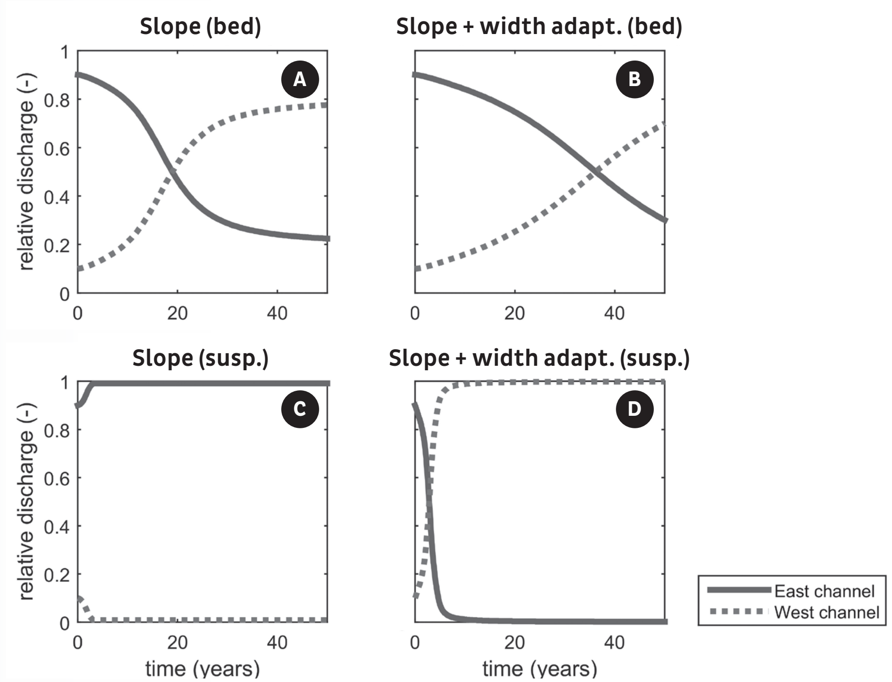

FIGURE 2.14 The temporal change of the discharge partitioning ratio in the two-channel system upstream of Colusa according to the 1D numerical model due to **(A)** a length difference between the downstream channels including only bed load **(B)** a length difference between the downstream channels including only bed load and adaptation of the channel width, **(C)** the development due to the length difference between the downstream channels including only suspended load, **(D)** a length difference between the downstream channels including only suspended load and adaptation of the channel width.

Photo: Bureau Beeldtaal Filmmakers

CHAPTER 3

Explaining artificial side channel dynamics using data analysis and model calculations

This chapter is published as Van Denderen, R.P., R.M.J. Schielen, S.G. Westerhof, . Quartel, and S.J.M.H. Hulscher, 2019: Explaining artificial side channel dynamics using data analysis and model calculations. *Geomorphology*, 327, 93–110, DOI:10.1016/j.geomorph.2018.10.016.

Side channel construction is a common intervention to increase both flood safety and the ecological value of the river. Three side channels of Gameren in the river Waal (The Netherlands) show amounts of large aggradation. We use bed level measurements and grain size samples to characterize the development of the side channels. We relate the bed level changes and the deposited sediment in the side channels to the results of hydrodynamic computations. Two of the three side channels filled mainly with suspended bed-material load. In one of these channels, the bed level increased enough that vegetation has grown and fine suspended load has settled. In the third side channel, the bed shear stresses are much smaller and, in addition to the suspended bed-material load, fine sediment settles. Based on the side channel system at Gameren, we identify two types of side channels: one type fills predominantly with suspended bed-material load from the main channel and a second type fills predominantly with fine suspended load. This gives an indication of the main mechanisms that lead to the aggradation in artificial side channel systems.

3.1 INTRODUCTION

Side channels are man-made or natural secondary channels that convey considerably less discharge compared to the main channel and are connected to the main channel at their upstream and downstream ends. In many regulated rivers, side channels disappeared due to human interventions (e.g., Hohensinner et al. (2014)) and currently, side channels are (re)constructed to, for example, increase the discharge capacity during peak flows (Simons et al., 2001; Nabet, 2014) or to restore the river to a more natural state (Schiemer et al., 1999; Formann et al., 2007; Riquier et al., 2015; Van Dyke, 2016). In side channels, which are constructed to increase the discharge capacity, aggradation is undesired. The aim of this paper is to get a better insight into the morphodynamic development of artificial side channels after construction.

Natural side channels can form in rivers, for example, as meander cutoffs or in anabranching rivers. Bed level changes in side channels are generally caused by a mismatch between the sediment supply and the transport capacity of the channel. In meander cutoffs, the downstream channels generally differ in length. This usually results in a steeper water surface gradient over the shorter channel leading to a relatively larger discharge conveyance and thereby transport capacity compared to the longer channel (Mendoza et al., 2016; Van Denderen et al., 2018a). The longer channel therefore starts to aggrade (Constantine et al., 2010; Dieras et al., 2013; Zinger et al., 2013; Van Denderen et al., 2018a). A plug bar can form if the transport capacity in the aggrading channel is much smaller than the supply (Constantine et al., 2010; Toonen et al., 2012; Kleinhans et al., 2013). Channels that receive a limited amount of bedload sediment due to, for example, a plug bar or a log jam are then slowly filled with finer sediment that is supplied to the channel during overbank flow conditions (Makaske et al., 2002; Constantine et al., 2010; Toonen et al., 2012). If the channel is still connected to the main channel at the downstream end, backflow can occur in the side channel leading to aggradation even during base flow conditions (Citterio and Piégay, 2009; Riquier et al., 2017). Channels without a blockage at the upstream entrance show deposition of coarse sediment that is spread over the channel until a certain bed level is reached after which fine sediment can be deposited (Makaske et al., 2002; Dieras et al., 2013).

The sediment supply to the downstream channels is a function of local flow patterns and bed slope effects at the bifurcation (Bulle, 1926; Bolla Pittaluga et al., 2003; Kleinhans et al., 2008; Kleinhans et al., 2013; Dutta et al., 2017; Van Denderen et al., 2018a). Large bifurcation angles and spiral flow at the bifurcation, due to the presence of an upstream river bend, can create a secondary flow over the cross section. This leads to near-bed flow velocities that direct more sediment towards the bifurcating channel or the channel in the inner bend (Bulle, 1926; Kleinhans et al., 2008; Kleinhans et al., 2012; Dutta et al., 2017). Bed slope effects at the bifurcation add a gravity component to the bedload transport direction that can divert sediment from a channel with a higher bed level towards a channel with a lower bed level (Bolla Pittaluga et al., 2003). Smaller particles go up a slope more easily than larger particles (Parker and Andrews, 1985) and this results a sediment supply that is finer to the channel with a higher bed level than the one with a lower bed level. Both the secondary flow and the bed slope mainly affect sediment transported as bedload and much less the sediment in suspension, and hence both processes can cause differences in grain size of the sediment supply to the downstream channels.

Artificial side channels, at least those in the Netherlands, are often limited in their discharge conveyance for their effect on the navigational function of the river (Simons et al., 2001). A large discharge withdrawal from the main channel can cause side currents and aggradation in the main channel, and might therefore hinder the navigational function of the main channel. For that reason, the discharge withdrawal from the main channel is in the Netherlands limited to 3–5% of the total discharge during bankfull flow conditions (Akkerman, 1993; Mosselman, 2001; Jans, 2004). This is achieved by constructing weirs or culverts (Simons et al., 2001) that likely affect the sediment supply and transport capacity of the side channels. In addition, the Dutch side channels are often constructed in between groynes that affect the flow field at the bifurcation and confluence. In general, the bed level in between groynes varies as a function of an import of sediment during peak flows (Yossef, 2005) and an export of sediment by navigation-induced currents (Ten Brinke et al., 2004). The sediment that is brought into suspension due to these currents might be supplied to the side channel. The large bed level gradient that occurs between the main channel and the groyne field likely reduces the sediment supply towards the side channel. These structures complicate the sediment dynamics at the bifurcation and confluence of the side channel system.

Most of the artificial side channels in the Netherlands show aggradation. It is unknown how fast and with which type of sediment these side channels aggrade. Maintenance efforts are therefore difficult to plan. The objective of this paper is to observe and explain the characteristics of the deposited sediment and the physical processes behind the bed level changes of a side channel system at Gameren in the river Waal. We first give an overview of the hydrodynamic and morphodynamic characteristics of the river Waal and the side channel system of Gameren (Section 3.2). We measured the bed level and collected grain size samples in the three channels (Section 3.3) to study the aggradation rate and the type of sediment that is deposited inside the three side channels. In addition, we set up a hydrodynamic model of the side channel system at Gameren to estimate the bed shear stresses in the side channels. We relate the bed level changes and the grain sizes in the side channels to the results of a hydrodynamic model (Section 3.4). We use these three channels to characterize the development of side channels (Section 3.5).

3.2 DESCRIPTION OF THE SIDE CHANNEL SYSTEM

More than 20 side channels have been constructed in the Dutch Rhine branches to reduce the water levels during peak flow and to increase the ecological value of the river (Simons et al., 2001; Baptist and Mosselman, 2002). One of these side channel systems is located near Gameren in the floodplain of the river Waal. A system of three side channels was constructed between 1996 and 1999 (Figure 3.1). The side channels were constructed to compensate for a dike relocation that reduced floodplain width. The East and the West channel were dug in 1996 and the Large channel was created in 1999. Since their construction, the side channels have been aggrading.

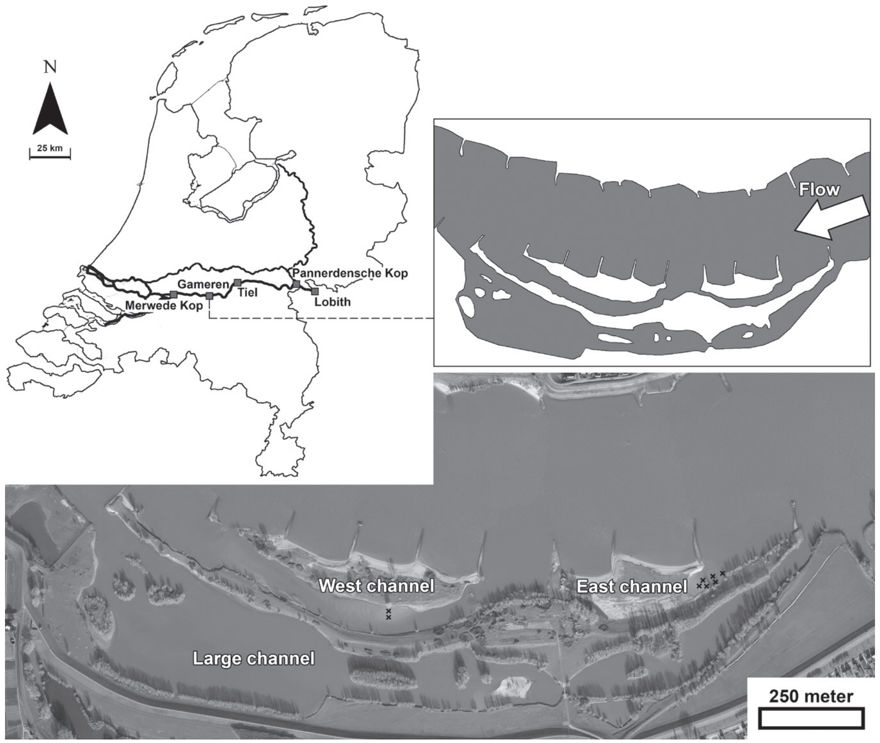

FIGURE 3.1 Aerial images of Gameren in the floodplain of the river Waal in the Netherlands (51° 48' 22.4" N 5° 12' 23.8" E) with the three side channels and the main channel (After images of Rijkswaterstaat). The black crosses in the aerial image denote the location of the sediment cores (Figure 3.14).

3.2.1 CHARACTERISTICS OF THE RIVER WAAL

The river Waal is one of the Rhine branches and flows from the Pannerdensche Kop to the Merwede Kop (Figure 3.1). The average annual discharge is about 1500 m^3/s, floodplains start to become inundated at 2900 m^3/s and the 10-yr flood (a peak discharge of an annual 0.1 probability) is about 6100 m^3/s (Hegnauer et al., 2014). The yearly average sediment transport in the river Waal is about 200,000 m^3/yr for sand (0.063 – 2 mm) and about 550,000 m^3/yr for fine sediment (< 0.063 mm) (Frings et al., 2015). Discharge measurements at Tiel in the river Waal show that in the first eight years after the construction of the first two channels (1996) two 10-yr floods occurred (Figure 3.2). After 2003, peak flows larger than 5300 m^3/s (5-yr flood) are much less frequent.

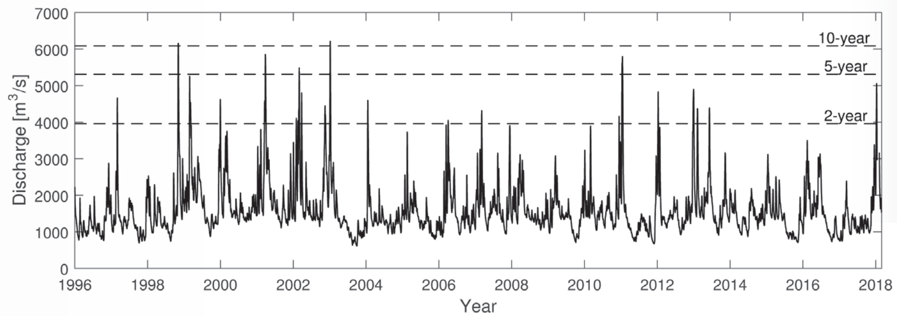

FIGURE 3.2 The discharge at Tiel between 1996 and 2018 with the discharge levels for three return periods of flood levels (*Hegnauer et al., 2014*).

The morphological conditions vary over the river Waal. The bed level in the river Waal decreases on average between 1 and 2 cm each year due to a shortage of the sediment supply from upstream (Sieben, 2009). The D_{50} in the top layer of the bed in the main channel of the river Waal decreases from 2.46 mm just downstream of the Pannerdensche Kop (river kilometer (rkm) 858) to 0.5 mm just upstream of the Merwede Kop (rkm 952) (Figure 3.3). In between the Pannerdensche Kop and the Merwede Kop, the D_{50} of the bed material decreases on average by about 0.8% per kilometer (Ten Brinke, 1997; Frings, 2007), but the variation over the width and length of the river is large (Figure 3.3B). At Gameren (rkm 936–939) the average D_{50} of the bed material in the main channel is 0.75 mm (Ten Brinke, 1997). The grain size of the suspended bed-material load was measured during peak flows in 1998 for the Pannerdensche Kop and in 2004 for the Merwede Kop (Figure 3.3). The width averaged sieve curve was averaged over samples from 0.2 m, 0.5 m and 1 m above the river bed and the samples were collected using a mesh size of 50 µm (Frings, 2007; Frings and Kleinhans, 2008). These samples therefore mainly consisted of suspended bed-material load. While the D_{50} of the bed material decreases over the length of the river, the grain size of the suspended bed-material load seems to be similar over the length of the river Waal.

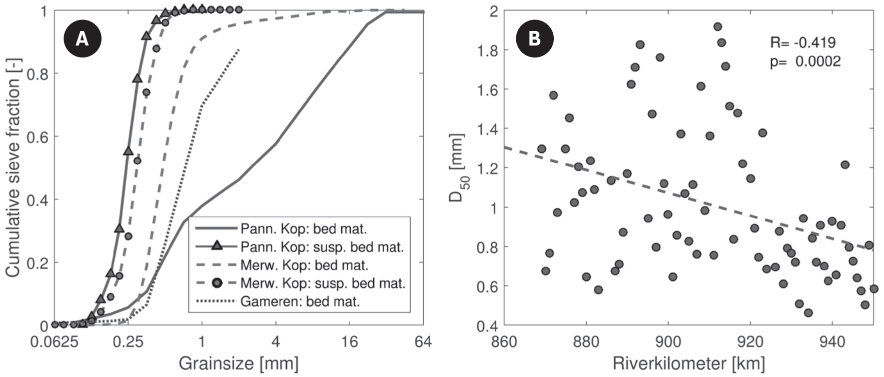

FIGURE 3.3 The variation of the grain size over the length of the river Waal. **(A)** The average sieve curve of the sediment at the top of the active layer of the bed and the suspended bed material during peak flows. The peak discharge in the river Waal for the measurements at the Pannerdensche Kop and the Merwede Kop are 6173 m³/s and 4527 m³/s, respectively (Frings and Kleinhans, 2008). The bed material in the main channel at Gameren is averaged over the river axis (rkm 936–939) and was collected in 1995/1996 (Ten Brinke, 1997). **(B)** The D_{50} in the top layer of the bed on the center line of the river Waal measured in 1995/1996 (Ten Brinke, 1997). The correlation parameters (*R* and *p*) are based on the Spearman's rank correlation.

During peak flows, sediment is deposited on the banks and in the floodplain of the river Waal (Sorber, 1997; Middelkoop and Asselman, 1998; Ten Brinke et al., 1998). Measurements during peak flows in 1993 and 1995 show that on average sand is deposited in the first 50–100 m of the floodplain (Middelkoop and Asselman, 1998). In the floodplain at Gameren, the peak flow of 1995 resulted in a bed level increase in the floodplain of up to 7 cm where the West and East channel currently are located (Sorber, 1997). The mean grain size of the deposited material was estimated to be ~0.3 mm (Sorber, 1997; Ten Brinke et al., 1998). This corresponds with the suspended bed-material load (Figure 3.3) (Frings and Kleinhans, 2008). Farther away from the main channel, the deposited sediment in the floodplain mainly consisted of silty clay and during the peak flow in 1993 the average deposition of overbank fines ranged between 0.5 and 1.5 mm (Middelkoop and Asselman, 1998).

Several other interventions were carried out in the river Waal to reduce the risk of flooding. One of these interventions was to reduce the groyne height in the main channel. A lower groyne height leads to less friction in the main channel and therefore increases its discharge capacity. In the upper part of the river Waal (rkm 887–915), the groyne height reduction resulted in a bed level increase in the main channel of about 5 cm between 2009 and 2012 (Klop, 2015). Within the groyne fields slight degradation occurred, but this was based on limited data (Klop and Dongen, 2015). In the lower part of the river Waal (rkm 915–953), the groyne height reduction was executed between 2013 and 2014, but the morphodynamic effect has not yet been analyzed. The groyne height reduction likely reduced the bed level between the groynes at Gameren and therefore affected the bed level in the side channels because the bifurcations and confluences of the side channels at Gameren are in the groyne fields.

3.2.2 THE SIDE CHANNELS AT GAMEREN

The side channels at Gameren were constructed to compensate for the water level increase due to a reduction of the floodplain width. The ecological objectives are secondary and are beyond the scope of this paper. The two small side channels were constructed in 1996 and are referred to as the *West* and *East* channel (Figure 3.1). The *Large* channel was finished in 1999 and connects an old clay mining pit with the main channel. The discharge capacity in the West and East channel is limited by weirs at their entrance, and in the Large channel a bridge acts as a culvert that limits the discharge capacity. The bed level and the weir of the East channel were designed such that the channel conveys discharge on average 100 d/yr corresponding to 2200 m³/s in the river Waal. The weir and bed level of the West channel were constructed lower such that the channel conveys discharge on average 265 d/yr corresponding to 1500 m³/s in the river Waal. The Large channel is connected with the main channel permanently. After the construction of the channels, their morphodynamic development caused the discharge conveyance and the connectivity of the side channels to change. For example, because bank erosion at the entrance of the West and the East channel, the flow is currently able to flow around the weir that was supposed to control the discharge conveyance in the channels. Between 2000 and 2002 several flow velocity measurements were carried out using an Acoustic Doppler Current Profiler (ADCP) (Jans, 2004) and from these measurements the discharge in each channel was computed (Figure 3.4). Both the discharge in the West channel and the East channel seem to increase linearly with increasing discharge in the main channel. In the Large channel the trend changes for discharges larger than 3300 m³/s, because for these discharges the water can flow around and over the bridge increasing the discharge capacity of the channel. The measurements show that during bankfull discharge conditions in the river Waal, the combined discharge in the three channels is about 5% of the total discharge in the main channel.

The floodplain near Gameren is covered with a clay and sandy clay layer that reaches 6–10 m below the average bed level (Data and Information of the Dutch subsoil: https://www.dinoloket.nl). The bed of the three channels was therefore initially covered with clay and sandy-clay. Below these layers, gravel and coarse sand can be found. Until 1996, a brick factory was present in the floodplain that created a large clay pit that currently is located at the downstream end of the Large channel. It was expected that this pit would slowly fill with sediment, but this was too slow for the ecological purpose of the channel and therefore sediment was dumped in the pit in 2009 (about 500,000 m³). A small channel was

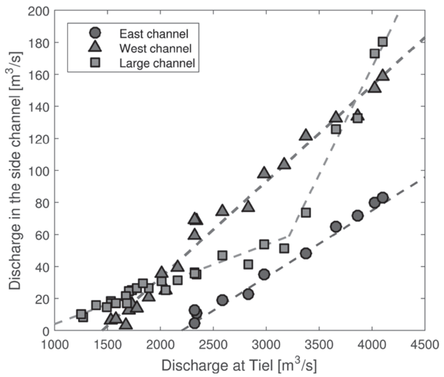

FIGURE 3.4 The conveyance of the three side channels, measured using an ADCP between 2000 and 2002, as a function of the discharge in the main channel of the river Waal at Tiel (Jans, 2004). The dashed lines are based on a linear least square fit of the measuring points. Two lines are fitted for the Large channel one for Q_{Tiel}<3500 m³/s and one for Q_{Tiel}>3500 m³/s.

dredged from the downstream end of the Large channel to dump this sediment. Other human interventions in the system are limited to the protection of groynes, which due to bank erosion in the side channel were bypassed, the application of bank protection just downstream of the bridge in the Large channel, and the maintenance of vegetation.

Bank erosion in the side channels has been, on average, very limited. The banks mainly consist of cohesive material and therefore the bank erosion primarily occurred at locations with large flow velocities. These locations are the surrounding banks of the weirs in the West and East channels, and just downstream of the bridge in the Large channel. In addition, at the downstream end of the West channel the bank has retreated up to 40 m (Figure 3.5). This region is not protected by groynes or floodplain and the bank retreat was therefore likely caused by the attack of waves from ships.

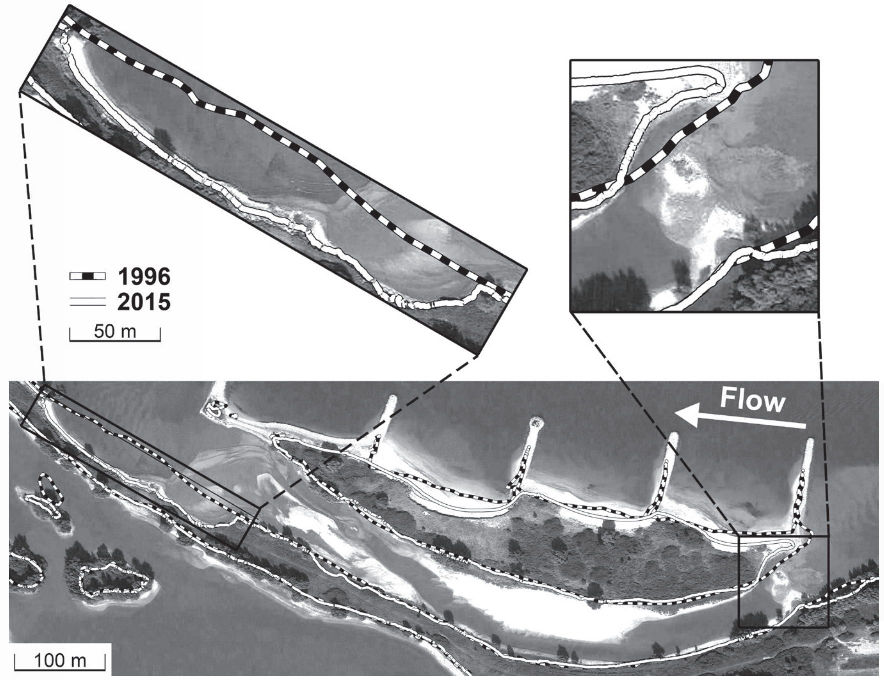

FIGURE 3.5 Bank erosion at the bifurcation and the confluence of the West channel. The blocked and open lines show the location where the bed level is 3m +NAP (Amsterdam Ordnance Datum) in 1996 and in 2015, respectively the background image is from 2016 *(Google Earth)*.

3.3 METHODS

Fourteen bed level measuring campaigns were carried out and sediment samples were collected from the three side channels in April 2017 and from the East channel in March 2018. We estimated the hydrodynamic conditions in the side channels using a hydrodynamic model.

3.3.1 BED LEVEL MEASUREMENTS

The bed level measurements vary in coverage and measuring method (Table 3.1). A dGPS (accuracy: 5 cm) was used to measure the bed level above the water level surface and the shallow areas. The Large channel and deeper areas of the West channel were measured using a single-beam echo sounder (accuracy: 10 – 15 cm). From 2003, regular LIDAR measurements (5 – 10 points per m^2, accuracy: 5 cm) were carried out. These do not penetrate the water column and therefore only the bed level in the East channel was retrieved from these measurements. Most of these measurements were carried out during base flow conditions. In 2018, multi-beam measurements (accuracy: 5 cm) were carried out during a peak flow (5050 m^3/s). The largest bed level changes are expected to occur during peak flow and therefore the measured aggradation rate depends on the moment of measurement.

Table 3.1 A list of the available bed level data for the side channels at Gameren with the measuring technique and the data coverage.

Date			Technique	Coverage
	December	1996	dGPS and single-beam echo sounder	East and West Channel
	December	1999	dGPS and single-beam echo sounder	Full area
	November	2000	dGPS and single-beam echo sounder	Full area
	December	2001	dGPS and single-beam echo sounder	East and Large Channel
	November	2002	dGPS and single-beam echo sounder	Full area
2	September	2003	LIDAR	East Channel
29	February	2008	LIDAR	East Channel
	October	2009	LIDAR and single-beam echo sounder	east and large channel
17	October	2010	LIDAR	East Channel
	March	2011	LIDAR	East Channel
24	August	2012	LIDAR	East Channel
8	September	2013	LIDAR	East Channel
25	June	2014	LIDAR	East Channel
15	February	2015	LIDAR	East Channel
31	January	2018	Multi-beam echo sounder	Full area, excl. upstream Large Channel

3.3.2 GRAIN SIZE SAMPLES

The grain size in the side channels is expected to vary over the length and width of the channels, and to vary in time as a function of the hydrodynamic conditions. In addition, we expect that the weir at the entrance of East and West channel reduces the sediment supply to the side channel. We took sediment samples in each channel along several cross sections and in the groyne fields at the bifurcations and confluences (Figure 3.12). In addition, we took three sediment cores upstream and three sediment cores downstream of the weir in the East channel (Figure 3.1). These cores show the effect of the weir on the grain size that enters the side channel. It was not possible to take similar samples around the weir of the West channel because of armoring in front of the weir and large scour behind the weir. However, we took two sediment cores from the point bar in the West channel to study the variation of the grain size of the deposited sediment through the channel in time (Figure 3.1).

We collected 86 sediment samples in the three side channels in April and May 2017. This was after a period of 10 months without discharges larger than 1800 m^3/s in the river Waal, suggesting a relatively calm period from morphological point of view. Large areas of the East and West channels were above the water level and in these areas, we collected the top layer of the bed with an auger. For the areas below the water level we used a Van Veen Grab sampler. After the peak flow of January 2018, we took 11 additional samples with an auger in the East channel to have an indication of the effect of peak flows on sediment deposition in the East channel. We used a dGPS to record the location of the samples and, where the water depth was less than 1 m, we also recorded the bed level.

We computed the grain size characteristics by sieving the sediment samples. We first wet sieved the samples to extract the fraction <0.063 mm and the remaining material we dry sieved. The dry sieving was carried out using mesh sizes: 63, 90, 125, 150, 212, 250, 300, 500, 600, 1000, 1400 and 2000 µm. Based on the sieve results, we computed the characteristic grain sizes (D_{10}, D_{50}, D_{90}), and the silt, sand and gravel fractions. Based on these measurements, we can determine what type of sediment is deposited in the side channels and relate this to how the deposited sediment is transported in the main channel, i.e., as suspended load, as suspended bed-material load or as bedload.

3.3.3 HYDRODYNAMIC MODEL

Hydrodynamic computations were carried out using a two-dimensional depth-averaged version of the Delft3D Flexible Mesh software (Kernkamp et al., 2011). The model computes the flow velocities and the water level in the river for a given bed level, bed roughness, upstream discharge and downstream water level. The model is created based on two GIS databases of the Rhine branches that are provided by Rijkswaterstaat (Becker et al., 2014). One describes the situation in 1995 without the side channels at Gameren and one describes the situation in 2017 in which the side channels are present. From these databases we extracted the bed level and the floodplain roughness. The main channel roughness is based on a calibration of water level measurements in the main channel. We calibrated the model for three discharge levels that occurred in 1994 and 1995 such that the model gives a good estimation of the hydrodynamic conditions in the river for a range of discharge levels (Appendix 3.A).

We used the model results to calculate the discharge conveyance of the side channels, the streamlines in the floodplain and the bed shear stress in the side channels as a function of the discharge in the main channel. We apply the model to three different states of the side channels: (1) representing 1996, (2) representing 1999 and (3) representing 2017. This corresponds with the initial state of the West and East channel (1996), the initial state of the Large channel (1999), and the state during the recent grain size measurements (2017). The 1996 and the 1999 model are based on the GIS database of 1995 with the measured bed level (Section 3.3.1) of the side channels in 1996 and 1999, respectively. The 2017 model is based on a GIS database of 2017. We computed the hydrodynamic conditions for twelve discharges ranging from 500 m^3/s to 7000 m^3/s using steady state boundary conditions. These discharge conditions range from base flow up to peak flow conditions.

We compare the computed discharge in the side channels with the measured discharge (Figure 3.6). The discharge was measured between 2000 and 2002. The model result that is closest to these years is 1999, and we compute the error based on the 1999 results. Due to the difference in years between the measurements and the model, the error is related to the aggradation rate in the channels. This results in an overestimation of the discharge by the 1999 model. The discharge measurements in the Large channel show a change in trend due to the presence of the bridge in the channel (Figure 3.4). This change in trend is not well captured by the model and this is likely caused by an incorrect representation of the culvert in the model resulting in an overestimation of the discharge between 2000 m^3/s and 4000 m^3/s. For larger discharges, the flow in the floodplain becomes more important and the effect of the bridge is smaller.

3.3.4 RELATION BETWEEN THE MEASUREMENTS AND THE MODEL RESULTS

To better understand the morphodynamic development of the side channels, we relate the bed level measurements, the grain size measurements and hydrodynamic model results. The bed level measurements vary in coverage, but the center line of the East and West channel, and the thalweg of the Large channel is for most dates available. We therefore use the measured average bed level height of these longitudinal profiles and combine these with the measured grain sizes and the computed hydrodynamic conditions in the channels. We focus on the East

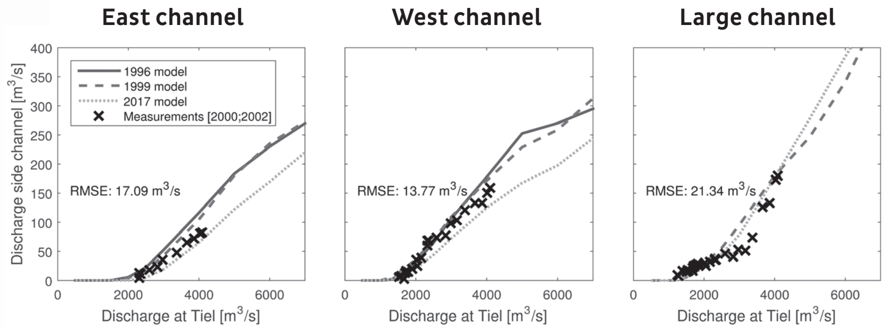

FIGURE 3.6 A comparison of the discharge at the entrance of the three side channels from the three models and the measurements between 2000 and 2002 (Figure 3.4). The root-mean-squared error (RMSE) is computed using the measurements and the 1999 model results.

channel, because the data of the West and Large channel is limited. The results of the other two channels are shown in the supplementary material. We compute the correlation using the Spearman's rank correlation that, in contrast to the Pearson's correlation, does not assume a linear relation between the parameters. The correlation results in a correlation coefficient (R) and a p-value for which we assume that $p < 0.01$ is sufficient to assume a correlation between the parameters. This corresponds with a false-positive probability of about 11% (Goodman, 2001; Nuzzo, 2014). In addition, we use a linear relation to show the trend of the correlation, but we immediately note that we have insufficient data to suggest any empirical relation.

3.4 RESULTS AND INTERPRETATION

In this section we present the bed level and grain size measurements. Next, we give an overview of the hydrodynamic results and we relate these with our measurements.

3.4.1 BED LEVEL CHANGES

EAST CHANNEL

The bed level in the East channel increased quickly after its construction in 1996 (Figure 3.7). This increase in bed level was mainly caused by an aggradation front that migrated through the East channel (Figure 3.8). Such an aggradation front is a bed wave that forms and migrates downstream due to a large difference between the sediment supply and the transport capacity of the channel (De Vries, 1971; Jansen et al., 1979). The point density of the bed level measurement in 2002 is too small to capture the front correctly. In 1999, the aggradation front had passed almost fully through the East channel and the bed level changes after 1999 were therefore much smaller. Apart from the aggradation front, the bed level continued to increase, but more slowly. The aggradation mainly occurred in the central part of the channel starting in the inner bend (Figure 3.7). The downstream end of the side channel was initially higher compared to the rest of the channel and showed the least aggradation. The bed level measurements of 2018 were carried out during peak flow. The flow velocities during this peak flow were sufficiently high such that small dunes (height ≈ 0.2 m; length ≈ 10 m) formed at the entrance of the East channel (Figure 3.7). This indicates that during peak flows the flow velocities are large and significant bedload transport occurs (Jansen et al., 1979).

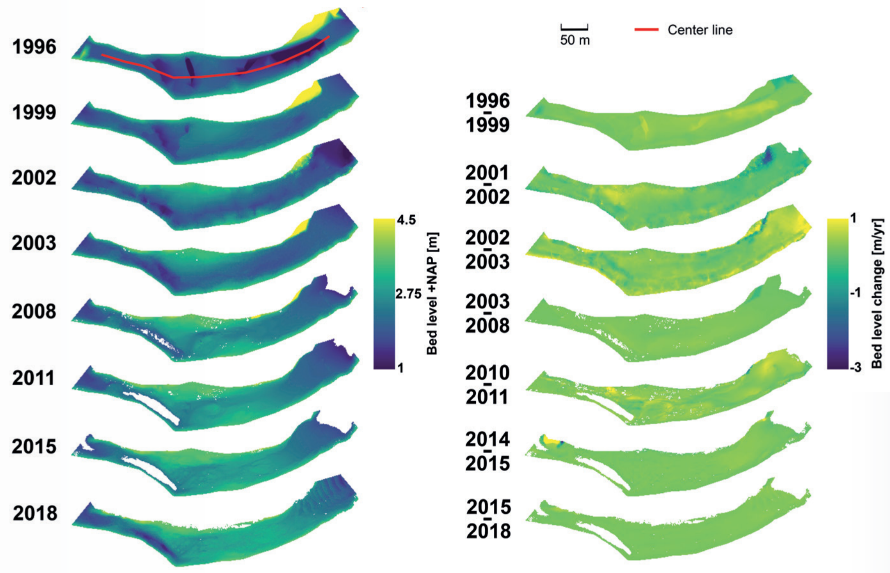

FIGURE 3.7 **Left:** The bed level of the East channel relative to NAP (Amsterdam Ordnance Datum) for several years. **Right:** The average bed level change per year between two measurements.

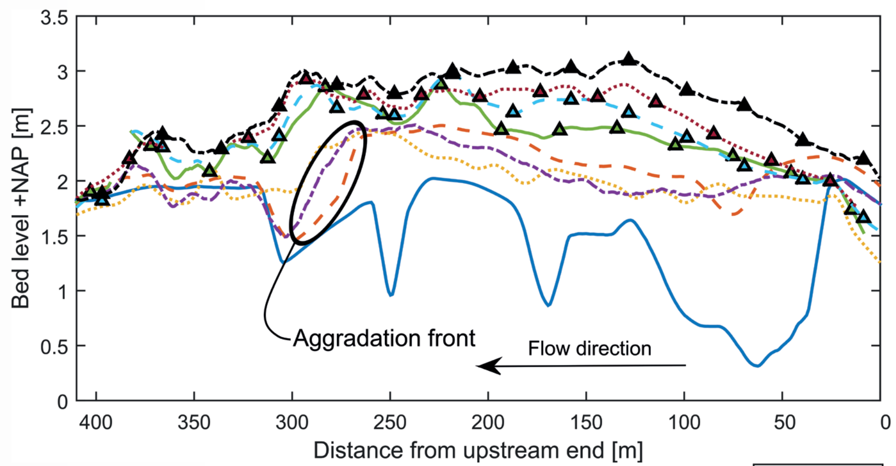

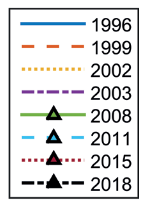

FIGURE 3.8 The change in bed level height on the center line of the East channel (Figure 3.7) filtered with a moving average over 10 m.

WEST CHANNEL

The West channel aggraded initially mainly in the inner bend where a point bar formed and just downstream of the outer bend where another bar formed (Figure 3.9). Initially large flow velocities at the entrance of the channel caused a large amount of scour just downstream of the weir and bank erosion that allowed the flow to circumvent the weir. The initial bed level change is large (up to 1 m/yr in the inner bend), but after 1999, the bed level changes were much smaller (Figure 3.10). The initial aggradation front is not visible in the measurements, but possibly went through the channel between 1996 and 1999. After 2002, the aggradation rate is small, but the bed level continues to increase.

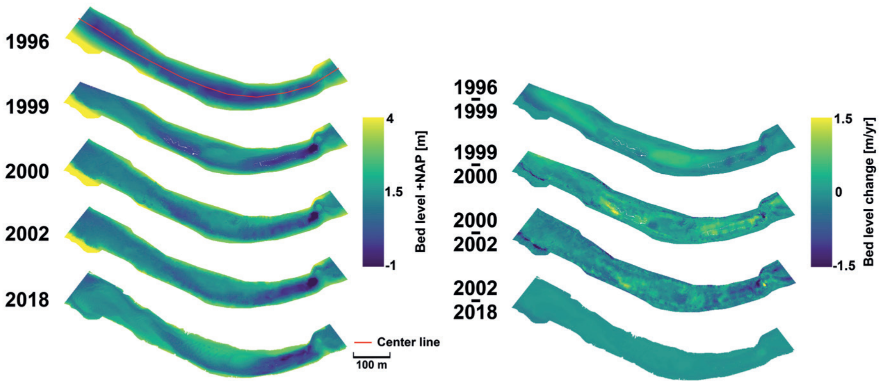

FIGURE 3.9 **Left:** The bed level of the West channel relative to NAP (Amsterdam Ordnance Datum) for several years. **Right:** The average bed level change per year between two measurements.

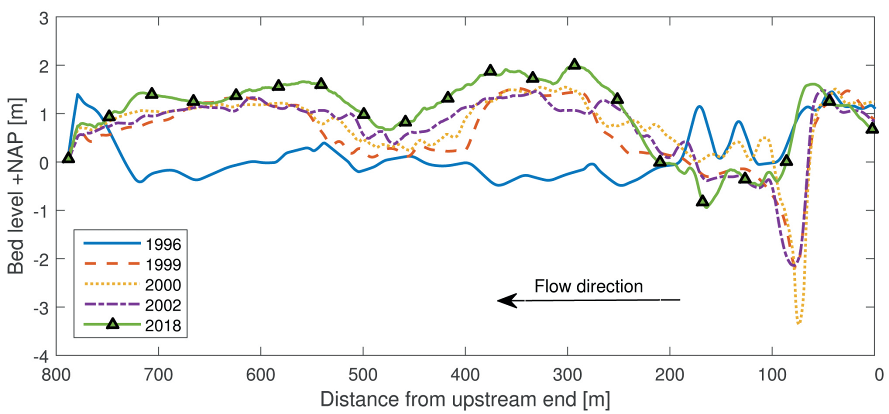

FIGURE 3.10 The change in bed level height on the center line of the West channel (Figure 3.9) filtered with a moving average over 10 m.

LARGE CHANNEL

The Large channel was constructed in 1999 and includes a large clay mining pit (Figure 3.11). The bed level in this pit goes down to -16 m +NAP (Amsterdam Ordnance Datum), while the bed level in the rest of the channel varies between -2 and +2 m +NAP. At the entrance of the channel the flow velocities are high, but the scour is limited due to the clay layer. The bridge limits the discharge through the Large channel and thereby creates a backwater effect in the upstream part of the channel that reduces the flow velocity. This resulted in aggradation in the upstream part of the Large channel. Below and downstream of the bridge large flow velocities occur due to the small channel width below the bridge. The bed below the bridge is protected and this leads to a large sediment transport capacity, but a limited sediment transport. This leads to large scour just downstream of the bridge (-10 m +NAP). Due to the widening of the channel, the flow quickly decelerates and the sediment that was eroded from the scour hole formed a small island. The bed level of 2009 shows that the mining pit was filled with sediment and to deliver this sediment to the side channel a small channel was dredged. It is likely that the sediment samples that were collected in the downstream part of the Large channel were affected by this intervention. The measurements of 2018 show that the dredged channel was partly refilled with sediment and the bed level in the mining pit has continued to increase. In the downstream part of the Large channel between the islands, the aggradation is limited between 2001 and 2009. This is a result of low flow velocities and a limited sediment supply, because most of the sediment was deposited in the mining pit.

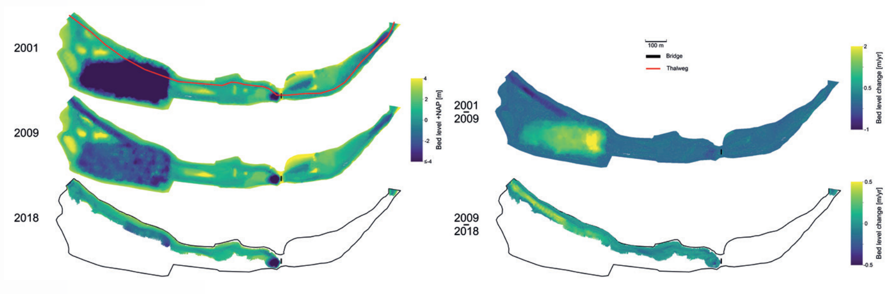

FIGURE 3.11 **Left:** The bed level of the Large channel relative to NAP (Amsterdam Ordnance Datum) for several years. The dark blue areas are lower than -4 m and down to -16 m. **Right:** The average bed level change per year between two measurements.

3.4.2 GRAIN SIZES IN THE TOP LAYER

We measured the grain size in the three side channels and first only present the samples collected in 2017 (Table 3.2). The average D_{10} in the Large channel is slightly overestimated, because the samples in which the silt/clay fraction is larger than 10% are not included here. The percentage of silt in the Large channel is much larger than in the other channels. The variation in grain size is also largest in the Large channel and this seems to be caused by the variation in width and the bridge that cause large gradients in the bed shear stress.

Table 3.2 An overview of the characteristic grain sizes for each channel including their groyne fields. The mean value (μ) and the standard deviation (σ) are based on a normal distribution with the number of samples (N).

	D_{10} [mm] $\mu\pm\sigma$ (N)	D_{50} [mm] $\mu\pm\sigma$ (N)	D_{90} [mm] $\mu\pm\sigma$ (N)	Silt frac. [%] $\mu\pm\sigma^1$ (N)	Sand frac. [%] $\mu\pm\sigma^1$ (N)	Gravel frac. [%] $\mu\pm\sigma^1$ (N)
West	0.19 ± 0.05 (27)	0.31 ± 0.08 (30)	0.52 ± 0.2 (28)	2.7 ± 5 (31)	94 ± 11 (31)	3.5 ± 10 (31)
East	0.14 ± 0.03 (16)	0.22 ± 0.05 (20)	0.38 ± 0.08 (19)	5.0 ± 7 (20)	94 ± 7 (20)	0.96 ± 3 (20)
Large	0.16 ± 0.07 (16)	0.21 ± 0.1 (30)	0.57 ± 0.3 (31)	17 ± 17 (33)	78 ± 18 (33)	4.2 ± 10 (33)

1 The mean and standard deviation are based on a normal distribution which does not fit the distribution of the silt, sand and gravel fraction since these fractions cannot be negative or larger than one. However, this distribution is used to clearly show the difference in variation between the channels.

Both the West and the East channels are mainly filled with sand. The sand that is deposited in the East and West channels is only in a small fraction present on the bed of the main channel. The D_{50} in the East and West channel is similar to the suspended bed-material load at the Pannerdensche Kop and the Merwede Kop during peak flows (Figures 3.1 and 3.3). Apparently, the suspended bed-material load in the main channel enters the side channels and is transported inside the channels as bedload. The sand deposited in the Large channel also corresponds with the suspended bed-material load in the main channel, but here also a large fraction of silt is found that in the main channel is transported as suspended load.

In the East channel, additional samples were collected of the sediment that was deposited during the peak flow in 2018 (5050 m³/s). A sand layer was deposited on top of the loamy sand layer that was found in 2017 (Figure 3.13). The deposited sediment is unimodal and comparable with the sand size previously found in the East channel. However, the silt fraction is much smaller and it seems likely that silt was deposited during the long period of low discharge before the 2017 measurement.

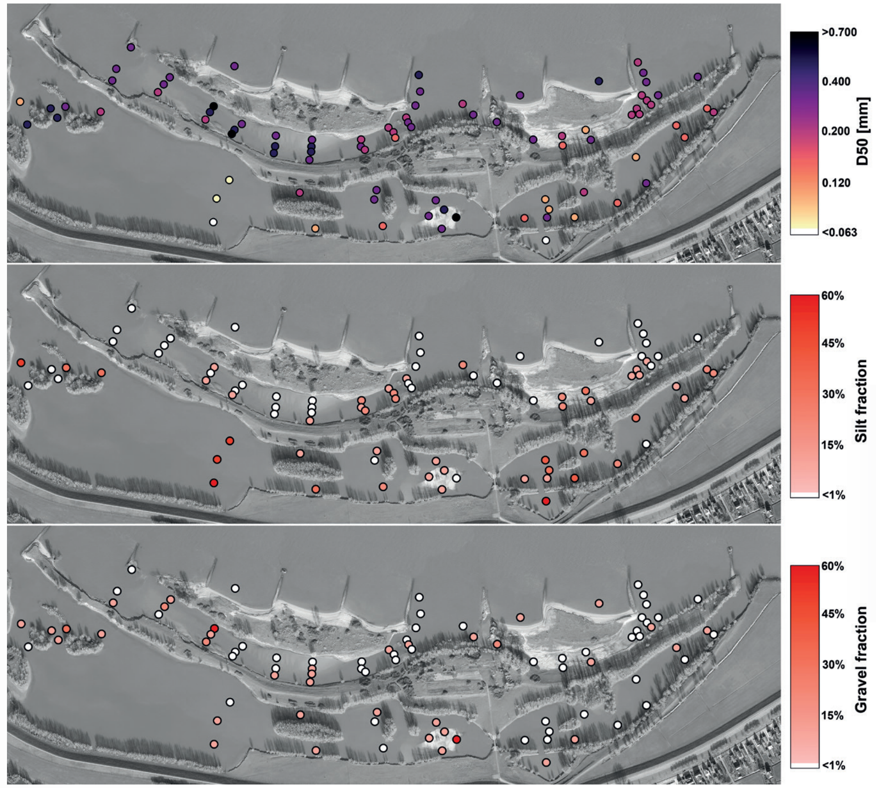

FIGURE 3.12 The spatial variation of the D_{50}, the silt/clay fraction, and the gravel fraction in the three side channels at Gameren.

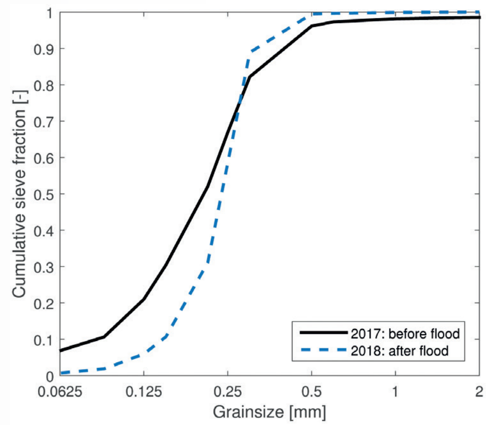

FIGURE 3.13 Comparison of the grain size in the East channel from 2017 before the peak flow and from 2018 after the peak flow.

3.4.3 SEDIMENT CORES IN THE EAST AND WEST CHANNELS

Several sediment cores were taken upstream and downstream of the weir in the East channel (Figure 3.14A). The deeper cores are affected by the original clay layer and are excluded from the statistical analysis. The graphs show a fining upward sequence except for D_{10} downstream of the weir. The sediment that was deposited in the East channel was apparently initially coarser and with the increasing bed level the grain size decreases. The sediment supply to the channel becomes finer with increasing bed level, because fine sediment is transported up a bed slope more easily (Parker and Andrews, 1985). The transport capacity in the channel is reduced due to the lower bed shear stress. The D_{10} and D_{50} do not show a clear difference upstream and downstream of the weir. For the D_{90}, the increase of the grain size with increasing distance below the bed level is larger upstream of the weir compared to downstream of the weir. The largest particles were blocked by the weir during the initial aggradation causing more coarse sediment to be deposited upstream of the weir compared to downstream of the weir. With increasing bed level upstream of the weir and lower bed shear stresses, the supply and thereby the deposition of coarse sediment upstream of the weir decreased. In 2017, the bed level upstream of the weir and downstream of the weir was the same as the weir height and therefore the grain size was very similar in front and behind the weir.

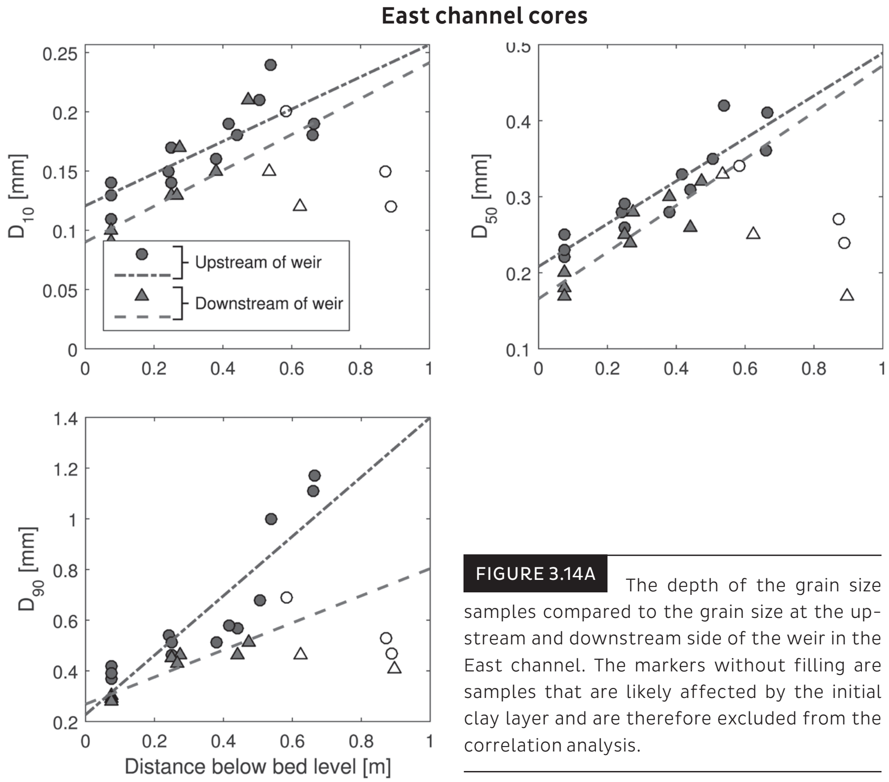

FIGURE 3.14A The depth of the grain size samples compared to the grain size at the upstream and downstream side of the weir in the East channel. The markers without filling are samples that are likely affected by the initial clay layer and are therefore excluded from the correlation analysis.

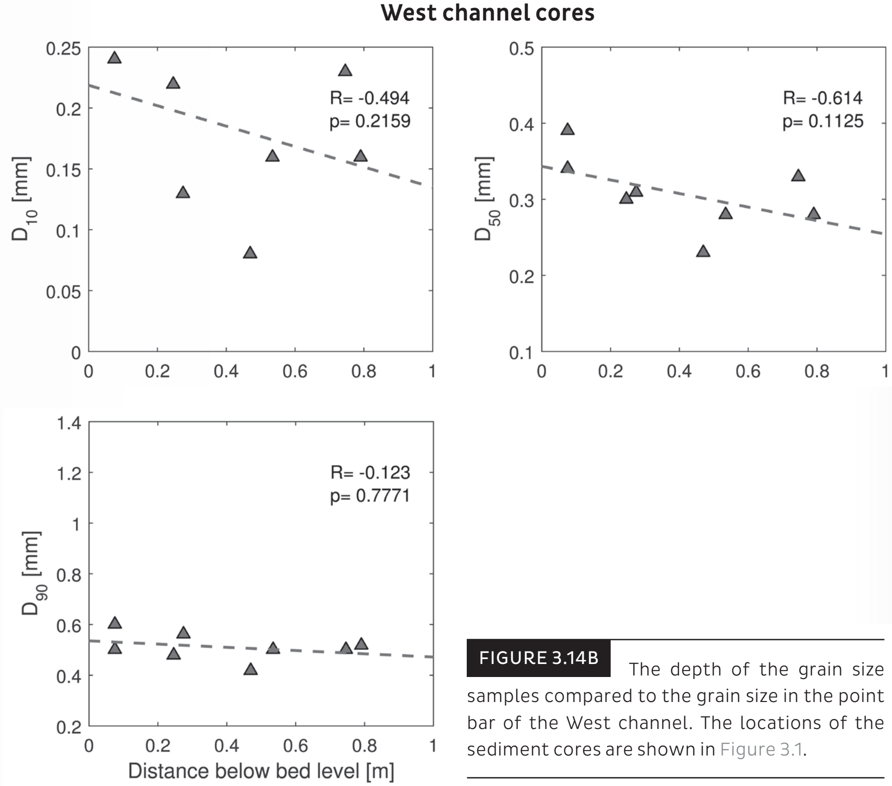

FIGURE 3.14B The depth of the grain size samples compared to the grain size in the point bar of the West channel. The locations of the sediment cores are shown in Figure 3.1.

The cores show that the sediment in the lower layers in the East channel is similar to the sediment that is currently found in the top layer of the West channel. In the point bar of the West channel, two cores were taken that do not show a clear trend in the grain size over the depth (Figure 3.14B). The grain size that was deposited in the West channel seems therefore constant in time. Initially, sediment deposited in the East and West channel was therefore more similar. The bed level increase and the decrease of the bed shear stress in the East channel resulted in a decrease of the D_{50}. In the West channel, the transport capacity has not decreased sufficiently such that fining of the bed occurs.

3.4.4 HYDRODYNAMIC MODEL RESULTS

The hydrodynamic model results show that the discharge in the side channels has generally decreased due to the bed level changes in these channels (Figure 3.6). In the Large channel the initial bed level changes that occurred at the entrance of the side channel results in an increase of the discharge through the channel. The discharge is not constant over the length of each channel (Figure 3.15). At Q = 4000 m^3/s a part of the discharge flows back from the East channel to the main channel and at Q = 5000 m³/s a part of the discharge flows from the East and West channel to the Large channel. In addition, at Q =4000 m³/s a part of the discharge enters the Large channel from the upstream floodplain (Figure 3.15).

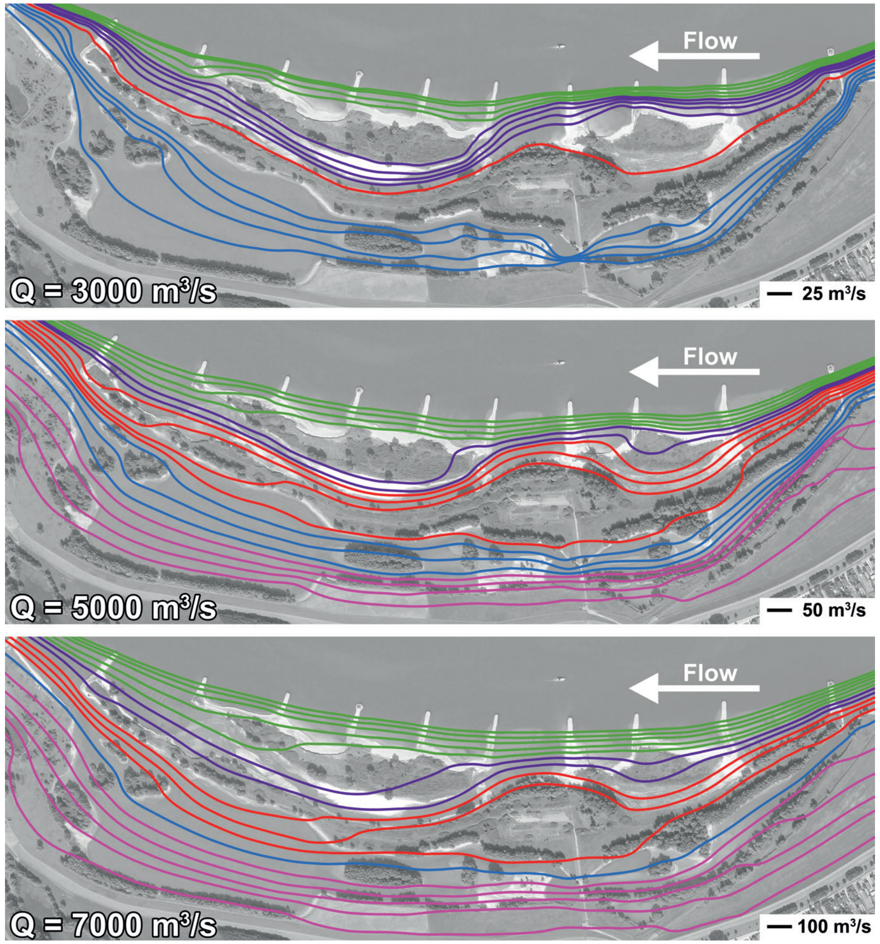

FIGURE 3.15 The streamlines in the side channel system near Gameren based on the depth-averaged hydrodynamic computations for three upstream discharges in the river Waal. The colors of the lines categorize the channel based on the location where they enter the floodplain. Pink lines enter the floodplain upstream of the side channel system, blue lines at the entrance of the Large channel, red lines at the entrance of the East channel, purple lines at the entrance of the West channel and green lines do not enter the floodplain. *(Background: Google Earth)*

The exchange of discharge between the channels and the floodplain affects the bed shear stress in the channels and therefore the sediment transport capacity (Figure 3.16). The bed shear stress increases with increasing discharge until exchange between the floodplain and other channels occurs. Over time, the bed shear stress in the West and Large channels has decreased. This is a result of bed level changes in the side channels which lead to, among other things, a reduction of the discharge conveyance. In the East channel, the bed shear stress increased between 1996 and 1999. At the entrance of the East channel, the channel is narrow resulting in large bed shear stresses, and due to the bank erosion that occurred in this period the discharge conveyance of the channel increased (Figure 3.6). With the continuing bank erosion and aggradation of the channel, the bed shear stress decreases between 1999 and 2017 (Figure 3.16).

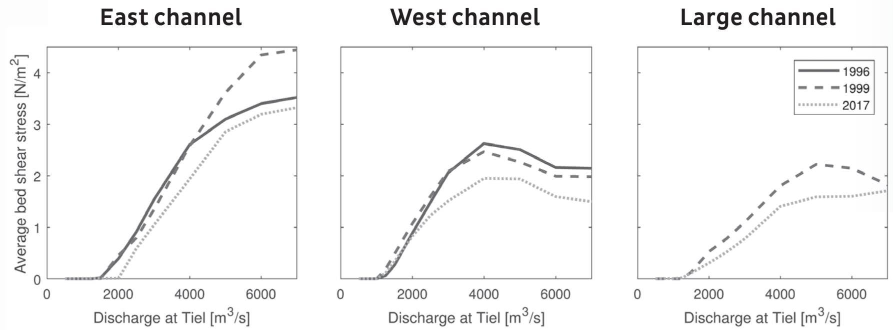

FIGURE 3.16 The average bed shear stress on the center line of the three channels for the bed level in 1996, 1999 and 2017. The discharge in the main channel ranges between 500 m³/s and 7000 m³/s.

3.4.5 RELATION BETWEEN THE MEASUREMENTS AND THE MODEL RESULTS

BED LEVEL

We compute the average bed level change over the length of the East and the West channel (Figure 3.17). The Large channel is not included because we have insufficient data, and in the downstream part of the Large channel, the bed level changes are strongly affected by the dredging and sediment dumping around 2009. In both the West and the East channel, the initial aggradation rate was large, and between 2000 and 2003 the bed level decreased. The bed level again increased in both channels after 2003, but the aggradation rates vary in time. On average, the bed level changes in the East channel seem to follow an exponential function (Figure 3.17B). An exponential function seems reasonable because the initial bed level change is large and with increasing bed level the sediment supply is expected to decrease until it reaches a bed level height from which much smaller floodplain aggradation rates occur (Riquier et al., 2017; Van Denderen et al., 2018a). The exponential function suggests that this bed level height is reached when bed level change is between 1.3 and 1.4 m (Figure 3.17). However, the aggradation rates of the side channel have not yet decreased significantly and therefore this bed level change is likely underestimated.

The aggradation rates vary due to the hydrodynamic conditions of the river and in the side channels (Figure 3.18). We compare the bed level changes in the East channel to the hydrodynamic conditions of the river. We ignore the initial bed level change, i.e., the change between 1996 and 1999, because this bed level change is dominated by the migration of the aggradation front. In addition, we scale the hydrodynamic and the bed level changes between measurements to yearly

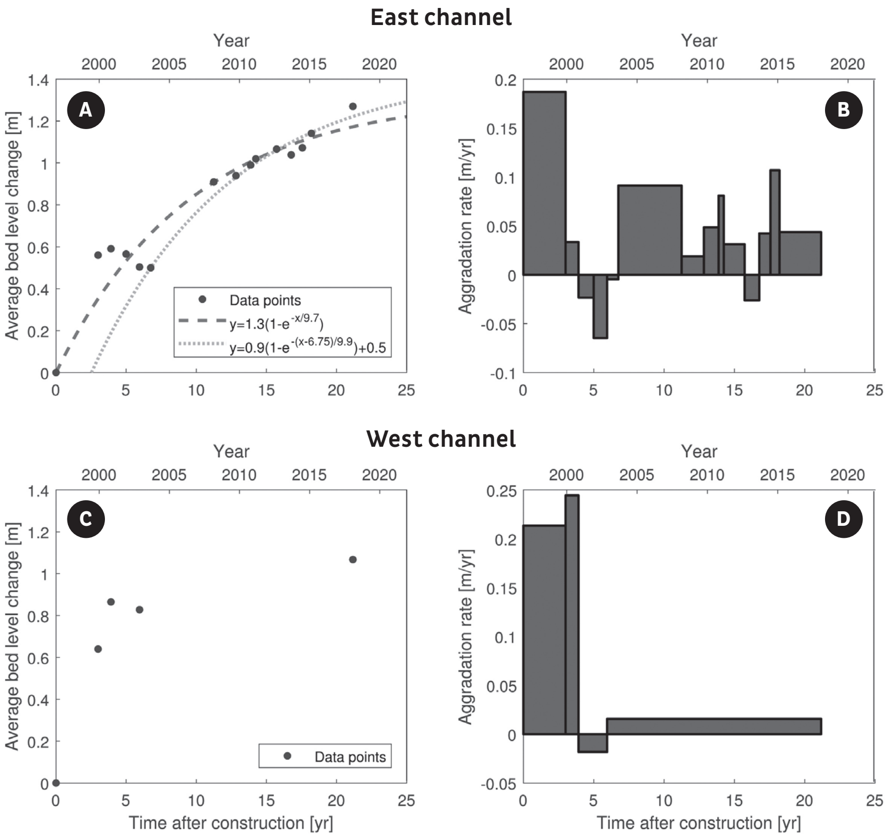

FIGURE 3.17 **(A)** The mean bed level change of the center line of the East channel (Figure 3.7) versus the number of years after construction. An exponential curve is fitted for the starting condition in 1996 and 2003 (Riquier et al., 2017; Van Denderen et al., 2018a). **(B)** The average aggradation rate of the East channel between each measurement. **(C)** The mean bed level change of the center line of the West channel versus the number of years after construction. **(D)** The average aggradation rate of the West channel between each measurement.

changes, and we therefore do not consider the measurements that are less than 10 months apart because otherwise the hydrodynamic conditions do not represent a full year. We find that the number of days that the East channel conveys discharge is negatively related to the bed level change (Figure 3.18A) and this relation is significant (p<0.01) using the Spearman's rank correlation. A similar result is found for the cumulative discharge (Figure 3.18C). The cumulative discharge is related to the bed shear stresses that occurred in the East channel. Long periods of high water can lead to degradation of the bed in the East channel. The bed shear stress in the East channel is large enough during the large discharges (Figure 3.16) such that a part of the deposited sediment is flushed from the channel (Figure 3.18D). The peak discharge is not a good predictor for the bed level change (Figure 3.18B, p>0.01), which makes sense as it does not include a time duration, which is relevant for the amount of sediment transported and therefore the bed level change. The same holds for the bed shear stress (Figure 3.18D).

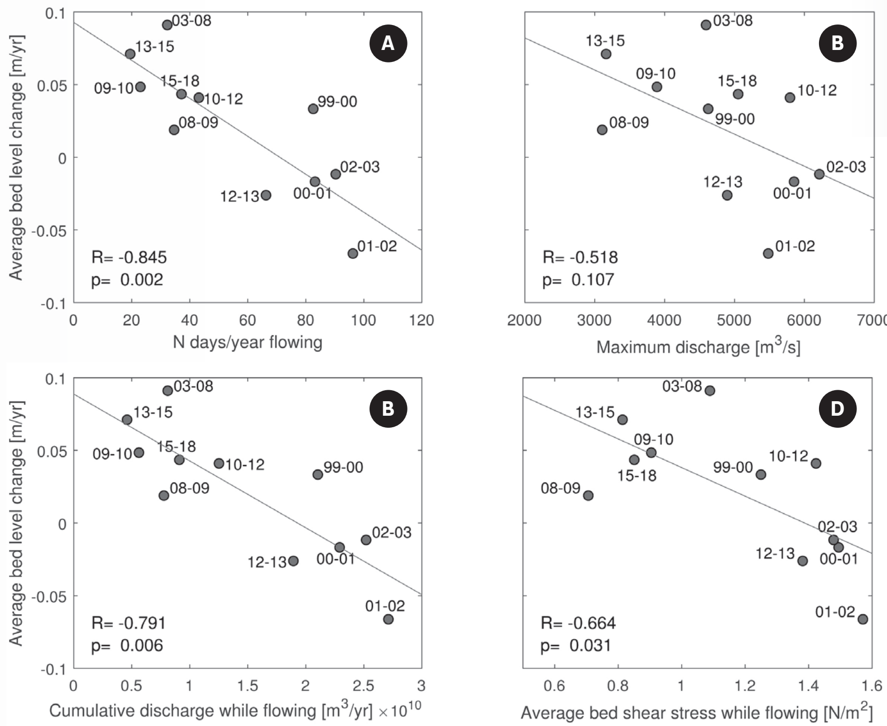

FIGURE 3.18 The correlation between the average bed level change and **(A)** the average number of days per year that the East channel flows (Q>2200 m^3/s), **(B)** the maximum discharge that occurred between each measurement, **(C)** the yearly averaged cumulative discharge during which the side channel flows between each bed level measurement, and **(D)** the averaged bed shear stress during which the side channel flows between each bed level measurement based on the hydrodynamic model. The correlation coefficients and the p-values are based on a Spearman's rank correlation and the linear regressions are based on a least-square fit.

GRAIN SIZE

The grain size that is deposited in the side channels is expected to be related to the sediment supply, the bed shear stress and the bed level. The sediment supply to the side channels is difficult to estimate because it is, among other things, a function of local three-dimensional flow patterns (e.g., Dutta et al., 2017). The depth-averaged streamlines (Figure 3.15) show that most of the discharge in the East channel comes directly from the main channel. The flow that enters the West channel comes for a large part from the East channel or its floodplain. This could suggest that the West channel receives less sediment since a part of the sediment can settle in the East channel. The size of this effect depends on the sediment exchange that occurs with the main channel in the groyne field at the bifurcation of the West channel, which requires more detailed data to estimate. The Large channel receives discharge from the East channel, the West channel, the main channel and the upstream floodplain. The discharge from the upstream floodplain flows parallel to the main channel and more than 100 m away from the main channel. Therefore, this discharge transports mainly silt/clay (Middelkoop and Asselman, 1998). We expect therefore that the sand supply to the Large channel is relatively small during peak discharges.

The longitudinal profile of the East channel shows that the highest bed level occurs halfway down the channel (Figure 3.19). Figure 3.20 shows a negative relation between the bed level and the D_{50}. Fine sediment is more easily transported up a bed slope compared to coarser sediment (Parker and Andrews, 1985) and the bed shear stress decreases with the increasing bed level (Figure 3.16). The silt fraction shows a positive relation with the bed level. The D_{50} decreases and the silt fraction increases from a bed level height of 1.5 – 2.0 m +NAP (Figure 3.20), i.e., in the whole channel except for its extremities. This suggests that from this bed level height the trapping of silt occurs. This is enhanced by the growth of vegetation and the low discharges that occurred in the months before the grain size sampling. The three points above a bed level of 2 m +NAP that are relatively coarse (Figure 3.20A) are in the downstream end of the side channel where the channel narrows and therefore higher bed shear stresses occur. The point with the lowest bed level and a high silt fraction (Figure 3.20B) is in the downstream groyne field. During base flow conditions, which was the case during the measurements, the flow velocity in the groyne field is low. The main flow is likely directed towards the entrance of the West channel and a flow circulation forms at the upstream side of the groyne field (Mosselman et al., 2004). The low flow velocity in the flow circulation can result in the deposition of fines at the downstream end of the East channel (Sukhodolov et al., 2002).

In the West channel the grain size is on average the largest of the three channels. The weir at the entrance does not block the flow and therefore during base flow conditions the scour hole at the entrance of the channel is filled with fines (Figure 3.21). The samples were collected after a long period with lower discharges,

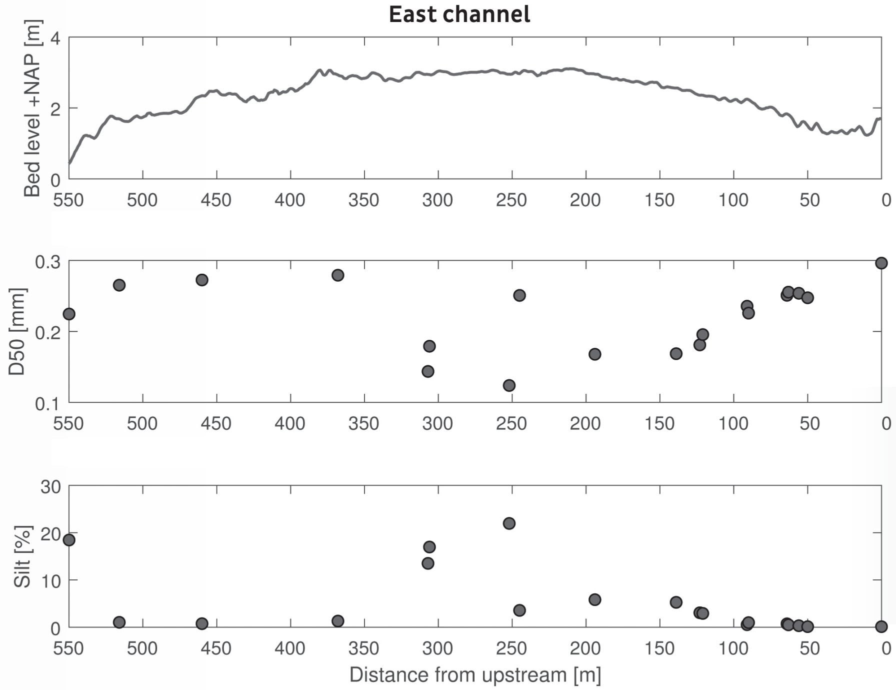

FIGURE 3.19 The bed level (2018), the grain size (2017) and the silt fraction (2017) on the center line of the East channel (Figure 3.7).

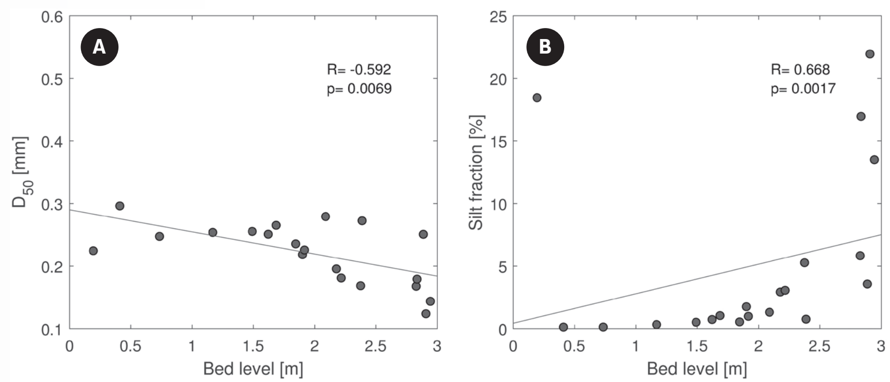

FIGURE 3.20 The D_{50} and the silt fraction in the East channel as a function of the bed level. The correlation coefficients were computed using Spearman's rank correlation and the linear regression is based on a least-square fit.

and it is therefore likely that during peak flows this deposited fine sediment erodes. In the remaining part of the channel, the silt fraction is small because the flow velocity is sufficiently high that fines do not settle. There is some variation of the D_{50} over the width of the channel (Figure 3.12) and this is related to the bend in which, due to the transverse bed slope, more fine sediment is deposited in the inner part of the bend (Parker and Andrews, 1985). The D_{50} in the West channel does not show a correlation with the bed shear stress, nor with the bed level (Appendix 3.B), because the bed level of 2.0 m +NAP at which in the East channel fining occurred is not yet reached in this channel. At the downstream end a few samples show a large gravel fraction. Since the gravel is not found in the rest of the channel, this is likely a result of the bank erosion that occurred here (Figure 3.5).

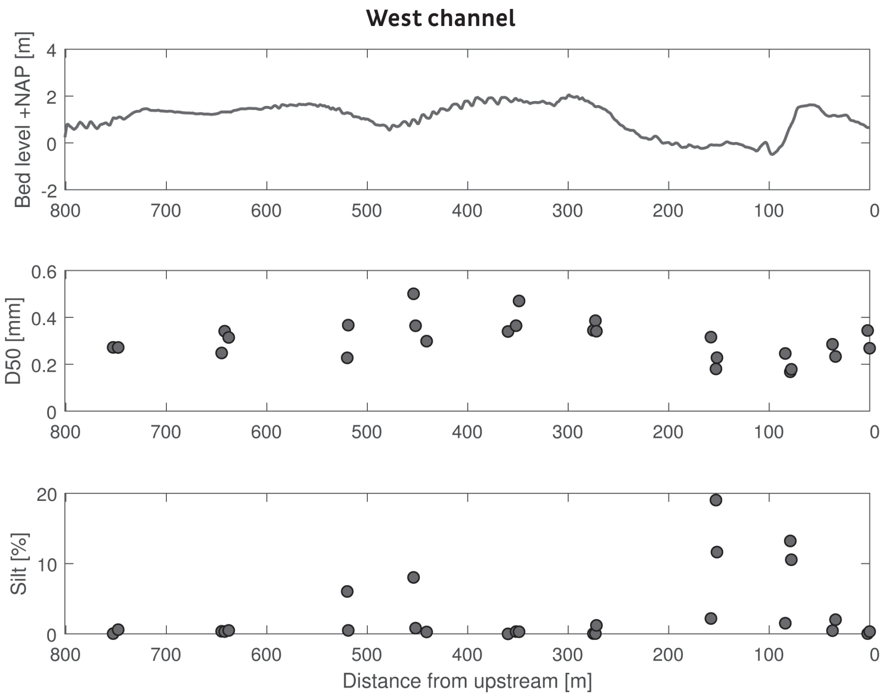

FIGURE 3.21 The bed level (2018), the D_{50} (2017) and the silt fraction (2017) on the center line of the West channel (Figure 3.9).

The largest silt fraction is found in the Large channel. The threshold value for the bed shear stress below which fines can settle is estimated at around 2.0 N/m² for the sediment in the river Waal (Middelkoop and Van der Perk, 1998; Asselman and Van Wijngaarden, 2002). On average, fines can settle in the Large channel even during peak flows (Figure 3.16). The large variation of the channel width and depth results in a large variation of the bed shear stress and thereby the D_{50} and the silt fraction (Figure 3.22). The thalweg of the Large channel is located next to the south bank upstream of the bridge and downstream of the bridge next to the north bank (Figure 3.11). In these areas we find coarser sediment, and the silt/clay fraction is lower than in the rest of the channel. At the entrance of the channel, large flow velocities occur and it was not possible to take a sample with the Van Veen grab. Here, the bed is likely covered with clay that limits the scour at the entrance. The island that formed just downstream of the bridge is partly covered with gravel and this originates from the deep scour hole just downstream of the bridge. The large acceleration at the bridge allows for the pickup of the gravel, but the deceleration just downstream causes it to be deposited. At the downstream end of the channel in between the islands, it is not clear whether the sampled sediment was deposited naturally or dumped due to dredging activities. In addition, the measurements show very limited aggradation and therefore the sediment could have been there since the construction of the channel.

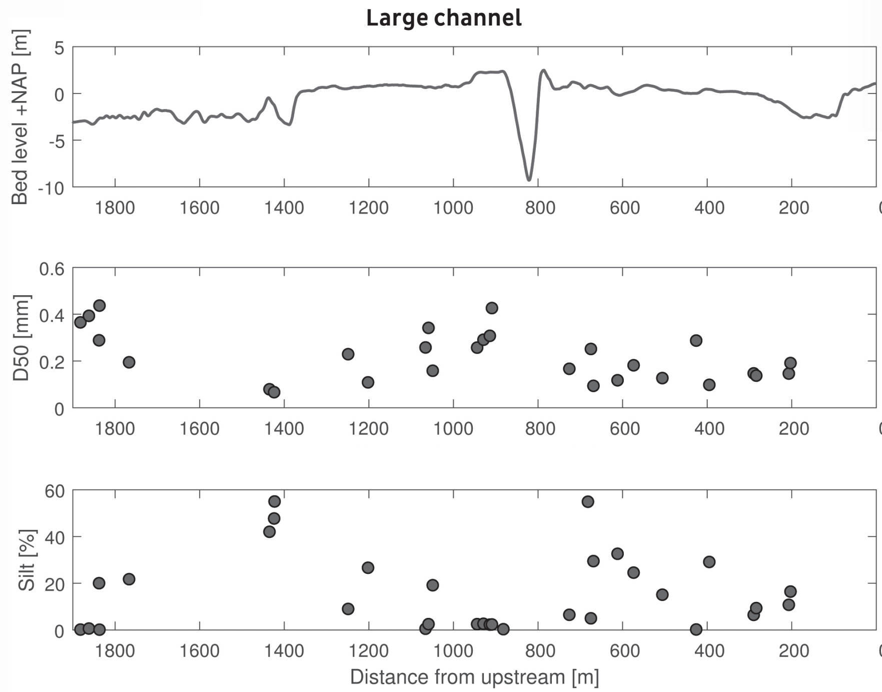

FIGURE 3.22 The variation of the bed level (2009), the D_{50} and the silt fraction on the thalweg of the Large channel (Figure 3.11).

3.5 DISCUSSION

3.5.1 CHARACTERIZATION OF THE SIDE CHANNELS AT GAMEREN

The three side channels at Gameren present two types of side channels. The East and West channel are mainly filled with sand from the main channel that in the main channel is transported as suspended bed-material load. The Large channel also shows the deposition of silt in addition to the suspended bed-material load. We expect that the West and East channel show a comparable development and that the difference in aggradation rate is caused by the design conditions of the channels.

Both the East and West channel have a similar relative length compared to the main channel (L_{side}/L_{main}), which was found to have large effect on the time scale of the side channel development (Van Denderen et al., 2018a). The initial bed level changes seem similar (Figure 3.17) and the corings in the East channel show that the sediment that was initially deposited in the East channel was similar in size to the sediment currently found in the West channel (Figure 3.14). We therefore expect both channels to have a similar equilibrium state, but that the aggradation time scale differs. An important factor is the initial geometry. The West channel is wider compared to the East channel, and the initial bed level and weir height are lower. Therefore, the West channel flows more frequently than the East channel and the aggradation rate is therefore likely smaller compared to the East channel (Figure 3.18A). In addition, the sediment supply might differ between the West and the East channel. The flow at the bifurcation of the West channel is affected by the outflow of the East channel (Figure 3.15). Based on the 2D hydrodynamic model, a large part of the flow first passes through the East channel before it enters the West channel. This suggests that the East channel can act as a sediment trap for the West channel during peak flow conditions. However, more detailed measurements or computations of the flow velocity in this groyne field are needed to confirm this.

The aggradation in the side channels affects the sediment supply and the transport capacity of the channel. The loamy sand layer that was found in the East channel means that fine sediment processes gained importance (Makaske et al., 2002). The aggradation in the East channel has made the channel sufficiently shallow such that vegetation can colonize and trap suspended load. In addition, the loamy sand layer can be a result of a long period of lower discharges that reduced the supply of coarse sediment. The recent peak flow (2018) resulted locally in large amounts of deposition of fine sand in the East channel. Coarser sediment is therefore supplied during peak flow conditions during which larger bed shear stresses occur.

The Large channel belongs to a second type of side channel. The Large channel is much longer than the main channel and, in combination with the large variations in width, this results in areas with small bed shear stresses. In these areas, we found large amounts of silt deposited. In addition, the channel is located in the floodplain and during peak flows, a large part of the flow originates from the floodplain that mainly carries fine sediment. Therefore, the supply of fines to the Large channel during peak flows might be relatively large compared to the supply of suspended bed-material load.

These two types of side channels are similar to the modes of infilling of channels that were found in anabranching rivers (Makaske et al., 2002). The way the channel is filled strongly depends on the sediment supply. The West and the East channel receive sediment that is transported inside the channel as bedload. This leads to a gradual aggradation in the channel until a certain bed level is reached and fines start to be deposited (Makaske et al., 2002; Dieras et al., 2013). The Large channel receives much less sand because it attracts relatively less discharge due to its length (Van Denderen et al., 2018a) and little sediment is supplied from the main channel during peak flows (Figure 3.15). This results in the deposition of fines (Makaske et al., 2002), which is similar to the aggradation in oxbow lakes (Constantine et al., 2010; Toonen et al., 2012).

3.5.2 KNOWLEDGE GAPS

In the Room for the River program in the Netherlands, over 20 side channels were constructed since 1996. Unfortunately, the monitoring of these side channels was limited except for Gameren. Therefore, the side channels at Gameren provide a unique opportunity to study the development of side channels in the Dutch Rhine branches. In this paper, a range of measuring techniques is used to characterize the sediment dynamics. Each technique has its limitations and inaccuracies. The regular LIDAR measurements between 2008 and 2015 provide insight into the development of the East channel. Unfortunately, the West and Large channel are permanently inundated and therefore aerial height measurements cannot give accurate information on the bed level changes in these channels.

In this paper, we mainly focus on the mechanisms that are not human-induced. However, there are several human-induced changes that might have influenced the development of the side channels. Between 2013 and 2014, the groyne height in the main channel was reduced over a large stretch. This led to higher flow velocities in the groyne field (Yossef, 2005) and a lower bed level (Klop and Dongen, 2015). This likely produces an increased sediment supply to the side channels because the larger bed shear stress allows for more sediment to be transported up a sloping bed (Parker and Andrews, 1985). The bed level of 2018 deviates from the proposed exponential function (Figure 3.17) and this might be due to the changed sediment supply during peak flows. Unfortunately, this cannot be confirmed because of the limited frequency of bed level measurements in the more recent years. A second example of human impacts are navigation-induced currents.

Navigation in the main channel causes an export of sediment from the groyne fields (Ten Brinke et al., 2004). The currents likely have a similar effect at the entrances of the side channels. For example, the bed level at the bifurcation of the East channel in 2018 is much higher than in the other years (Figure 3.8). These measurements were collected during the peak flow in 2018 and therefore navigation had a limited effect on the bed level. All the other measurements were carried out at the beginning of the flood season, and therefore navigation-induced currents might have reduced the bed level at the entrance of the East channel. In addition, it is possible that during base flow conditions fine sediments are supplied to the channels due to the navigation-induced currents. Vessels that pass through the main channel cause a depression of the water level in the side channel, and after the vessel passes the water level rises again. This water level variation is enough to bring fine sediment into suspension (Ten Brinke et al., 2004) and might therefore lead to aggradation of the channel. Especially in the Large channel, which is continuously connected with the main channel and in which the bed shear stress is generally low (Figure 3.16), this can result in the deposition of fines.

Besides the groyne field dynamics, the bed level changes and the aggradation rates of the side channels are also related to the flow conditions in the main channel (Figures 3.17 and 3.18). Just after the construction of the side channel system several large peak discharges occurred, but during other periods, e.g., 2004–2010, the flood frequency was much lower (Figure 3.2). The duration needed to fill in a side channel will increase with regular large peak discharges (Figure 3.18).

3.6 CONCLUSION

The three side channels near Gameren all show aggradation after their construction. The East and West channels are very similar in terms of sediment dynamics. In both channels large aggradation occurred and mainly sand was deposited. The aggradation rate of the East channel shows a relation to the hydrodynamic conditions of the river. The measurements show that a more frequent flowing side channel results in lower aggradation rates. The aggradation in the East channel was large enough such that vegetation has grown and silt has deposited. The East channel is therefore slowly becoming a part of the floodplain. The aggradation in the West channel initially reacts to hydrodynamic events similarly to the East channel. The aggradation rate in the West channel is slower after the initial 5 yr after construction, but the bed level continues to increase and we expect that the bed level will continue to increase until it reaches a similar bed level as the East channel. The smaller aggradation rate of the West channel seems to be related to a different initial geometry, which allows the channel to flow more frequently compared to the East channel, and a difference in sediment supply compared to the East channel. The West channel is located just downstream of the East channel and might therefore receive a smaller sediment supply.

The aggradation of the Large channel was different than that of the other two channels. The length of the channel is much larger than the length of the main channel and in combination with variation in channel width this results in areas with low bed shear stresses. In addition to suspended bed-material load, silt is deposited in the Large channel due to the low bed shear stresses. During peak flows a large part of the discharge in the Large channel originates from the floodplain and therefore mainly carries fines. The supply of sand to the channel relative to the discharge in the channel is therefore likely lower during peak flows and this reduces the aggradation rate.

ACKNOWLEDGEMENTS *This research is supported by the Netherlands Organisation for Scientific Research (NWO), which is partly funded by the Ministry of Economic affairs, under grant number P12-P14 (RiverCare Perspective Programme) project number 13516. This research has benefited from cooperation within the network of the Netherlands Centre for River studies. Datasets related to this article can be found at https://doi.org/10.4121/uuid:2704f813-d23b-43b5-b837-fdb02ceef261, hosted at 4TU.Centre for Research Data (Van Denderen et al., 2018b). We thank Anouk Bomers for her help in setting up and calibrating the hydrodynamic numerical model. The Editor Scott Lecce and three anonymous reviewers are acknowledged for their valuable comments that helped to improve the paper.*

APPENDIX

3.A SET UP OF THE HYDRODYNAMIC MODEL

We use a hydrodynamic to better estimate the hydrodynamic conditions in the side channels and to see how they have changed since the construction of the channels. The hydrodynamic computations are carried out using a depth-averaged version of the Delft3D Flexible Mesh software (Kernkamp et al., 2011) that allows for a combination of a curvilinear and triangular grid. In the main channel and the surrounding floodplain, we use a curvilinear 20x10m grid. In the floodplain of Gameren, we create a curvilinear grid in each side channel separately and connect these with the rest of the model using triangles. This allows us to use a much finer grid at the side channels of Gameren without a too large computational effort.

The model is created based on two GIS databases of the Rhine branches that are provided by Rijkswaterstaat (Becker et al., 2014). One describes the situation in 1995 without the side channels at Gameren and one describes the situation in 2017. The GIS databases include interventions in the river that were carried out between 1995 and 2017.

The side channels are assumed to have a Nikuradse roughness length of 0.2 m corresponding with the bed forms found in the West and East channel. The roughness in the main channel is used to calibrate the model. We base the roughness length in the main channel on the simplified relation by Van Rijn (1984), in which the dune height and length are expressed as a function of the water depth:

$$k = Ah^{0.7}\left(1 - e^{-Bh^{-0.3}}\right) \tag{3.1}$$

in which h is the water depth, A is a calibration parameter of the bed form height and $B = 2.5$ is a calibration parameter of the bed form steepness (Becker, 2015). For calibration, the model results are compared to observations at five water level measuring stations along the river Waal. Between each of these water level stations the main channel roughness parameters are assumed constant. We use the sparsedud algorithm of OpenDA (https://www.openda.org) to estimate the main channel roughness. The calibration criterion is an average error smaller than 0.005 m which corresponds with the guidelines of the Rijkswaterstaat (Becker, 2015). We calibrate the model based on three flow conditions in 1995 that occurred between December 1994 and February 1995 (Figure 3.23) (Becker, 2015). The model should therefore also give reasonable results for lower discharges in the river Waal.

The calibrated model results in the following average errors for all measuring stations: Low = $-3.4 \cdot 10^{-3}$ m, Medium = $-2.9 \cdot 10^{-5}$ m and High = $-2.7 \cdot 10^{-4}$ m. We consider that the model is sufficiently calibrated.

We use the model to compute the water level, flow velocities and discharges in the side channels. We assume steady flow conditions with a discharge at the upstream boundary condition ranging from 500 m^3/s to 7000 m^3/s in the river Waal. For the simulated discharges that are between the calibrated discharges, we linearly interpolate the values of A.

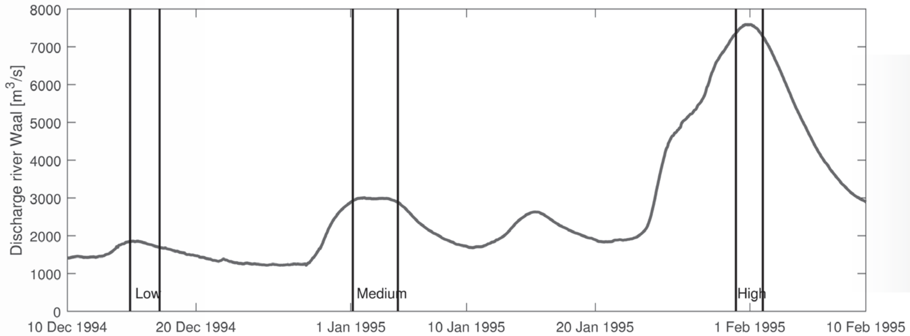

FIGURE 3.23 The discharge in the river Waal and the time windows (Becker, 2015) between which the water level is calibrated by adjusting the main channel roughness.

3.B COMPARISON OF THE BED LEVEL, GRAIN SIZE AND THE BED SHEAR STRESS IN THE SIDE CHANNELS

The bed level of the West and Large channel are not presented in the paper in relation to the grain size and the bed shear stress, because they do not show a clear correlation. We present them here as background information. Figure 3.24 shows the relation between the grain size and the bed level in the three channels.

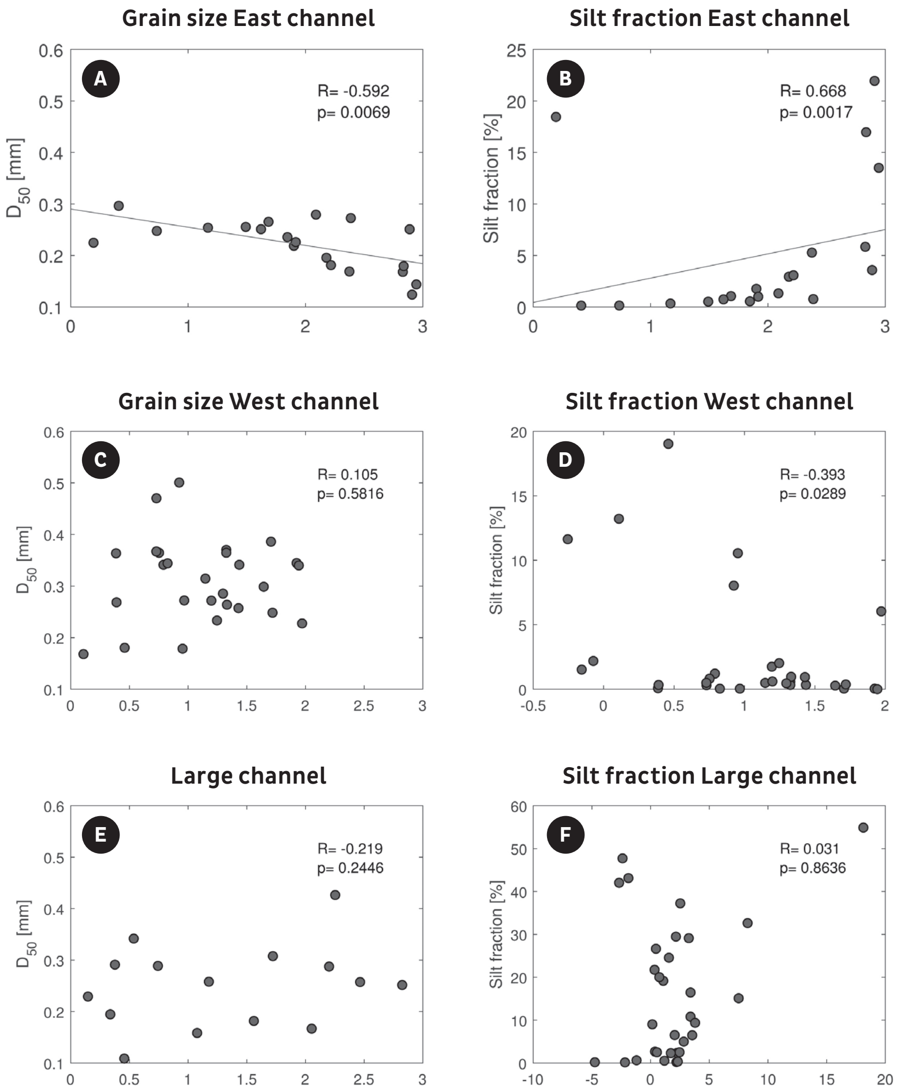

FIGURE 3.24 The D_{50} and the silt fraction versus the bed level for each of the channels. The correlation is computed with the Spearman rank correlation.

Only in the East channel this results in a clear correlation. There does not seem to be a correlation between the bed shear stress and the grain size (Figure 3.25). We only have one grain size measurement available and we do not know which discharge level is governing. In addition, the governing discharge level likely varies between the channels and within a channel due to differences in the bed levels.

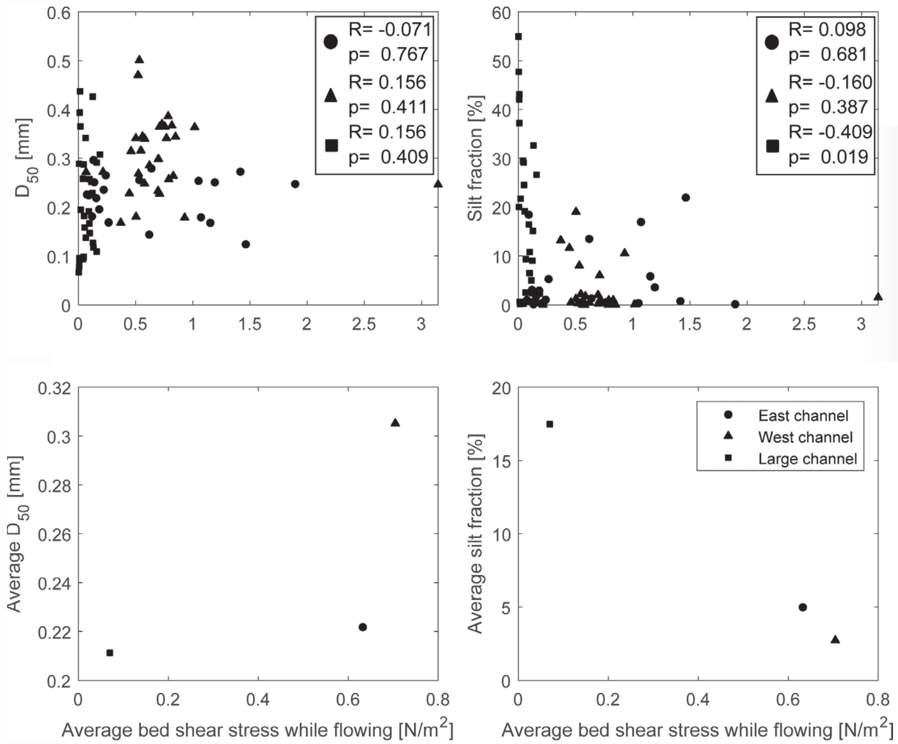

FIGURE 3.25 The average bed shear stress in the last three years (2015-2017) correlated with the grain size and the silt fraction.

Photo: Bureau Beeldtaal Filmmakers

CHAPTER 4

Numerical modelling of morphodynamic changes in side channel systems

This chapter is submitted as
Van Denderen, R.P., R.M.J. Schielen, and S.J.M.H. Hulscher: Numerical modelling of morphodynamic changes in side channel systems.

Side channels are constructed to reduce the flood risk and increase the ecological value of the river. Measurements of a side channel system at Gameren show that suspended bed-material load from the main channel is deposited in the side channel and that floods have an important role in the morphodynamic development of the system. We use a two-dimensional morphodynamic mixed-sediment model with varying hydrodynamic conditions to estimate the development of such systems. The objective of this paper is to evaluate the morphodynamic development of a side channel system as a function of its characteristics and the hydrodynamic conditions. The bed level changes and the grain size variation in the side channel is computed and shows a relation with the transverse bed slope, the upstream sediment supply, upstream discharge, the roughness and the initial bed level. Our model shows that a mixed-sediment model is needed to correctly estimate the sediment supply and the transport capacity in a side channel system. In addition, we show that proper estimates of the side channel development need varying hydrodynamic conditions, because it results in a large variation of the sediment supply and the transport capacity in the side channel.

04

4.1 INTRODUCTION

Side channels are secondary channels that convey much less discharge than the main channel; at the upstream and the downstream end they are connected with the main channel. Naturally-formed side channels occur, for example, in braiding, meandering or anabranching rivers. Due to human interference, side channels have disappeared in many regulated rivers (e.g., Hohensinner et al., 2014). Artificial side channels are now (re)constructed to increase the discharge capacity of the river (Simons et al., 2001; Nabet, 2014; Van Denderen et al., 2019), to increase the ecological value of the river (Schiemer et al., 1999; Buijse et al., 2002; Formann et al., 2007; Riquier et al., 2015; Van Dyke, 2016; Riquier et al., 2017), to restore river branches (Henry et al., 1995; Helfield et al., 2012) and to reduce the degradation in the main channel (Tockner et al., 1998; Formann et al., 2007). These constructed side channels generally aggrade (e.g., Riquier et al., 2017; Van Denderen et al., 2019). The aggradation rate and the type of sediment that is deposited in the side channel, depend on the characteristics of the side channel system (Dépret et al., 2017; Riquier et al., 2017; Van Denderen et al., 2018; Van Denderen et al., 2019). Measurements show that aggrading side channels generally fill with finer sediment than the sediment that is found on the bed of the main channel (Riquier et al., 2017; Van Denderen et al., 2019). This means that sediment sorting occurs at the bifurcation and mixed sediment processes are important. Here, we study the side channel development using a two-dimensional mixed-sediment morphodynamic model to better understand the dynamics of side channel systems.

The sediment that is deposited in side channels depends on the sediment supply and the transport capacity within the side channel. Mechanisms that affect the sediment supply in the downstream channels are, for example, the transverse bed slope (Bolla Pittaluga et al., 2003) and spiral flow at the bifurcation (Bulle, 1926; Kleinhans et al., 2008). Smaller particles are more easily transported up the transverse bed slope (Parker and Andrews, 1985). Spiral flow, i.e. generated by an upstream bend (Kleinhans et al., 2008) or a large bifurcation angle (Bulle, 1926; Dutta et al., 2017), changes the direction of the sediment transport near the bed. Sediment that is transported in suspension is less affected by a change in flow direction near the bed and by bed slope effects. This can lead to sediment sorting at the bifurcation (Kleinhans et al., 2012).

The effect of the transport capacity on the side channel development is, for example, seen in the development of cutoff channels in meandering rivers. A cutoff channel attracts generally more discharge than the old meander, because the length of the cutoff channel is generally smaller. This results in a larger water level slope over the cutoff and therefore this channel attracts relatively more discharge compared to the main channel (Mendoza et al., 2016). Therefore, the old meander aggrades and depending on the transport capacity of the channel, the channel closes with a plug bar that mainly consists of coarse sediment (Constantine et al., 2010; Toonen et al., 2012) or the aggradation is more spread over the length of the channel (Toonen et al., 2012; Dieras et al., 2013). In the first case, the channel will continue to aggrade with fines that are supplied during flood conditions (Makaske et al., 2002; Constantine et al., 2010; Toonen et al., 2012). In the second case, the deposition of fines starts when a certain bed level is reached above which the supply of coarse sediment is limited and the channel is sufficiently shallow such that vegetation colonizes which results in the trapping of fines (Makaske et al., 2002; Van Denderen et al., 2019).

In this paper, we look at an idealized side channel system with properties that are loosely based on the West channel at Gameren in the river Waal (The Netherlands) (Figure 4.1). The side channel was constructed in 1996 and a weir was constructed at the upstream entrance to control the discharge in the side channel. The West channel is separated from the floodplain with a levee and therefore the exchange of sediment and discharge between the channel and the rest of the floodplain is limited (Van Denderen et al., 2019). Between 1996 and 1999, an initial bed level increase occurred which is an adjustment of the originally constructed side channel with a trapezoidal cross-section to a more natural-formed cross-section. After 1999, the aggradation continued and the aggradation rate seems to be related to the discharge in the main channel. The grain size deposited in the side channel decreases with increasing bed level and during floods relatively more coarse sediment is supplied to the channel (Van Denderen et al., 2019). Measurements show that mainly fine sand is deposited in the West channel that in the main channel is transported as suspended bed-material load (Frings and Kleinhans, 2008; Van Denderen et al., 2019). Therefore, both sediment sorting at the bifurcation and varying hydrodynamic conditions are important mechanisms to correctly simulate the side channel development.

Measurements show the importance of using a mixed sediment morphodynamic model with varying hydrodynamic conditions to estimate the development of a side channel system. However, regardless of these observational results, we cannot yet estimate the effect of these mechanisms on the development of side channels in a quantitative way. Therefore, the objective of this paper is to evaluate the morphodynamic development of a side channel system as a function of the transverse bed slope effect, the upstream sediment supply, the roughness, the active layer thickness, the initial bed level, structures and the hydrodynamic conditions. We first present the model and the main equations used (Section 4.2) and introduce the base case and several variations on the base case (Section 4.3). Then, we present the results and make a comparison with the measurements at Gameren (Section 4.4). We conclude with a discussion on uncertainties and modeling challenges (Section 4.5).

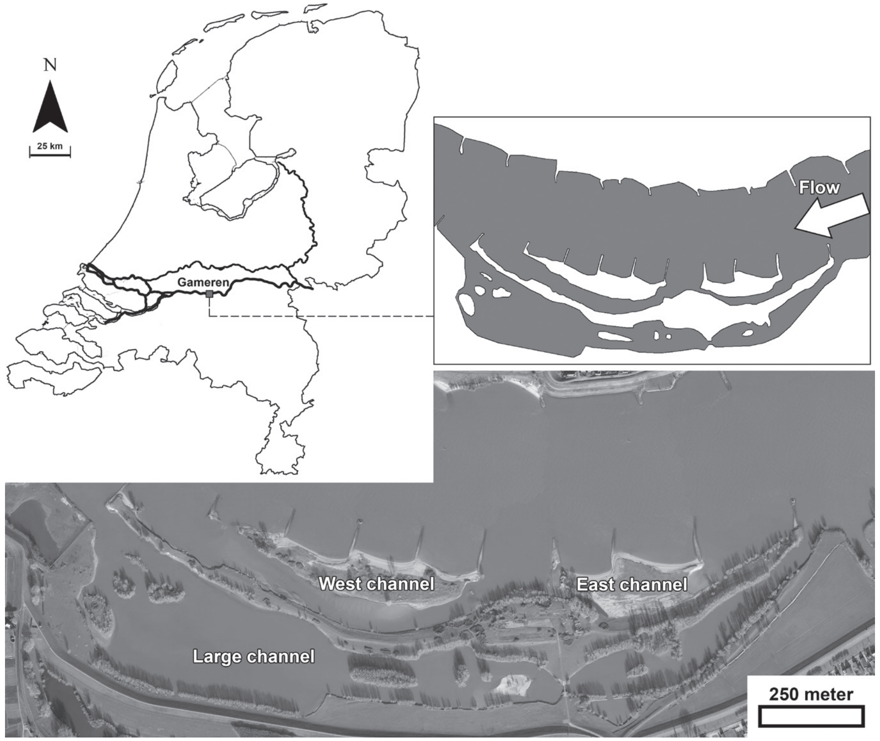

FIGURE 4.1 A map of the Netherlands with the most important Rhine branches, a sketch of the side channel system at Gameren, and an aerial image of the side channels at Gameren from 2014 *(after images of Rijkswaterstaat).*

4.2 MODEL DESCRIPTION

We use a two-dimensional depth-averaged (2DH) version of Delft3D (adapted from Version 6.02.10.7204) including a morphodynamic module for mixed sediment morphodynamics (Sloff et al., 2001; Lesser et al., 2004). Delft3D is a widely used model for coastal, estuarine and riverine applications and solves the nonlinear shallow-water equations. The model is able to reproduce the two-dimensional morphodynamic development of a river (e.g., Schuurman et al., 2013; Duró et al., 2016) and was previously used to study the development of bifurcations (e.g., Kleinhans et al., 2008). The implementation of the mixed sediment module was previously verified with straight and curved flume experiments (Sloff et al., 2001) and applied to a large river bifurcation (Sloff and Mosselman, 2012). A parametrization for the secondary flow is included based on the streamline curvature (Jansen et al., 1979; Sloff and Mosselman, 2012). The secondary flow causes a deviation of the sediment transport direction compared to the depth-averaged flow direction. If vertical flow variations are unsolved, a parametrization is needed to correctly reproduce the 2D morphology in a river. However, studies show that the validity of this parametrization is uncertain due to the limitations in its derivation (Ottevanger, 2013).

The variation and the changes in grain size are computed using the Hirano active layer model (Hirano, 1972). The active layer represents the volume of sediment in the bed that interacts with the flow. The measured sieve curve is discretized in sediment classes and the volume fractions of these classes are assumed to be uniformly distributed in the active layer within a computation cell. If degradation occurs, sediment is transferred from the substrate to the active layer and if aggradation occurs, sediment is transferred from the active layer to the substrate. To keep track of the deposited sediment, the substrate is divided in different layers. The active layer thickness is a model parameter and is, in case of irregular dunes, best represented by the mean dune height (Blom, 2008). The active layer model is known to become ill-posed (Ribberink, 1987). The most likely cause of ill-posedness is the degradation of the active layer into a finer substrate. Since we look at an aggrading side channel, we expect this effect to be limited for the purpose of this study. In addition, we check the results for non-physical oscillations that coarsen the substrate and that are caused by the ill-posedness of the model (Chavarrías et al., 2018).

The sediment transport is a sum bed load transport and suspended load transport. We compute the bed load transport using Ashida and Michiue (1972):

$$q_{sib} = 17F_i\sqrt{\Delta g D_i^3}(\theta_{si} - \alpha_s\xi_i\theta_c)\left(\sqrt{\theta_{si}} - \sqrt{\alpha_s\xi_i\theta_c}\right) \tag{4.1}$$

in which subscript i denotes the sediment class, q_{sib} is the bed load transport, F_i is the volume fraction, Δ is the relative density, D_i is the grain size, θ_{si} is the

Shields stress due to skin friction, ξ_i is the hiding and exposure parameter, α_S the effect of the bed slope in stream-wise direction on the critical Shields stress and $\theta_c = 0.035$ the critical Shields parameter (Van Rijn, 1984a) based on the mean grain size in the river Waal. The Shields stress based on skin friction is given by:

$$\theta_{si} = \frac{u^2}{C_{90}^2 \Delta D_i}$$
$$where\ C_{90} = 18\log\left(\frac{12h}{3D_{90}}\right) \tag{4.2}$$

in which u is the depth-averaged flow velocity and h is the water depth. The parameter α_S is given by (Fernandez Luque and Van Beek, 1976):

$$\alpha_s = \frac{\sin(\phi_s + \beta)}{\sin\phi_s} \tag{4.3}$$

in which ϕ_S is the angle of internal friction of the sediment (30°) and β is the bed slope in flow direction. The hiding and exposure coefficient (ξ_i) is given by (Ashida and Michiue, 1972):

$$\xi_i = \begin{cases} 0.8429\dfrac{D_m}{D_i} & \dfrac{D_i}{D_m} < 0.38889 \\ \left(\dfrac{\log_{10} 19}{\log_{10} 19 + \log_{10}\left(\dfrac{D_i}{D_m}\right)}\right)^2 & \dfrac{D_i}{D_m} \geq 0.38889 \end{cases} \tag{4.4}$$

in which D_m is the mean grain size.

We compute the suspended bed-material load with Wright and Parker (2004). This relation is a correction of the relation by Garcia and Parker (1991) which overestimates the sediment transport rate for large sand-bed rivers (Wright and Parker, 2004). We assume that in each computational cell the reference concentration is equal to the equilibrium concentration which is then given by $C_{ei} = F_i E_{si}$. The entrainment rate (E_{si}) is given by:

$$E_{si} = \frac{B(\lambda X_i)^5}{1 + \frac{B}{0.3}(\lambda X_i)^5} \tag{4.5}$$

$$X_{si} = \left(\frac{u_{*s}}{w_{si}} Re_{pi}^{0.6}\right) S_0^{0.08} \left(\frac{D_i}{D_{50}}\right)^{0.2} \tag{4.6}$$

in which $B = 7.8 \cdot 10^{-7}$, D_{50} is the median grain size of the sediment mixture, $\lambda = 1 - 0.28\sigma_\phi$ is the reduction of the entrainment due to mixing effects with σ_ϕ the standard deviation of the bed material on ϕ-scale, u_{*s} is the shear velocity due to skin friction, $Re_{pi} = \sqrt{\Delta\, gD_i}D_i/\nu$ is the particle Reynolds number, ν is the kinematic viscosity and S_0 is the average bed slope of the river that we assume constant in time. The suspended sediment transport for each sediment class can be computed with:

$$q_{sis} = 9.70 u_* h F_i E_{si} \left(\frac{h}{k_c}\right)^{\frac{1}{6}} I \tag{4.7}$$

in which I can be solved by integrating the Rouse profile over the depth, but to reduce the computational effort, we use the proposed approximation by Wright and Parker (2004):

$$I \approx \begin{cases} 0.679exp(-2.23Z_{Ri}) & Z_{Ri} \leq 1 \\ 0.073Z_{Ri}^{-1.44} & Z_{Ri} > 1 \end{cases} \tag{4.8}$$

in which Z_{Ri} is the Rouse number for sediment class i.

The direction of the bed load transport is a function of the depth-averaged flow direction, the effect of secondary flow that is included in a parametrized way and the transverse bed slope. The change in the direction of bed load sediment transport due to slope effects is given by (Koch and Flokstra, 1980):

$$\tan\beta_s = \frac{\sin\beta_\tau - \dfrac{1}{f(\theta_i)}\dfrac{\partial\eta}{\partial y}}{\cos\beta_\tau - \dfrac{1}{f(\theta_i)}\dfrac{\partial\eta}{\partial x}} \tag{4.9}$$

in which β_s is the angle between the sediment direction and the bed shear stress, β_τ is the angle between the bed shear stress and the depth-averaged flow direction which can differ due to spiral flow (Jansen et al., 1979), $f(\theta_i)$ is the transverse bed slope intensity as a function of the Shields stress (θ_i) for sediment class i, and $\partial\eta/\partial x$ and $\partial\eta/\partial y$ are the bed slope in x and y direction, respectively. Many relations have been developed to estimate transverse bed slope intensity ($f(\theta_i)$), but these relations are often based on a limited amount of data and show large variation (Baar et al., 2018). In addition, the transverse bed slope intensity has a large influence on the 2D morphodynamic development of a river (e.g., Schuurman et al., 2013). Therefore, we estimate $f(\theta_i)$ using both a physically derived relation (Parker and Andrews, 1985) and an empirical based relation (Struiksma and Crosato, 1989). In contrast to the relation implemented in Delft3D by default, we use a Shield parameter based on skin friction (Johannesson and Parker, 1989). The transverse bed slope effect is given by (Parker and Andrews, 1985):

$$f(\theta_i) = \frac{f_* c_L}{1 + r c_L} \sqrt{\frac{\theta_{si}}{\alpha \xi_i \theta_c}} \tag{4.10}$$

in which f_* = 1.19 is a calibration parameter, c_L = 0.43 is the coulomb friction and r = 0.85 is the lift-drag ratio. The values for these parameters are based on a calibration by Johannesson and Parker (1989). Talmon et al. (1995) propose an empirical relation based on a limited amount of experiments and field data (Struiksma and Crosato, 1989).

$$f(\theta_i) = A\sqrt{\theta_i} \tag{4.11}$$

in which A = 0.85. We assume that only bed load transport is affected by the bed slope and therefore, the transverse bed slope effect on the total sediment load is a function of ($q_{sib}/(q_{sib} + q_{sis})$). The two relations (Equations 4.10 and 4.11) give averaged over all the grain size classes, similar values (Figure 4.2). However, for Talmon et al. (1995) the difference in $f(\theta_i)$ between the smallest and the largest grain size class is larger than for Parker and Andrews (1985). This is a result of the critical bed shear stress ($\xi_i\theta_c$) that is not taken into account in Talmon et al. (1995). In Parker and Andrews (1985), the transverse bed slope intensity for the two smaller sediment classes is the same, but the smallest sediment class is transported more as suspended load reducing the transverse bed slope effect for this sediment class (Figure 4.2).

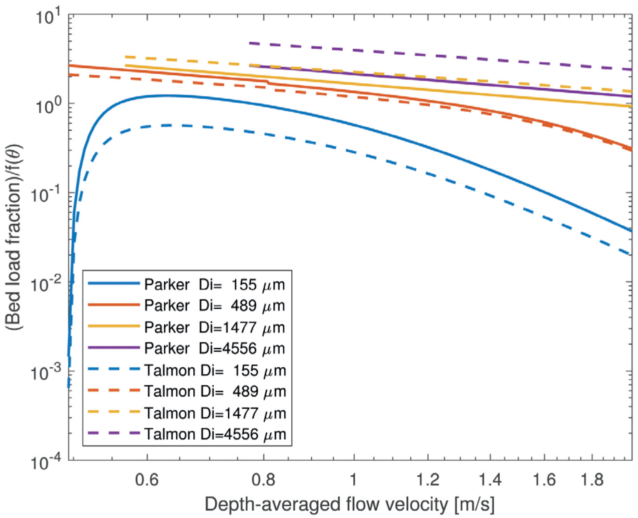

FIGURE 4.2 The transverse bed slope effect for each sediment class (Table 4.1) as a function of the flow velocity.

4.3 METHOD

We simplify the West channel at Gameren to a two-channel system with a smooth bifurcation and confluence such that a curvilinear grid can be used (Figure 4.3). We use a spatially varying numerical grid that in the side channel is 20 m by 14 m. At the upstream boundary of the domain, we apply a discharge and sediment supply, and at the downstream boundary a water level. Both the sediment supply and the water level are a function of the discharge and they correspond to equilibrium conditions of the main channel without the side channel. We apply an average yearly discharge wave (Figure 4.3) that represents the discharge in the river Waal excluding the floodplain (Yossef et al., 2008) and that is repeated each year. The roughness length and active layer thickness in the main channel and the side channel are based on measurements (Sieben, 2009; Van Denderen et al., 2019). This results in a Nikuradse roughness length of 0.5 m and 0.2 m for the main channel and side channel, respectively (Van Rijn, 1984c) and an active layer thickness of 1 m and 0.2 m for the main channel and side channel, respectively.

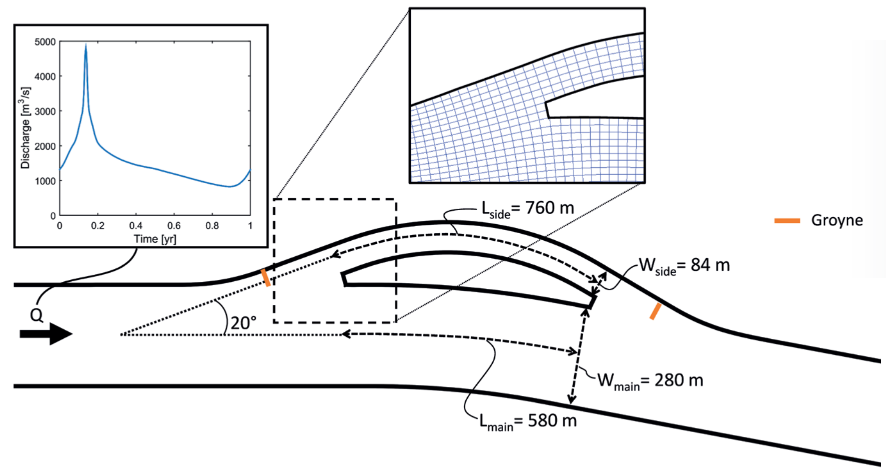

FIGURE 4.3 The domain of the side channel system, a close up of the grid, and the discharge at the upstream boundary condition.

We define four sediment classes and determine their corresponding volume fractions (Table 4.1) based on grain size measurements (Ten Brinke, 1997). We compute the equilibrium upstream sediment supply for each sediment class such that the total yearly sediment supply equals 200,000 m³/yr (Frings et al., 2015). The sediment supply for each sediment class therefore depends on the chosen sediment transport relation, and on the chosen input parameters. The upstream sediment supply is shown in Table 4.1 for the base case (Table 4.2).

Table 4.1 The sediment classes, the representative grain size (D_i), the fall velocity (w_{si}) (Van Rijn, 1984b) and the yearly sediment supply ($Q_{si,yr}$) for the base case (Table 4.2).

Class	D_{min} [mm]	D_{max} [mm]	D_i [mm]	F_i [-]	w_{si} [mm]	$Q_{si,yr}$ [m³/yr]
1	0.088	0.273	0.155	0.0173	0.0172	12,022
2	0.273	0.841	0.489	0.5384	0.0696	128,542
3	0.841	2.594	1.477	0.3451	0.1701	53,983
4	2.594	8.000	4.556	0.0992	0.2980	5,452

The initial bed level and grain size variation in the main channel are given by a morphodynamic computation without the side channel in which the main channel develops to a dynamic equilibrium. The average bed slope of this equilibrium is found to be $1.1{\cdot}10^{-4}$ which corresponds with the average bed slope of the river Waal. We assume the initial bed level of the side channel 3 m higher than the average bed level in the main channel, which corresponds with the design of the West channel at Gameren, and the initial volume fractions in the side channel are the same as those in the main channel (Table 4.1). The initial cross-section in the side channel is uniform over the length of the channel, which corresponds with how a side channel is commonly constructed.

4.3.1 VARIATIONS OF THE BASE CASE

We vary the transverse bed slope, the roughness, the boundary conditions and the initial conditions to study their effect on the development of a side channel system (Table 4.2). The total upstream yearly sediment supply and the D_{50} is assumed similar to the base case.

1. The development of a bifurcation is generally expected to be influenced by the transverse bed slope relation (e.g., Bolla Pittaluga et al., 2003). Since such a relation is uncertain (Baar et al., 2018), we apply a second relation by Talmon et al. (1995) (Case *Tal*). A second uncertainty is the supply of the finer sediment fractions at the upstream boundary of the model. The supply is based on the grain size measurements of the bed in the main channel (Section 4.3) and therefore does not include the sediment in suspension. We increase the supply of the smallest sediment class by increasing its volume fraction on the bed while keeping the D_{50} constant (Case F_1=10%).

2. The bed roughness and the active layer thickness are both smaller in the side channel than in the main channel due to smaller dune heights. However, the total hydraulic roughness is higher than just the bed form roughness due to the roughness of the channel banks and vegetation (e.g., Warmink et al., 2013). Therefore, we apply the same roughness in the side channel as in the main channel (Case *k*=0.5). We increase the active layer thickness in the side

Table 4.2 List of cases with the mechanism and the corresponding relation or parameter that is adjusted compared to the base case (Table 4.1).

Case name	Mechanism	Relation/Parameter
Base case		
	Bed load transport	Ashida and Michiue (1972)
	Hiding and Exposure parameter	Ashida and Michiue (1972)
	Suspended load transport	Wright and Parker (2004)
	Particle fall velocity	Van Rijn (1984b)
	Transverse bed slope effect	Johannesson and Parker (1989)
1. Transverse bed slope and sediment supply		
Tal	Transverse bed slope	Equation 4.11 with A = 0.85
F_1 = 10%	Initial volume fraction whole domain	F_1 = [0.1000;0.4461;0.3499;0.1040]
2. Bed roughness and active layer thickness		
k=0.5	Nikuradse roughness length side channel	k = 0.5 m
δ=1	Active layer thickness side channel	δ = 1 m
k=0.5; δ=1	Case *k*=0.5 and Case *δ=1*	k = 0.5 m; δ = 1 m
3. Initial bed level		
η_{side}-2m	Initial bed level side channel	$\eta_{side} = \eta_{side,base}$ -2 m
η_{side}+2m	Initial bed level side channel	$\eta_{side} = \eta_{side,base}$ +2 m
4. Comparison with the field		
tdgr	Thin dam as groynes (Figure 4.3)	Infinite height
Qreal	Upstream discharge	Real discharge between 1997 and 2017

channel from 0.2 m to 1 m (Case *δ=1*), which affects the mixing celerity (e.g., Sloff and Mosselman, 2012; Stecca et al., 2014). In addition, we look at a combination of an increased roughness and an increased active layer thickness in the side channel (Case *k=0.5;δ=1*).

3. We change the initial bed level of the side channel (Cases η_{side}*-2m* and η_{side}+2m), because this affects the aggradation rate and the grain size in the side channel (Van Denderen et al., 2019).

4. We compare the model results with the field and simulate therefore more realistic conditions. In Case *tdgr*, we include the effect of high groynes at the bifurcation and at the confluence of the side channel system (Figure 4.3). In addition, we found, based on measurements, that the aggradation rate of the side channel varies with the hydrodynamic conditions. Therefore, we apply a hydrograph that represents the discharge that occurred between 1997 and 2017 in the river Waal (Figure 4.4, Case *Qreal*).

04

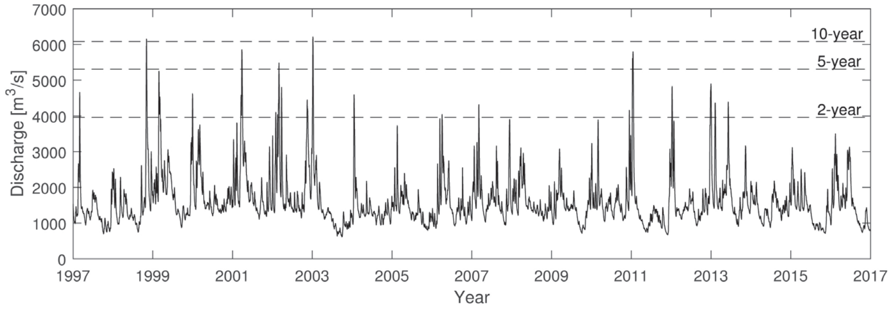

FIGURE 4.4 The measured discharge in the river Waal between 1997 and 2017 (Case *Qreal*).

4.3.2 ANALYSIS RESULTS

We first present the base case in detail by studying (1) the initial development, (2) the yearly development and (3) the long-term development of the side channel. Then, we compare the other cases to the base case using the discharge partitioning, the average bed level change in the side channel and the average grain size in the side channel. The discharge that is conveyed by the side channel during bankfull discharge condition is expected to follow an exponential function (Riquier et al., 2017; Van Denderen et al., 2018). This means that in the case of an aggrading side channel, the equilibrium discharge in the side channel during bankfull conditions approaches zero.

$$Q_{side}(t) = Q_{side,0}\exp(-t/T_{Qbank}) \tag{4.12}$$

in which $Q_{side,0}$ is the initial relative discharge in the side channel, t is the time since construction in years and T_{Qbank} is the time scale of the discharge development. We determine $Q_{side,0}$ and T_{Qbank} using a non-linear least-square fit. The resulting parameters are used to estimate the initial closing rate of the side channel ($Q_{side,0}/T_{Qbank}$) and the closing duration of the side channel. In the base case, we will show that when the model result reaches Q_{side} = 0%, the exponential function returns Q_{side} = 0.25%. We assume this to be the closing threshold.

4.4 RESULTS

4.4.1 RESULTS OF THE BASE CASE

The initial adjustment of the side channel bed is caused by a large difference between the sediment supply and the transport capacity (De Vries, 1971). This initial adjustment of the bed causes an aggradation front to pass through the side channel and adjusts the bed level and the bed slope in the side channel (Figure 4.5A). The migration rate of this bed wave is, among others, affected by the sediment transport rate and the water depth in the side channel (e.g., Jansen et al., 1979).

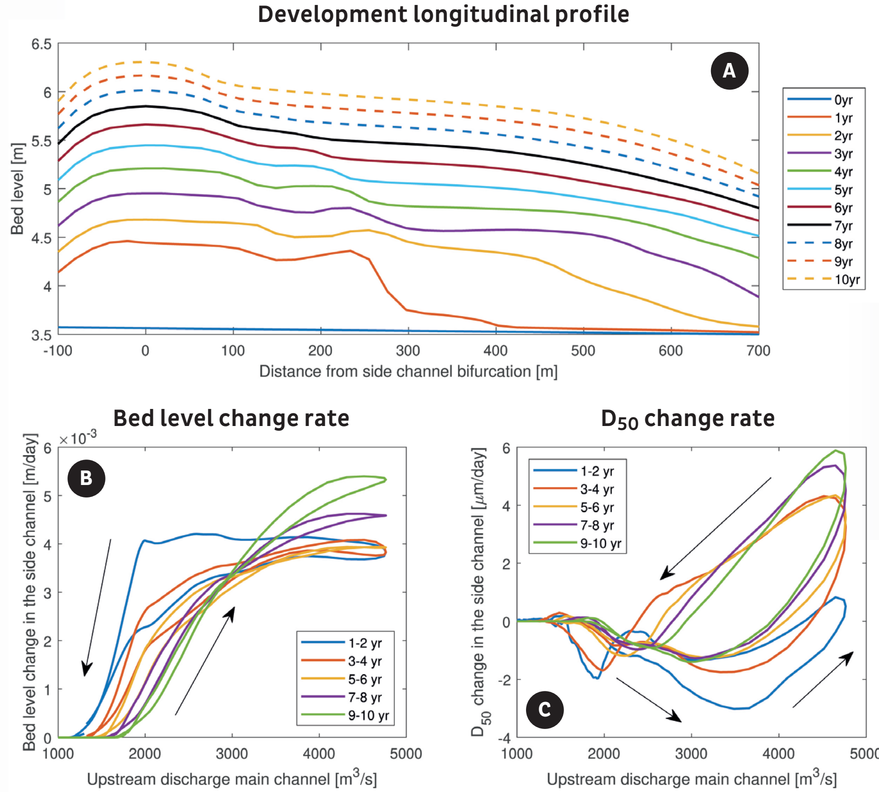

FIGURE 4.5 **(A)** The longitudinal bed level profile averaged over the width of the side channel at the start of each year. **(B)** The bed level change per day during a year as a function of the upstream discharge in the main channel. **(C)** The change of the D_{50} per day during a year as a function of the upstream discharge in the main channel. The arrows denote the chronological order.

The change of the bed level and the grain size during each year varies with discharge (Figures 4.5B and C). During the rising of the discharge, sediment is deposited in front of the side channel. The finer sediment is able to quickly migrate through the side channel leading to a fining of the aggrading bed (Figure 4.5C). The coarse sediment that is supplied to the side channel is first deposited in the upstream part of the side channel, due to the low transport capacity in the side channel. Both the sediment supply and transport capacity increase with increasing discharge and the upstream-deposited coarse sediment starts to migrate through the side channel resulting in a bed level increase and a coarsening of the bed. This lagged aggradation effect causes the hysteresis between the discharge and the aggradation rate, and between the discharge and the D_{50} (Figures 4.5B and C). The hysteresis is initially largest, because the initial aggradation front results in much larger bed level changes (Figure 4.5A). With increasing bed level in the side channel, the discharge and the sediment supply to the side channel decreases. This reduces the aggradation rate for lower discharges and increases the importance of floods. In addition, the hysteresis during one flood becomes smaller each year, because less sediment is deposited at the upstream part of the side channel. The bed of the side channel generally fines, but during each peak flow the bed coarsens slightly. The effect of the floods on the coarsening of the bed becomes more important with increasing bed level, because the coarser grains remain immobile for a longer period each year and less coarse sediment is supplied to the side channel with increasing bed level.

The long-term results show that the side channel stops to flow during bankfull conditions after about 31 years (Figure 4.6). The decrease of the discharge in the side channel during bankfull conditions seems to follow the expected exponential function (Equation 4.12). After 31 years, only flood events cause bed level changes in the side channel system. Before and after a flood the grain size decreases and during the flood the grain size increases (Figure 4.5C). This results in small spikes in the decreasing trend of the grain size each year (Figure 4.6). Hence, with increasing bed level in the side channel, the supply of coarse sediment decreases leading to a continuing fining of the side channel bed.

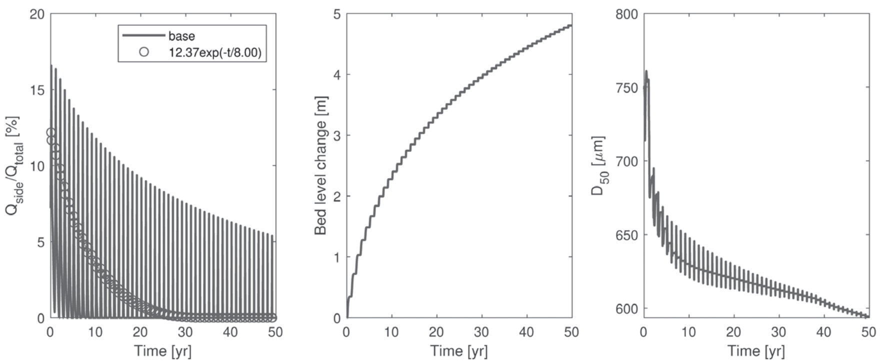

FIGURE 4.6 The relative discharge in the side channel with the bankfull discharge marked with circles, the average bed level change and the average D_{50} in the side channel for the base case.

4.4.2 VARIATIONS ON THE BASE CASE

We now compare the development of the base case with each of the variations. As the initial response of the bed to the side channel construction disappears within 5 years after construction (Figure 4.5A) and the exponential decrease of the discharge in the side channel can be estimated by the first 10 years accurately (Figure 4.6), we study only the first 10 years of the variations of the base case which reduces the computational effort. We compare the average bed level and the average D_{50} in the side channel after 10 years (Figure 4.7A) and we estimate the initial closing rate ($Q_{side,0}/T_{Qbank}$) and the closing time of the side channels using Equation 4.12 (Figure 4.7B).

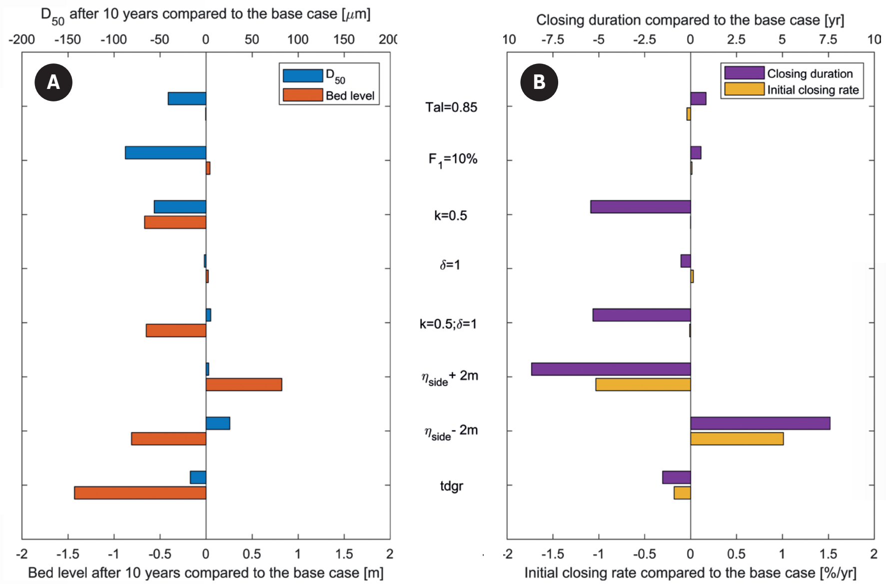

FIGURE 4.7 (A) The grain size and the bed level compared to the base case ($\Delta\eta_{t=10yr}$ = 5.8 m and $D_{50,t=10yr}$ = 630 μm). (B) The closing duration and the the initial closing rate ($Q_{side,0}/T_{Qbank}$) compared to the base case ($Q_{side,0}/T_{Qbank}$ = 1.5 %/yr and t_{closed} = 31 yr).

TRANSVERSE BED SLOPE AND SEDIMENT SUPPLY

The transverse bed slope affects the sediment supply to the side channel. The bed level change of Case *Tal* is quite similar to the base case, but the D_{50} becomes smaller (Figure 4.7A). This is an effect of the hiding exposure relation that is not included in Talmon et al. (1995), and therefore the transverse bed slope effect is smaller for the smaller grain sizes and larger for the larger ones (Figure 4.2). The relation by Parker and Andrews (1985) is physically more sound and therefore the comparison indicates that Talmon et al. (1995) generally overestimates the sorting due to transverse bed slope effect.

If we increase the sediment volume fraction of the first sediment class (Case F_1=10 %), we increase the sediment supply in the main channel of this sediment class. The sediment supply to the side channel is therefore finer and larger compared to the base case, because a larger fraction of the sediment is transported as suspended load which is less affected by the transverse bed slope effect (Figure 4.2). This results in a fining of the bed and a small bed level increase. The fining of the bed leads to a larger transport capacity in the side channel and therefore, the bed level increase in the side channel is limited.

BED ROUGHNESS AND ACTIVE LAYER THICKNESS

In Case k=0.5, the roughness in the side channel is increased which leads to smaller discharge conveyance in the side channel. The lower Shields parameter reduces the sediment supply. The supply of larger grain sizes reduces relatively more compared to the smaller grain sizes, because their Shields stress is closer to the critical Shields stress. This leads to a finer bed in the side channel compared to the base case. The initial discharge in the side channel is larger compared to the base case and therefore, although the initial closing rate is the same, the closing duration decreases (Figure 4.7B).

The active layer thickness has a limited effect on the bed level changes in the side channel system (Figure 4.7). However, a larger active layer thickness reduces the celerity of the sorting waves (Ribberink, 1987). For Case δ=1, the effect of the active layer thickness on the development of the side channel is negligible, but in Case k=0.5;δ=1 there is much less fining of the side channel bed (Figure 4.7). In case of a larger active layer thickness, relatively more sediment is needed to adjust the D_{50} of the active layer. In Case δ=1, the aggradation is large enough such that the grain size difference with the base case is limited. However, in Case k=0.5;δ=1, less sediment is deposited in the side channel resulting in less fining of the side channel bed (Figure 4.7A).

INITIAL BED LEVEL

The initial bed level changes the aggradation rate of the side channel. An increase of the bed level leads to a smaller initial discharge, transport capacity and sediment supply. This results in a smaller migration rate of the initial aggradation front and a smaller overall aggradation rate (Figure 4.7B). The bed level difference with the base case therefore reduces over time (Figure 4.7A). The smaller initial discharge reduces the closing duration, even with the smaller aggradation rate.

A decrease of the initial side channel bed level increases the closing rate of the side channel and the bed level difference with the base case decreases over time (Figure 4.7). The grain size in the side channel is larger for Case η_{side}-2m

compared to the base case, because the lower bed level results in a larger supply of coarse sediment. In Case η_{side}-2m, degradation occurs during the flood (Figure 4.8) and lower discharges are more important for the aggradation in the side channel compared to the base case (Figure 4.5C). This is caused by the sediment supply that is too large during the higher discharges, which results in deposition upstream of the side channel that during lower discharges is transported into the side channel.

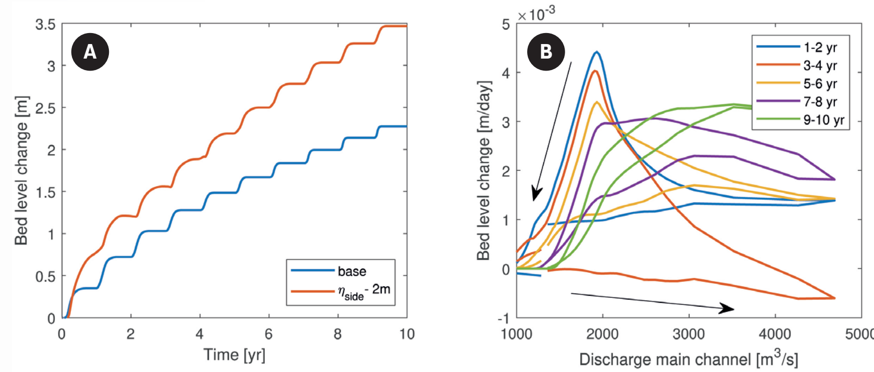

FIGURE 4.8 **(A)** The average bed level change and **(B)** the average bed level change per day of Case η_{side}-2m as a function of the upstream discharge. The arrows denote the chronological order.

4.4.3 COMPARISON WITH THE FIELD

GROYNES

The groynes at the bifurcation and the confluence (Figure 4.3) reduce the discharge and flow velocity in the side channel. The lower bed shear stresses result in a smaller sediment supply and a lower transport capacity, leading to less aggradation and an increased fining of the side channel bed (Figure 4.7).

COMPARISON WITH GAMEREN

Our model is loosely based on a simplified version of the West channel in the side channel system near Gameren. The dimensions are overall quite similar except that we assume a constant channel width and overbank flow is ignored. The latter assumption is based on hydrodynamic computations that show that the exchange of discharge between the main channel or the other side channels over the floodplain is limited (Van Denderen et al., 2019).

So far we looked at a yearly repeated hydrograph, but now we take discharge variations into account by applying the actual discharge that occurred between

1997 and 2017 (Figure 4.4). The variation of the discharge and the variation of the aggradation rate are therefore much larger (Figure 4.9). Initially the peak discharges are shorter and smaller than the repeated hydrograph leading to a smaller migration of the initial bed wave. However, from 2000 onwards, several large floods occurred resulting in a large increase of the bed level. In the period between 2004 and 2011, large floods did not occur and the aggradation rate is smaller and the grain size in the side channel decreases. The flood in 2011 resupplies the channel with coarse material and increases the aggradation rate of the side channel. On average, the repeated average yearly hydrograph of the base case corresponds well with the bed level changes of the real hydrograph. Individual flood events or the absence of flood events causes deviations from the average bed level change in the base case.

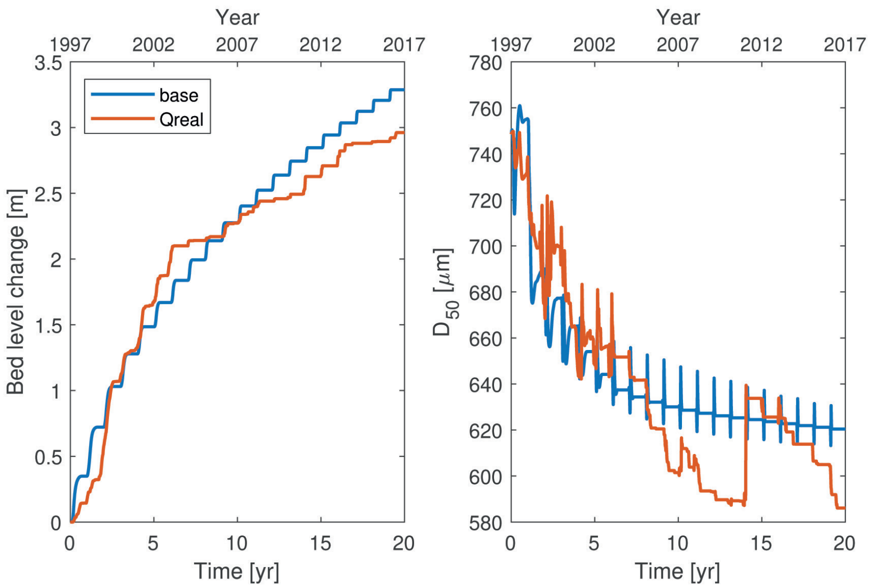

FIGURE 4.9 The relative discharge in the side channel, the bed level change and the grain size variation over time for Case *Qreal*.

4.5 DISCUSSION

We compared the results of the base case with measurements (Van Denderen et al., 2019) and find that in the base case the bed level changes in the side channel are overestimated. In addition, the model overestimates the grain size in the side channel after 10 years. We have studied the effect of several model parameters and side channel characteristics. The results show that a combination of these cases could reproduce the correct aggradation rate and grain size. The model presented here seems to overestimate the bed shear stress in the side channel compared to more realistic hydrodynamic computations (Van Denderen et al., 2019). This seems to be a result of the vegetated floodplain and channel banks that are not included in the model. The overestimated bed shear stress increases both the sediment supply and transport capacity. However, in general, the results of the base case show similar mechanisms compared to measurements. Each of the cases shows aggradation and a fining of the side channel bed. The model simulates also the importance of floods on the aggradation rate in the side channel and the supply of coarse sediment to the side channel during floods.

4.5.1 SUPPLY VERSUS CAPACITY

The development of a side channel system is based on the difference between the sediment supply and the transport capacity. Both are a function of the Shields stress and studies have shown that an equilibrium state of the bifurcation varies with the Shields stress (Edmonds and Slingerland, 2008; Bolla Pittaluga et al., 2015). The Shields parameter is a function of the grain size and the bed shear stress. Therefore, these parameters need to be correctly estimated by the model. Using a morphodynamic model with a single grain-size class that is equal to the D_{50} in the main channel will overestimate the grain size of the sediment that is supplied and deposited in the side channel. This results in an underestimation of the sediment volume that is supplied to the channel and the transport capacity in the channel. The resulting aggradation rate will be incorrect and an unrealistic equilibrium state of the side channel might be reached in which the side channel remains open. Measurements show that grain-size sorting occurs at the bifurcation of a side channel system and that the deposited sediment in the side channel is much finer than the sediment on the bed of the main channel (Van Denderen et al., 2019). The supply of coarse material to the side channel can reduce due to, for example, bed slope effects (Case *Tal*), the fraction of the sediment that is transported as suspended load (Case F_1=10%). or a reduced Shields stress at the bifurcation (Case *tdgr*). The transport capacity of a side channel with a bed of fine sediment is larger than one with a bed of coarse sediment. This means that, under the same hydrodynamic conditions, the total sediment transport in the side channel with a finer bed is larger compared to the base case, e.g. Case F_1=10%. Mixed sediment processes are therefore important in estimating the sediment supply and the transport capacity, and thereby, the aggradation and degradation of the side channel.

The second parameter in the Shields stress is the bed shear stress, which is a function of, for example, the bed roughness, the bed level of the side channel and the upstream discharge. Generally, a constant discharge is used in bifurcation modeling. Therefore, we simulate four additional cases that highlight the difference between a varying upstream discharge and a stationary discharge. We select a constant upstream discharge of 2000 m^3/s, 2300 m^3/s (bankfull discharge), 2900 m^3/s and 4750 m^3/s (peak discharge). The results show that the development of the side channel varies with the discharge (Figure 4.10). The migration of the initial aggradation front is visible as a change in the aggradation rate that occurs for each of the cases within five years (Figure 4.10B). The migration rate in Case *Q4750* is smallest, because more coarse sediment is supplied to the side channel resulting in a slower migration of the bed wave. The four computations show that when a certain bed level is reached that the side channel's bed starts to become finer. The bed level height at which this occurs depends on the upstream discharge and from this bed level height the bed shear stress is too small to supply the coarser sediment classes to the side channel. Until that point is reached, the grain size in the side channel is more or less constant and similar as in the main channel. Cases *Q2000* and *Q2300* reach an equilibrium state, because the transverse bed slope upstream of the bifurcation diverts sediment away from the entrance of the side channel. In the case with a constant bankfull discharge, the side channel does not fully close and the aggradation rate of the side channel is larger compared to the base case. Therefore, it seems that computing the development of bifurcations with a mixed-sediment model and a constant upstream discharge leads to unrealistic equilibrium states of the side channel's bed level. Both mixed-sediment and varying-discharge mechanisms are required to estimate the sediment supply and transport capacity of the side channel in a realistic way.

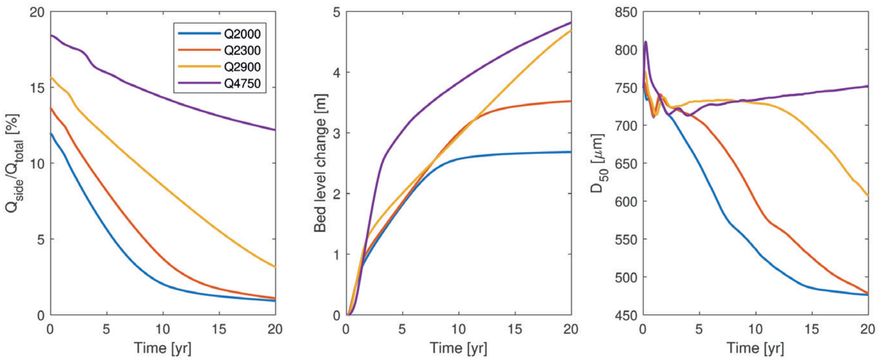

FIGURE 4.10 The relative discharge in the side channel, the bed level change and the grain size variation over time for four cases with a constant upstream discharge in the main channel.

4.5.2 MAIN UNCERTAINTIES

There are several assumptions that seem to affect the side channel development. Firstly, floodplains were not taken into account and for the Gameren case this seems to be a reasonable assumption, because due to levees the West channel is almost fully separated from the floodplain. However, this assumption causes an overestimation of the bed shear stress in the side channel, because the bed shear stress reduces in the channels when overbank flow occurs (Van Denderen et al., 2019). This effect is similar to a higher side channel roughness during floods and including it would result in a smaller sediment supply and aggradation rate during flood conditions, similarly to Case *k=0.5*.

Secondly, the transverse bed slope and the spiral flow just upstream of the bifurcation affect the sediment supply to the channel. The transverse bed slope intensity ($f(\theta_i)$) is still uncertain (Baar et al., 2018) and clearly affects the sediment supply and sorting at the bifurcation (Case *Tal*). Spiral flow occurs at the bifurcation due to the bifurcation angle. In the model, we assume that the suspended bed-material load is similarly affected by the spiral flow as bed load. This is reasonable because measurements of the side channels at Gameren show that sediment that is deposited in the side channels is transported in suspension up to 1 meter from the bed (Frings and Kleinhans, 2008; Van Denderen et al., 2019). However, both the suspended sediment concentration and the spiral flow intensity vary over the depth. The amount of suspended load that is affected by the spiral flow in a 2DH model should therefore depend on the variation of the transverse flow velocity over the depth and the Rouse number.

Finally, the groynes seem to significantly affect the side channel development. We assume that nor water nor sediment is able to flow over the groyne and this is very simplistic. Our simple assumption allows for a first estimation of the influence of groynes, since physical and numerical experiments have shown that current modeling of the flow and sediment over weirs is still limited (Busnelli, 2001; Lauchlan, 2004). In addition, the bed level changes within a groyne field are affected by navigational currents. Measurements showed that the aggradation in a groyne field is a balance of an import of sediment during high discharges and an export of sediment during lower discharges caused by navigational currents (Ten Brinke et al., 2004; Yossef, 2005). The effects are ignored in the model, but likely results in the removal of the deposited sediment within a groyne field during base flows and thereby increases the time scale of side channel development.

4.6 CONCLUSION

Multiple grain size classes and varying hydrodynamic conditions are needed to study the stability of a bifurcation. Therefore, we use a mixed-sediment morphodynamic model with varying hydrodynamic conditions to estimate the development of the side channel system in a quantitative way. We find that the initial aggradation in an artificial side channel is large due to the migration of the initial aggradation front. After this front has passed through the system, the aggradation is much slower. The lower discharges are responsible for the fining of the sediment on the side channel bed. The larger discharges cause a coarsening and the largest aggradation. The base case shows that the side channel closes during bankfull conditions due to the supply of sediment during floods.

The development of the side channel is affected by the transverse bed slope effect, the grain size of the supply sediment in the river, the bed roughness in the side channel, the active layer thickness in the side channel, the initial bed level of the side channel, structures at the bifurcation and confluence, and the variation in the hydrodynamic regime. Each of these mechanisms and characteristics of a side channel system affect the sediment supply and transport capacity in the side channel and thereby, the aggradation rate and the grain size in the side channel. With the proposed model, we can, for the first time, estimate the development of side channels in a quantitative way.

ACKNOWLEDGEMENTS *This research is supported by the Netherlands Organisation for Scientific Research (NWO), which is partly funded by the Ministry of Economic affairs, under grant number P12-P14 (RiverCare Perspective Programme) project number 13516. This research has benefited from cooperation within the network of the Netherlands Centre for River studies (https://ncr-web.org).*

Photo: Bureau Beeldtaal Filmmakers

CHAPTER 5

A characterization of side channel development

This chapter is submitted as
Van Denderen, R.P., R.M.J. Schielen, M.W. Straatsma, M.G. Kleinhans and S.J.M.H. Hulscher: A characterization of side channel development.

Side channels are commonly constructed to reduce the flood risk or to increase the ecological value of a river. Such artificial side channels generally aggrade. We characterize the development of side channels based on the sediment that is deposited in these channels. Based on this characterization, we determine the main mechanisms that affect their development and we propose an initial framework on how to predict the long-term development of side channels. The results can be used to design, operate and maintain side channel systems.

5.1 INTRODUCTION

It is well known that artificial side channels generally aggrade (e.g., Simons et al., 2001; Riquier et al., 2017; Van Denderen et al., 2019). There is a need for a better understanding of the mechanisms and the processes that result in an aggrading side channel. Our objective is to propose a categorization of side channel development and to present its practical implications. The categorization is based on the sediment deposited in the side channel and the sediment transport properties in the main channel. The categorization can help to assess which mechanisms and processes are important in the development of a side channel system and can support the design, operation and maintenance of a side channel. The practical implications of the categorization are based on a one-dimensional model that was previously used to reproduce the development of side channel systems (Van Denderen et al., 2018). We use the model to estimate the temporal scale of the side channel development for each of the categories as a function of the width/depth ratio of the side channel and its length relative to the main channel, which are both common design parameters of side channels.

5.2 CONCEPTUAL CHARACTERIZATION OF SIDE CHANNELS

Mechanisms such as bed slope effects or spiral flow at the bifurcation usually determine the sediment partitioning (Kleinhans et al., 2011), but sediment that is transported in suspension is much less affected by such mechanisms than sediment that is transported near the bed. We present three main categories of side channels based on the classification of the sediment transport in the main channel: predominantly (1) bed load supplied side channels, (2) suspended bed-material load supplied side channels and (3) wash load supplied side channels (Figure 5.1). Note that the sediment transport classification represents the sediment that the predominantly deposited in the side channel and that also other types of sediment can be supplied. For example, wash load is also supplied to a bed load supplied channel, but is not deposited due to, for example, a high bed shear stress. The category can change over time due to an increasing bed level (Makaske et al., 2002; Van Denderen et al., 2019) or due to changes in the flow conditions (Riquier et al., 2015). Each category corresponds with mechanisms that affect the sediment supply to a side channel or the transport capacity in a side channel. Differences between the sediment supply and the transport capacity lead to morphodynamic changes.

5.2.1 BED LOAD SUPPLIED SIDE CHANNELS

Bed load supplied side channels are supplied with sediment that is transported as bed load in the main channel (Figure 5.1) and therefore consist mainly of gravel or sand (Church, 2006). The sediment supply to the side channel is affected by transverse bed slope effects (Bolla Pittaluga et al., 2003) and spiral flow. Spiral flow can be a result of a river bend upstream of the bifurcation (Kleinhans et al., 2008) or a large bifurcation angle (Bulle, 1926). Spiral flow causes a near-bed flow velocity that has a different direction compared to the depth-averaged flow direction and hence, it can direct relatively more sediment to the side channel if the bifurcation is located in an inner bend. The transverse bed slope effect is a function of the Shields stress and the bed level difference between the side channel and the main channel (Bolla Pittaluga et al., 2003). Therefore, bed load sediment can only be supplied to the side channel if a sufficiently small bed level difference is combined with a sufficiently large Shields stress. If the transport capacity in the side channel is relatively low, a plug bar of coarse sediment forms at the entrance of the channel (Constantine et al., 2010) and if the transport capacity is sufficiently high, the deposition of coarse sediment is more evenly distributed over the channel (Dieras et al., 2013) (Figure 5.1).

A typical example of a bed load supplied side channel is the filling of a meander just after the initiation of a cutoff channel. Initially, the bed level difference between the main channel and the meander is relatively small and therefore bed

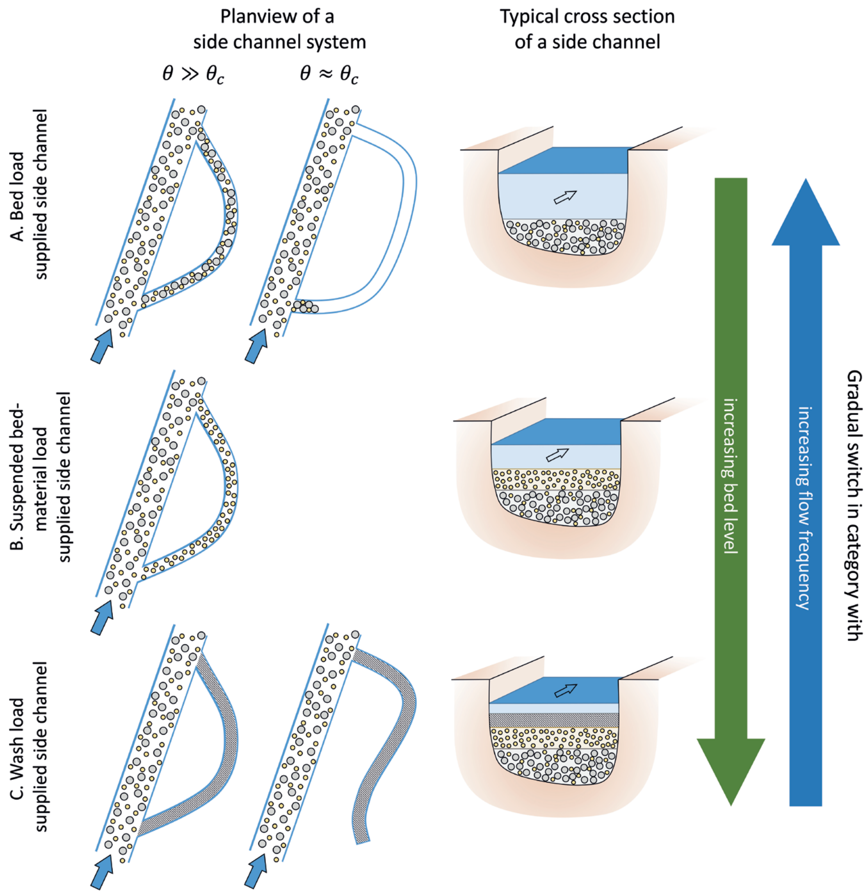

FIGURE 5.1 Schematic of the categorization of side channels compared to the main channel and the typical infilling of a side channel cross section that due to the increase of bed level changes in category. θ represents the Shield's stress and θ_c the critical Shield's stress. The largest gray circles represent sediment transported in the main channel as bed load, the smaller yellow circles represent sediment transported in the main channel as suspended bed-material load and the shaded areas denote deposited wash load.

load sediment can enter the channel. In the river Ain (France), two cutoff events occurred between 1996 and 2005. Near Mollon (Figure 5.2A), the East channel used to be the main channel, but after a flood in 1996 the West channel started flowing and became the dominant channel in 2003 (Dieras et al., 2013). The deposition of gravel occurred over the length of the channel (Dieras et al., 2013). This is in contrast to a strongly curved meander in the river Ain that shows the formation of a plug bar (Figure 5.2C). The meander is much longer than the cutoff. The sediment supply to the meander is large due to the small bed level difference and, due to a limited sediment mobility in the channel, a plug bar formed (Dieras et al., 2013).

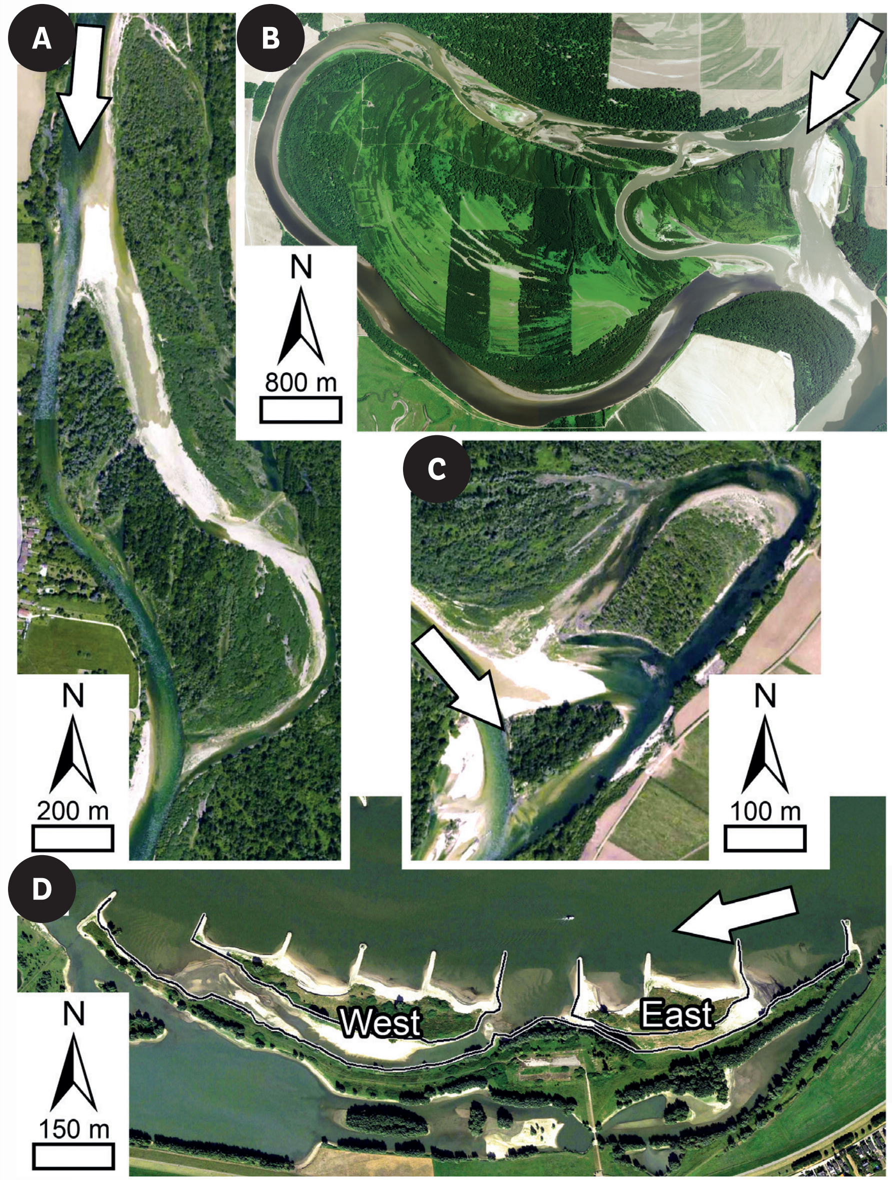

FIGURE 5.2 Aerial images of side channel systems. **(A)** Old meander in the river Ain (France) near the Mollon. **(B)** The Mackey Bend in the Wabash river (USA). **(C)** An old meander in the river Ain (France) near Martinaz. **(D)** A constructed side channel system near Gameren in the river Waal (The Netherlands). (*Images from IGN France, NAIP and Google Earth*)

5.2.2 SUSPENDED BED-MATERIAL LOAD SUPPLIED SIDE CHANNELS

Suspended bed-material load supplied side channels are filled with sediment that can be found on the bed of the main channel and that is partly transported in suspension (Figure 5.1). Suspended bed-material load consists primarily of sand (Church, 2006). The sand is mainly transported in the bottom half of the water column in the main channel and once supplied to the side channel, it is likely transported as bed load (Van Denderen et al., 2019). The sediment on the bed of the side channel is finer than the sediment found on the bed of the main channel (Van Denderen et al., 2019). Sorting occurs at the bifurcation, because a large bed level difference between the channels is combined with a low Shields stress such that the coarse bed load cannot enter the side channel. The suspended bed-material load, which has a smaller grain size compared to bed load, is partly transported in suspension and is transported more easily up the bed slope (Parker and Andrews, 1985). Deposition of silt and clay can occur if the bed shear stress in the side channel is low (Van Denderen et al., 2019) or if the channel is sufficiently shallow such that vegetation colonizes the channel bed and traps fines (Makaske et al., 2002). The bed level at which this occurs depends on the hydrodynamic conditions in the main channel (Figure 5.1). During periods of low discharge, finer sediment is deposited compared to periods with regular floods (Riquier et al., 2015).

Suspended bed-material load channels are present in the river Waal in the Netherlands (Van Denderen et al., 2019) and also seem to occur in the river Rhône in France (Riquier et al., 2015). At Gameren in the river Waal (Figure 5.2D), the East and the West channel are mainly filled with suspended bed-material load (Van Denderen et al., 2019). The West channel flows more frequently than the East channel. In addition, groynes are located at the bifurcations and at the confluences of the side channels reducing the discharge conveyance in the side channel and the bed shear stress at the bifurcation (Van Denderen et al.). The East channel reached a bed level that allows for the growth of vegetation and the trapping of fines (Van Denderen et al., 2019), making the transition into a wash load supplied side channel.

5.2.3 WASH LOAD SUPPLIED SIDE CHANNELS

Wash load supplied side channels are filled with sediment that is transported as wash load in the main channel and that is generally not found on the bed of the main channel (Figure 5.1). Wash load transport consists generally of silt and clay (Church, 2006), occurs more or less uniformly over the water column and does not affect the river slope or width (Paola, 2001). Side channels filled with wash load deposits are often blocked at the bifurcation with a logjam or a plug bar (e.g., Makaske et al., 2002) or are located further away from the main channel. Artificial side channels show similar behavior if they are only connecting to the main channel at the downstream end. The sediment supply to the side channel occurs during overbank flow conditions and is proportional to the discharge conveyance of the channel. The distance between the upstream side of the side channel and the main channel can become important, because the sediment concentration reduces in the floodplain with increasing distance from the main channel (Middelkoop and Asselman, 1998). Inside the side channel, the deposition processes are expected to be similar to deposition processes in the floodplains. This means that non-equilibrium sediment transport is important (Asselman and Van Wijngaarden, 2002), and the sediment deposition is lagged in time and space compared to a change in transport capacity as a function of the settling velocity.

The Mackey bend in the Wabash River is an example of a wash load supplied side channel (Figure 5.2B). The large meander was cutoff twice and the East channel is now the main channel. Measurements showed that in the other two channels mainly silt and some clay is deposited (data from USACE and Zinger, 2016). The discharge in the channels is limited allowing fines to settle. Wash load supplied side channels were also found in the Columbia River in Canada (Makaske et al., 2002) and in the river Rhône in France (Riquier et al., 2015).

5.3 PRACTICAL IMPLICATIONS

Each category of side channels (Figure 5.1) develops differently. Here we propose a preliminary method to estimate the time scale of side channel development for each category. The method is based on a previously published 1D model (Kleinhans et al., 2012). The development of bed load and suspended bed-material load supplied side channels can be estimated using a simple backwater model. Van Denderen et al. (2018) apply such a model to bed load supplied side channel systems. The transport capacity in such channels is best represented using a transport relation that includes the initiation of motion (Bolla Pittaluga et al., 2015). The roughness and grain size in the side channel are assumed similar to the main channel (Table 5.1). For suspended bed-material load supplied channels, the sediment sorting at the bifurcation is significant and in order to compute the transport capacity in the side channel, a smaller grain size and bed roughness should be taken into account compared to the main channel (Table 5.1). In addition, we use a sediment transport relation that includes both bed load and suspended bed-material load transport (Bolla Pittaluga et al., 2015). The sediment supply is assumed to be equal to the discharge partitioning, which is reasonable since the sediment is transported near the bed in suspension. The development of wash load supplied channels is more difficult to model, since the bed level changes are a function of the peak flow frequency, peak flow intensity and the 2D flow patterns in the floodplain. Deposition of fines occurs below a critical bed shear stress for sedimentation. A first estimate of the bed level changes in the side channel can then be made based on the average flow velocity and an estimate of the sediment concentration in the main channel (e.g., Asselman and Van Wijngaarden, 2002).

Table 5.1 The relations that can be used to estimate the side channel development for the three categories.

	Bed load	Suspended bed-material load	Wash load
Sediment supply (Q_s)	Bolla Pittaluga et al. (2003)	$\frac{Q_{s,side}}{Q_{s.main}} = \frac{Q_{side}}{Q_{main}}$	$\frac{Q_{s,side}}{Q_{s.main}} = \frac{Q_{side}}{Q_{main}}$
Transport capacity	e.g., Meyer-Peter and Müller (1948)	e.g., Engelund and Hansen (1967)	e.g., Asselman and Van Wijngaarden (2002)
Grain size	Similar to main channel	Based on grain size measurements	-
Roughness	Similar to main channel	Based on ripple/dune height in side channel	Based on ripple/dune height or vegetation in side channel

As an example, we apply our modeling approach to the three categories for various initial geometries. We assume that the side channels are connected to the main channel during bankfull conditions. This allows for the usage of a simple one-dimensional model (Appendix 5.A). We vary the initial width/depth ratio and the length of the side channel while keeping the initial discharge partitioning constant. The initial discharge is assumed 10%, 1% and 0.1% for a bed load, a suspended bed-material load and a wash load supplied side channel, respectively. Using these conditions, we compute the time scale needed to reach an equilibrium state where the discharge in the side channel does not change more than 0.01% of the upstream discharge during 100 years (Figure 5.3). We normalize the time scale to (1) incorporate changes in the sediment volume that is needed to fill in the side channel with the changing geometry and (2) make it more generally applicable (Appendix 5.B). In addition, we show the estimated time scale for cases in the river Waal and the Mississippi River (Figure 5.3). The bed load supplied case shows that the time scale decreases towards a switch from an aggrading to a degrading side channel. This switch corresponds with a case where the initial condition is the same as the equilibrium state of the side channel system. For suspended bed-material load supplied side channel systems, one of the channels always closes. The largest time scale (Figure 5.3C) occurs close to the switch from a dominant main channel to a dominant side channel that occurs for small length and width/depth ratios. The closing time scale of wash load supplied side channels is generally much larger (Figure 5.3F). Only for high width depth ratios, the bed shear stress is small enough such that erosion does not occur. The region in which erosion does not occur is much larger for side channels that are not connected to the main channel at both its extremities.

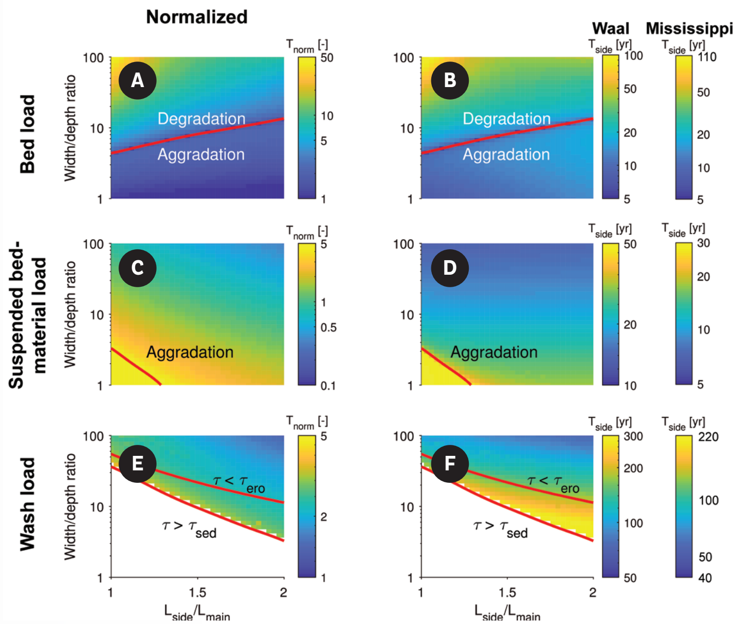

FIGURE 5.3 The normalized time scale **(A, C, E)** needed to reach an equilibrium state of a side channel and the time scale applied to cases in the river Waal and the Mississippi River **(B, D, F)** as function of the length ratio with the main channel and the width/depth ratio of the side channel.

5.4 CONCLUDING REMARKS

We present a categorization for side channel systems such that the main mechanisms for its development are easily identified (Figure 5.1). In addition, we propose an initial framework to easily estimate the side channel development (Table 5.1) that will help to optimize the design, operation and maintenance of side channels. For a combined assessment of planimetric forcing and mixtures of sediment, it would be essential to run a two or three-dimensional flow and morphodynamic model with multiple grain-size classes.

ACKNOWLEDGEMENTS *This research is supported by the Netherlands Organisation for Scientific Research (NWO), which is partly funded by the Ministry of Economic affairs, under grant number P12-P14 (RiverCare Perspective Programme) project number 13516. This research has benefited from cooperation within the network of the Netherlands Centre for River studies (https://ncr-web.org). We thank an anonymous reviewer for his/her comments that helped to improve the paper.*

APPENDIX

In these appendices, we give a brief overview of the parameters for the model used. For a more detailed description, we refer to Kleinhans et al. (2011) and Van Denderen et al. (2018).

5.A MODEL DESCRIPTION

The three defined categories indicate the governing mechanisms for the development of a side channel system. We use a one-dimensional (1D) bifurcation model that previously was used to estimate bifurcation development (Kleinhans et al., 2011; Van Dijk et al., 2012, Gupta et al., 2014; Van Denderen et al., 2018). We assume a constant upstream bankfull discharge with a constant downstream water level. The water depth in the channels is solved using a second-order numerical backwater solver (Parker, 2004). We introduce an intermittency factor for the bed load and suspended bed-material load cases, which corrects for the overestimation of the yearly sediment supply at the upstream boundary of the model. This factor is defined as the measured yearly-averaged sediment transport rate of the river divided by the yearly-averaged sediment transport rate as estimated by the model with constant bankfull discharge conditions (Van Denderen et al., 2018).

BED LOAD SUPPLIED SIDE CHANNELS

The sediment supply is computed using Kleinhans et al. (2011) which is an adaptation on Bolla Pittaluga et al. (2003). This relation is able to reproduce the development of bed load supplied side channels (Van Denderen et al., 2018). We choose to use Meyer-Peter and Müller (1948) for the sediment transport.

SUSPENDED BED-MATERIAL LOAD SUPPLIED SIDE CHANNELS

The sediment supply is computed using:

$$\frac{Q_{s,side}}{Q_{s,main}} = \left(\frac{Q_{side}}{Q_{main}}\right) \tag{5.1}$$

in which $Q_{s,side}$ and $Q_{s,main}$ are the sediment supply to the side channel and the main channel, and Q_{side} and Q_{main} are the discharges in the side channel and the main channel. The sediment transport in the channels is computed using Engelund and Hansen (1967).

WASH LOAD SIDE CHANNELS

In wash load side channels, we assume a sediment concentration in the main channel such that after a year during bankfull conditions, the sediment transport rate of wash load equals the measured yearly-averaged wash load of the river. We assume the sediment concentration uniformly distributed over the depth and width of the river and the sediment supply to the side channel is then given by Equation 5.1. The sediment deposition is computed in each cell following Asselman and Van Wijngaarden (2002). They assume that deposition does not occur when the bed shear stress is above a critical bed shear stress and that erosion does not occur. The latter is a reasonable assumption for an aggrading side channel under constant hydrodynamic conditions. The deposition flux is given by:

$$Q_{sus,dep} = Q_{sus}\left(1 - e^{-w_s\frac{A}{Q}}\right) \tag{5.2}$$

in which $Q_{sus,dep}$ is the deposition flux, Q_{sus} the sediment supply of wash load, w_s the particle fall velocity, A the horizontal surface area of the channel or computational cell and Q the discharge to the cell.

5.B MODEL CONDITIONS

We assume conditions similar to the river Waal in the Netherlands. The yearly-averaged sediment supply of sediment larger than 63 µm is 200,000 m³/yr and for sediment smaller than 63 µm is 550,000 m³/yr. The bankfull discharge is assumed 2900 m³/s and the average width of the main channel 280 m. The downstream water level is chosen such that water depth in the downstream main channel is (initially) uniform. We assume that the initial discharge varies for each category such that the initial geometry is more representative for this category (Table 5.2). We compute the side channel development until the discharge in the side channel does not change more than 0.01% of the upstream discharge during 100 years. The time scale shows at which moment this discharge is first reached. We present the time scale in a normalized way and in a way that is representative for the river Waal and the Mississippi River (Table 5.3).

NORMALIZED TIME SCALE

We normalize the time scale by dividing the model result with a time scale that is a balance between the sediment supply and the transport capacity. The way the time scale is normalized differs therefore for each type of side channel.

$$T_{norm} = \frac{T_{side}}{T_{cat}} \tag{5.3}$$

in which T_{norm} is the normalized time scale, T_{side} is the time scale of the model result and T_{cat} is the time scale based on a balance between the sediment supply and the transport capacity, and changes for each category: T_{bed}, T_{susbed} and T_{wash}.

Table 5.2 Main parameters for the hydrodynamic and morphodynamic conditions for the main channel and for the side channel categories. Empty cells denote that the parameter is unused in such a side channel. The roughness height is found from Van Denderen et al. (2019), the grain size from Ten Brinke (1997); Van Denderen et al. (2019) and the wash load parameters from Asselman and Van Wijngaarden (2002).

	Main channel	Bed load supplied	Suspended bed-material load supplied	Wash load supplied
Initial discharge side channel		10%	1%	0.1%
Roughness height [m]	0.5	0.5	0.2	0.2
Grain size [mm]	0.75	0.75	0.3	
Critical Shields stress [-]		0.035		
Particle fall velocity [m/s]				$7{\cdot}10^{-5}$
Critical bed shear stress sedimentation [N/m²]				2.0
Critical bed shear stress erosion [N/m²]				0.5

Table 5.3 The main parameters for the river Waal and the Mississippi River. The particle fall velocity is chosen the same for the river Waal and the Mississippi River to reduce the uncertainty in the comparison associated with this parameter. The chosen particle fall velocity falls within the expected range (Fernández et al., 2018).

	River Waal	Mississippi River
Annual sediment load (bed load + suspended bed-material load) [m³/yr]	200,000 (Frings et al., 2015)	7,500,000 (Nittrouer et al., 2008)
Annual sediment load (wash load) [m³/yr]	550,000 (Frings et al., 2015)	26,000,000 (Nittrouer et al., 2008)
Grain size [mm]	0.75 (Ten Brinke, 1997)	0.44 (Fernández et al., 2018)
Bankfull discharge [m³/s]	2900	30,000 (Harmar, 2004)
Bankfull width [m]	280	1650 (Harmar, 2004)
Particle fall velocity (wash load) [m/s]	$7{\cdot}10^{-5}$ (Asselman and Van Wijngaarden, 2002)	$7{\cdot}10^{-5}$
Assumed main channel length [m]	380	1000

In the case of a bed load supplied side channel, we assume that the sediment supply to the channel is principally determined by the channel width. The transport capacity in the channel is given by Meyer-Peter and Müller (1948). An first estimate of the side channel filling in is therefore given by:

$$T_{bed} = \frac{L_{side} W_{side} h_{side}}{\frac{W_{side}}{W_{side} + W_{main}} \; Q_{s,yr} - 8\left(\left(\frac{C}{C_{90}}\right)^{3/2} \theta - \theta_c\right)^{3/2} D_{side}^{3/2} \sqrt{g\Delta} W_{side}} \tag{5.4}$$

in which T_{bed} is the initial estimate of the time scale for bed load supplied side channels, L_{side}, W_{side} and h_{side} are the length, width and depth of the side channel which represent the volume that has to be filled with sediment, $Q_{s,yr}$ is the yearly sediment supply in the upstream channel, C is the total Chézy roughness, C_{90} is the Chézy roughness corresponding with the skin friction of the sediment, θ and θ_c are the Shields stress and the critical Shields stress, D_{side} is the grain size in the side channel and Δ the relative density.

The sediment supply in a suspended bed-material load channel is given by the discharge partitioning and the sediment transport capacity using Engelund and Hansen (1967). This results in

$$T_{susbed} = \frac{L_{side} W_{side} h_{side}}{\frac{Q_{side}}{Q_{upstream}} Q_{s,yr} - \frac{0.05 u_{side}^5 W_{side}}{\sqrt{g} C^3 \Delta^2 D_{side}}} \tag{5.5}$$

in in which T_{susbed} is the initial estimate of the time scale for suspended bed-material load supplied side channels and u_{side} is the depth averaged flow velocity in the side channel.

In the case of a wash load supplied side channel, we can use Equation 5.6 to estimate the time scale of filling in.

$$T_{wash} = \frac{L_{side} W_{side} h_{side}}{Q_{fine,yr}\left(1 - \exp\left(-\frac{L_{side} W_{side} h_{side}}{Q_{side}} \frac{w_s}{h_{side}}\right)\right)} \tag{5.6}$$

in which T_{wash} is the initial estimate of the time scale for wash load supplied side channels, $Q_{fine,yr}$ is the yearly sediment supply of fines in the upstream channel and w_s is the particle fall velocity.

REFLECTION ON THE CHOSEN CONDITIONS

In this paper, we do not take into account a switch in category. Figure 5.4 gives an indication of the average bed level change for each category. The initial condition for each category is different and therefore we scale the bed level change with the initial water depth. The normalized averaged bed level for the suspended bed-material load and the wash load supplied channel theoretically goes to 1. However, the aggradation is not uniform over the length of the side channel and therefore the discharge in the side channel reaches zero before a normalized averaged bed level of 1 is reached. In practice, the further aggradation of the channel occurs during peak flow conditions. The bed load supplied side channel remains open and reaches an equilibrium. The graphs show that the initially the largest aggradation occurs in a bed load supplied channel. The aggradation rate in a wash load supplied channel is much lower.

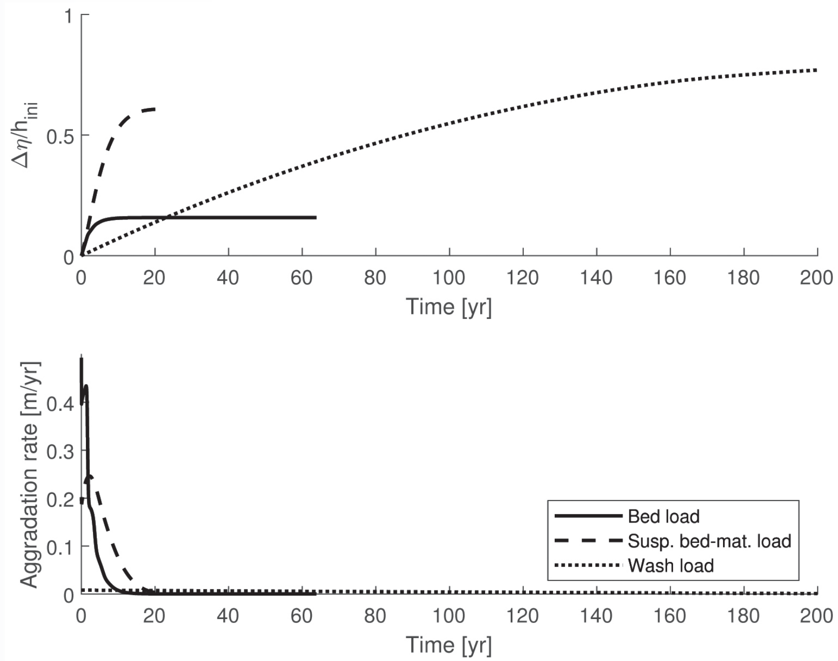

FIGURE 5.4 The average bed level change ($\Delta\eta$) scaled with the initial water depth (h_{ini}) and the aggradation rate over time for the three categories. The bed load and suspended bed-material load supplied results are given for L_{side}/L_{main} = 1.3; W/h = 4.5. The wash load supplied results are for L_{side}/L_{main} = 1.7; W/h = 10.

Photo: Johan Roerink / Aeropicture.nl

CHAPTER 6

Discussion

The main goal of this project is to understand the dynamics of side channel development such that maintenance efforts can be optimized. Several of the Dutch side channels are constructed to increase the discharge capacity of the channel and the observed aggradation is therefore a problem in many side channels. In this chapter, we discuss the possibility of a 'maintenance-free' side channel system, give some guidance for an optimal side channel design, discuss the main knowledge gaps and review some considerations.

06

6.1 A MAINTENANCE-FREE SIDE CHANNEL

Maintenance-free side channels seem to only occur under specific conditions. We first describe why, in our opinion, side channels in lowland rivers generally always aggrade, but then we give two examples in which, due to special conditions, this does not occur. We assume that a side channel is not allowed to erode, since this would lead to aggradation issues in the main channel that hinder navigation and might result in a cutoff of the main channel. Therefore, side channels are generally constructed longer than the main channel or the conveyance in the channel is limited by, for example, a weir.

6.1.1 THE AGGRADING SIDE CHANNEL

In Chapter 5, we described three categories of side channel systems, i.e. (1) bed load, (2) suspended bed-material load and (3) wash load supplied side channels. The category can change over time as a function of the aggradation in the side channel or due to changes in the hydrodynamic regime of the river. For each of these categories, we suggested a method to estimate the development of a side channel system and we use these methods to estimate the equilibrium state of a side channel.

A bed load supplied side channel that is longer than the main channel generally aggrades (Chapter 2). With an increasing bed level in the side channel, less sediment is supplied to the side channel due to the increasing transverse bed slope and this generally leads to an equilibrium state in which the side channel remains open (Bolla Pittaluga et al., 2003; Bolla Pittaluga et al., 2015). Such an equilibrium state forms, because the sediment supply balances with the transport capacity. This balance is a function of the Shields stress and with increasing Shields stress, the bed level difference between the channels has to increase to maintain such a balance (Bolla Pittaluga et al., 2015). The Shields stress increases with increasing flow velocity and is larger for smaller grain sizes. In rivers with a wide distribution of sediment, there will be a smaller grain size which corresponds with a higher Shields stress that is less affected by the bed slope effects or that is transported in suspension and therefore unaffected by bed slope effects. In addition, bed load can still be supplied to the side channel during peak flow events. Therefore, a bed load supplied side channel will continue to aggrade and change to another side channel category.

For both suspended bed-material load and wash load supplied channels, the sediment partitioning at the bifurcation is assumed to be proportional with the discharge partitioning (Chapter 5). For a suspended bed-material load channel, the sediment supply is then by definition larger than the transport capacity because of the lower flow velocity in the side channel compared to the main channel. The side channel will continue to aggrade. The side channel can become predominantly wash load supplied when a certain bed level is reached or when a plug bar formed at the bifurcation. The deposition of wash load continues the aggradation in the side channel and the side channel becomes part of the floodplain.

This theory suggests that only in case of bed load supplied side channels an equilibrium state can occur in which both channels remain open. However, due to peak flows in the river that can supply coarse material to a side channel and the limited transport capacity of a side channel that allows for the deposition of finer sediment, the channel continues to aggrade until it becomes a suspended bed-material load or a wash load supplied side channel. Following this reasoning, we hypothesize that in general side channels in lowland rivers always close.

6.1.2 SPECIAL CASES

A side channel typically aggrades and becomes part of the floodplain, but under special conditions an equilibrium state might be reached in which the side channel remains open. We relate these special conditions to the transport capacity in the side channel and the sediment supply to the side channel. We first look at a special case of the transport capacity and then a special case of the sediment supply.

The first type of side channels is one with a high transport capacity that have a limited or a non-erodible bed, and to which, due to a high bed level or structures at the bifurcation, bed load from the main channel is not supplied. Such side channels were observed in the river Rhône, in which sixteen side channels were reconstructed and monitored (Riquier et al., 2017). Four of these channels did not aggrade. The bed of these channels is covered with gravel and fines are deposited in the side channels during regular flow conditions (Riquier et al., 2015). During peak flow, the bed shear stress in these channels is such that the fine material is flushed out of the channel, but that the gravel remains (Riquier et al., 2017). Based on this principle, a side channel was constructed near Rees in the German part of the river Rhine. The side channel is constructed in the inner bend and is therefore shorter than the main channel, i.e. the transport capacity in the side channel is large, and the channel bed and banks are protected with geotextile and riprap. In addition, a high sill was constructed at the entrance of the channel, which blocks the supply of bed load from the main channel. Such a channel is possibly maintenance free, but it is questionable whether such a channel with limited morphodynamic changes and fixed banks is valuable from an ecological point of view (e.g., Duel et al., 2002; Amoros et al., 2003).

A second type of side channels is one to which the sediment supply of certain grain sizes that would normally lead to the aggradation of a side channel is limited. In our reasoning concerning the aggrading side channel (Section 6.1.1), we assume that a wide range of sediment grain sizes are transported in the main channel. However, if in the river there is a limited supply of suspended bed-material load, then a suspended bed-material load supplied side channel might remain open. The coarser sediment is not supplied to the channel due to the transverse bed slope effect and at the same time, the flow conditions in the side channel can be such that the wash sediment load does not deposit. This an hypothetical situation because this type of side channels has not yet been observed. We suggest that it could be found downstream of a hydro dam, because the dam affects both the sediment supply and the hydrodynamic regime of the river.

These two cases present suggestions for maintenance-free side channels, but heavily engineered solutions, such as at the side channel at Rees, might be needed to apply it in practice. This is in contrast with the current view on side channel construction as a Nature Based Solution.

6.2 GUIDANCE ON SIDE CHANNEL DESIGN

A side channel can have various objectives. A side channel can be constructed, for example, to increase the discharge capacity, to increase the ecological value of the river, or to reduce degradation of the main channel. These objectives determine the design of a side channel, but often conflict with each other or with other functions of the river, such as its navigability. This makes the design of a side channel more complex. Therefore, we focus in this discussion on reducing the aggradation of a side channel given a certain discharge conveyance.

In Chapter 5, we proposed a characterization of side channels and we use this to suggest a method to give a first estimate of side channel development. This method can be used to evaluate the side channel design in a quantitative way (Chapters 2 and 5). The aggradation rate seems to reduce when the flow frequency of the side channel increases (Chapter 3 and Riquier et al. (2017)). With increasing bed level, regular peak flows seem to become more important for the aggradation of the side channel (Chapter 4). Generally, a channel with a small width/depth ratio is beneficial, because the effect of the bed roughness is smaller and therefore the flow velocities are higher, increasing the transport capacity of the side channel (Figure 5.3). In addition, we suggest that, with our design requirements, a bed load supplied side channel, i.e. a channel in which sediment is deposited that in the main channel is transported as bed load, should be avoided since the transport capacity of the coarse material is likely limited within a side channel. This makes it more likely that a plug bar forms, which reduces the discharge capacity of the side channel significantly in a short period of time. To prevent bed load to enter the side channel, a side channel could be constructed with a high bed level such that a large transverse bed slope is created and the Shields stress at the bifurcation can be reduced by, for example, structures at the bifurcation.

The effect of the geometric characteristics of the side channel on the aggradation rate can be evaluated using the proposed method. However, there are other effects that are not included. We found that structures such as groynes and weirs affect the aggradation rate. Groynes reduce the bed shear stress at the entrance of the side channel and therefore seem to reduce the sediment supply to the side channel (Chapter 4). Groynes can therefore reduce the aggradation rate and side channels are less likely to be predominantly bed load supplied. Weirs reduce the flow frequency of a side channel and therefore might increase the aggradation rate (Chapter 3). The effect of structures on the side channel development should be studied in a more generalized way, but the results show that they can reduce the aggradation rate.

After the construction of a side channel, the development of the side channel should be monitored. Regular bed level measurements give insight into the development of the side channel and can be used to evaluate whether the side channel meets its requirements. In the first few years, the bed level changes are primarily a result of the initial adjustment of the bed and therefore gives less information on the long-term development of the side channel. After the initial change, the measuring frequency can be based on the time scale based on model computations (Chapter 5). In addition, it was found that the largest variation in aggradation rate occurs during peak flow conditions. Bed level measurements just after peak flow conditions are therefore important for a correct estimation of the aggradation time scale. In addition to the bed level measurements, we recommend to take grain size samples regularly. The frequency of these measurements can be smaller compared to the bed level measurements. A large change in the grain size over time can suggest a change in the sediment supply and thereby the category of the side channel.

Predicting the development of side channels still has challenges. The simple estimation method (Chapter 5) allows us to estimate the development of side channel in a quantitative way. The effect of other mechanisms such as peak flow events or groynes can only be estimated qualitatively because the limited amount of data.

6.3 KNOWLEDGE GAPS

6.3.1 SEDIMENT SUPPLY

The development of a side channel is a balance between the sediment supply and the transport capacity. The largest uncertainty is found in the sediment supply that for each type of bifurcation is difficult to determine. This is, for example, due to uncertainties in the estimation of the transverse bed slope effect (Baar et al., 2018), a varying sediment supply in time (Chapter 4) and a varying sediment supply as a function of the grain size (Schielen and Blom, 2018). In the Dutch side channels, the groyne field at the bifurcation complicates the estimation of the sediment supply to the side channel. Eddies occur in between the groynes that trap sediment or direct it towards the side channel (Sukhodolov et al., 2002; Mosselman et al., 2004). In addition, the sediment supply likely changes when the groynes start to overflow. A prediction of side channel development could significantly improve if we have more detailed data on the flow field at the bifurcation as a function of the discharge in the river and the sediment transport at the bifurcation as a function of the transported grain size and the discharge in the river.

6.3.2 NAVIGATION

The river Waal in the Netherlands is an important shipping route. The size and the design of a side channel in this river is generally restricted by its effects on the navigability of the main channel. Such effects are, for example, transverse currents in the main channel at the bifurcation and the confluence, and aggradation in the main channel due to the withdrawal of discharge from the main channel. In addition, navigation turns out to be an important driving force for the bed degradation within a groyne field (Ten Brinke et al., 2004) and bank erosion (Duró et al., 2018). The development of the side channel is likely affected by the shipping. Navigation induced currents and waves are sufficiently strong to bring sediment into suspension within a groyne field (Ten Brinke et al., 2004). If a side channel is connected at the downstream end, but closed at the upstream end during base flow conditions (e.g. the West channel at Gameren, Chapter 3), the navigation induced water level variations in combination with shipping waves likely transport fines into the side channel from the downstream end. This mechanism is similar to backflow in which fines are supplied to the side channel via the downstream end due to variations in the water level in the main channel (Citterio and Piégay, 2009; Riquier et al., 2017). A part of the deposited fines is likely flushed away from the side channel during peak flow events due to the larger bed shear stresses (Riquier et al., 2015).

We expect that terrestrialized side channels (e.g. the East channel at Gameren) are differently affected by the navigational currents. At the upstream and the downstream end of such a side channel, the bed level likely decreases due to shipping in the main channel, similarly to the bed level decrease within groyne fields. This would result in a lower bed level at the extremities of the side channel.

6.4 CONSIDERATIONS ON BIFURCATION RESEARCH

6.4.1 1D, 2D, AND 3D MODELING OF BIFURCATIONS

At a bifurcation three-dimensional (3D) flow structures occur which are important for determining the sediment partitioning (e.g., Thomas et al., 2011; Dutta et al., 2017). A three-dimensional numerical model is therefore regularly used to study the flow at a bifurcations and its effect on its development (e.g., Dargahi, 2004; Kleinhans et al., 2008; Hardy et al., 2011; Dutta et al., 2017). Such models are able to solve for the spiral flow that occurs at a bifurcation due to the bifurcation angle (Dutta et al., 2017), a bed slope advantage (Hardy et al., 2011) or an upstream river bend (Kleinhans et al., 2008). In addition, the bed shear stress can be better predicted with a 3D model when vertical velocities become important (Lane et al., 1999). In case of complex bifurcations, e.g. bifurcations with structures or with 90o corners, a 3D approach seems necessary (Mosselman et al., 2004; Dutta et al., 2017). However, 3D models generally require more boundary conditions and modeling choices, and these can have a large effect on the result. One of these modeling choices is selecting the turbulence closure model. The turbulence closure model influences, for example, the size of the flow separation zone at a bifurcation (Dutta et al., 2017) and the secondary flow development in a river bend (Ottevanger, 2013). In addition, due to the high computational costs of 3D models, generally only a limited number of vertical layers are used. Both the number and the vertical distribution of the layers have a large effect on the flow velocity and thereby the sediment transport of the river (Gaweesh and Meselhe, 2016). Therefore, using a 3D model adds additional modeling uncertainties compared to a 2D model.

In a two-dimensional (2D) model, the variation of the flow velocity over the water column is ignored. Secondary flow that occurs at a bifurcation or in a river bend needs to be included in a parametrized way to correctly reproduce the morphology of a river. With the parametrization for the secondary flow and including a relation for bed slope effect, the sediment partitioning at the bifurcation is implicitly solved with a 2D numerical model. However, there are several limitations in the derivation which makes the parametrization less accurate for complex geometries and sharp river bends (Ottevanger, 2013).

A 1D model requires an explicit relation for the sediment partitioning at the bifurcation. Such a nodal point relation contains coefficients that have to be defined empirically and only the mechanisms that are explicitly included in the nodal point relation will affect the partitioning of the bifurcation. This allows for a quick assessment of the effect of such mechanisms, but raises the question whether all the relevant mechanisms are included. However, due to its small computational effort, a 1D bifurcation model is most practical because its simplicity allows for a quick evaluation of many side channel designs.

Each type of model has its advantages and disadvantages. A detailed investigation of the flow at a bifurcation requires a 3D model in combination with detailed measurements. A 2D model inherently includes more physical processes than a 1D model and can be easily applied to morphodynamic computations of a time span in order of a decade. The choice of a model is therefore a balance between the detail needed to study important flow patterns and the required mechanisms that are included in the model combined with the temporal and spatial scale of the computational domain.

6.4.2 VEGETATION

Vegetation plays an important role in development of a side channel system. When the side channel becomes sufficiently shallow, vegetation is able to colonize and trap wash load (Makaske et al., 2002; Rodrigues et al., 2006). Therefore, vegetation can accelerate the development of the side channel to become part of the floodplain. Vegetation in the side channel also affects the roughness of the side channel. Hence vegetation can reduce the flow velocity in the side channel and at the bifurcation, changing the aggradation rate compared to a case without vegetation (Baptist and Mosselman, 2002; Burge, 2006). Vegetation also affects other morphodynamic mechanisms such as bank erosion (Simon and Collison, 2002; Duró et al., 2018). The stabilizing effect of vegetation on river banks can result in a smaller width/depth ratio of the channel (Van Dijk et al., 2013) and changes the migration rate of meandering channels (Van Oorschot et al., 2016).

Vegetation can affect and increase the aggradation rate of a side channel (Baptist and Mosselman, 2002). At Gameren, the role of vegetation varies between the channels (Chapter 3). In the West channel at Gameren only suspended bed-material load is deposited and the deposited sediment remains unvegetated. In East channel at Gameren, vegetation grows on the deposited sediment and likely aids the deposition of wash load. Both the colonization of vegetation and the category of the side channel show a relation with the flow velocity and the bed level (Makaske et al., 2002; Van Oorschot et al., 2016). Whether vegetation is important for an artificial side channel might therefore be related to the category of the side channel.

6.4.3 OTHER BIFURCATIONS

So far, we mainly discussed river bifurcations. However, bifurcations also occur in other fluid dynamic problems such as in tidal deltas or in arteries. The flow structures at such bifurcations are even more complex because the flow intensity and flow direction changes regularly due to tides (Buschman et al., 2013; Hoitink et al., 2017) or the pumping of the heart (Ku, 1997; Berger and Jou, 2000). This can generate complex secondary flow patterns at the bifurcation (Ku, 1997; Buschman et al., 2013). In tidal deltas, river peak flow events seem to be less supplied for the development of bifurcation compared to river bifurcations and the tidal variation of the discharge in the branches can have a stabilizing effect on the bifurcation (Hoitink et al., 2017). In addition, mud has a large effect on the development of a tidal delta or an estuary (e.g., Braat et al., 2019). In a side channel, mud may become important in the wash load supplied side channels. Therefore, the models used in estuary modeling can aid in evaluating the transition of a side channel into a floodplain. In artery bifurcations, flow separation can occur similarly as in river bifurcations (Figure 6.1). In arteries this can lead to the accumulation of plaque and thereby it reduces the conveyance of an artery (Berger and Jou, 2000). This seems similar to the formation of a plug bar in a river bifurcation. Bifurcations remain a complex problem in fluid dynamics. Our study increases the understanding of the mechanisms and processes that affect the development of asymmetric bifurcations. This can increase the flood safety, reduce maintenance costs and improve maintenance interventions.

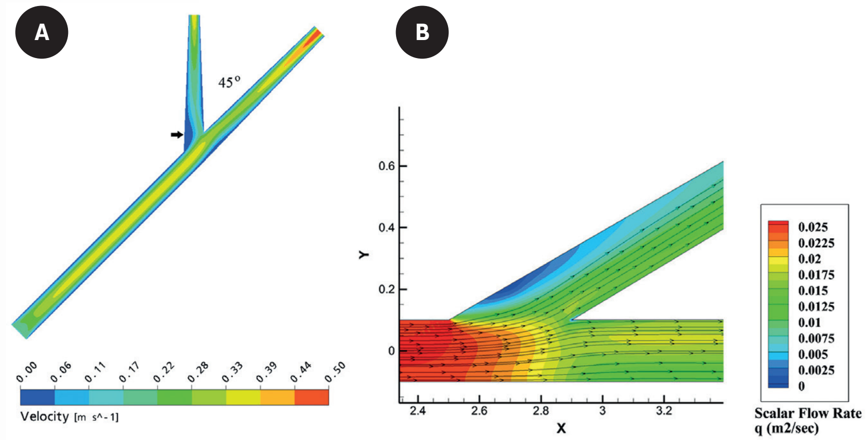

FIGURE 6.1 The flow velocity at **(A)** an artery (Chaichana et al., 2011) and **(B)** a river bifurcation (Dutta et al., 2017). The results are computed using detailed 3D hemodynamic and hydrodynamic models, respectively.

06

Photo: Bureau Beeldtaal Filmmakers

CHAPTER 7

Conclusions and recommendations

7.1 CONCLUSIONS

The aim of this thesis is to better understand the mechanisms that drive the morphodynamic development of side channels to enable estimating their development. We studied several side channel systems using aerial images with a simple numerical model, detailed bed level and grain size measurements and a detailed morphodynamic mixed-sediment model. Based on these result we are able to categorize side channel system which can be used in estimating side channel development in the future. In this section, we answer the research questions as formulated in Section 1.3.

Q1 *Which mechanisms make side channels aggrade or degrade and at which rate?*
We looked at four side channel systems and reproduced their development using a simple one-dimensional model. We found that in bed load supplied side channels, the length of the channel in combination with the curvature of the channel upstream of the bifurcation are the main mechanisms that determine the equilibrium state. In general, both of the branches remain open, but with discharge partitioning that is asymmetric. We found that flow separation at the entrance of a side channel reduces its discharge conveyance and thereby its transport capacity. The width adaptation of the downstream channels has a limited effect on which channel becomes the dominant channel, but has a large effect on the time scale of the side channel development. Using the 1D model, we computed the time scale of the side channel development for several ranges of parameters and the results can be used in estimating the development of bed load supplied side channels (Figures 2.4 and 2.5).

Q2 *How is the aggradation rate and the deposited sediment size in Dutch side channels related the hydrodynamic conditions?*
The side channel system at Gameren (river Waal, the Netherlands) was regularly measured since its construction. The measurements give insight into the variation of the aggradation rate in time and space. In addition, we collected sediment samples in the three channels and estimated the hydrodynamic conditions in the channels using a hydrodynamic model. We found that there is a relation between the aggradation rate and hydrodynamic conditions in the main channel. The measurements show that a more frequent flowing of the side channel results in a lower aggradation rate of the side channel. The side channels are mainly filled with suspended bed-material load from the main channel. This means that sediment-size sorting occurs at the bifurcation. The grain size variation between the channels seems to be a function of the bed level (i.e. a higher bed level results in deposition of finer sediment) and the bed shear stress (i.e. a lower bed shear stress results in more deposition of fines).

Q3 *How is the aggradation rate of a side channel related to varying hydrodynamic conditions and its design conditions?*
The measurements (Q2) show that the aggradation rate is a function of the hydrodynamic conditions in the river and that grain-size sorting occurs at the bifurcation of the side channel. Therefore, we use a mixed-sediment morphodynamic model with varying hydrodynamic conditions and focus on side channels that are mainly filled with suspended bed-material load. Both the aggradation rate and the grain size that is deposited in the side channel are a function of past and current discharge conditions. Peak flow events become more important for the aggradation of the side channel with increasing bed level and with increasing bed level, the deposited grain size decreases. Both the change in bed level and the change in grain size are therefore a function of the size and the frequency of the peak flow events that occurred since the construction of a side channel. In addition, we show that a constant discharge, which is commonly used in bifurcation modeling, gives significantly different aggradation rates and fining of the side channel bed.

Q4 *How can we characterize the side channel development and how can we use this characterization to estimate the development of side channels?*
We find that there are three main categories of side channel systems based on how the sediment that is deposited inside the side channels is transported in the main channel. These categories are (1) bed load supplied side channels, (2) suspended bed-material load supplied side channels and (3) wash load supplied side channels. For each category, we identify the main mechanisms that affect the sediment supply and the transport capacity in the side channel. With the relations for the sediment supply and the transport capacity, we can estimate the temporal development of a side channel system. This a first estimation can aid the design, operation and maintenance of side channels (Figure 5.3).

We studied the development of side channel in various ways and found that mechanisms such as a length difference between the downstream channels, sediment sorting at the bifurcation and varying hydrodynamic conditions have a large effect on the morphodynamic development of a side channel system. The mechanisms that are important are not the same for each side channel and can vary in time. Therefore, we propose three categories of side channel based on how the sediment that is deposited in the side channel is transported in the main channel: (1) bed load supplied, (2) suspended bed-material load supplied and (3) wash load supplied side channels. These categories can help in determining the main mechanisms that affect the development of a side channel system. In addition, we propose a method based on the categorization that can aid the design, operation and maintenance of side channels.

7.2 RECOMMENDATIONS

We divided the recommendations in two sections: recommendations for further research and recommendations for river managers.

7.2.1 RESEARCH

A DETAILED STUDY OF THE FLOW AND SEDIMENT TRANSPORT AT THE BIFURCATION

The sediment partitioning at the bifurcation of artificial side channels is often complex due to structures or complex geometries (Section 6.3.1). The sediment supply seems to change as a function of the discharge of the main channel and this seems to be related to the flow between the groynes. Detailed measurements and three-dimensional simulations can aid in characterizing the flow at the bifurcation and can give insight into the sediment partitioning as a function of the discharge in the river.

THE EFFECT OF PEAK DISCHARGES ON THE SIDE CHANNEL DEVELOPMENT

In this thesis, we could not give a definitive answer of the effect of floods on the side channel development. Peak flows seem to be able to cause degradation in a side channel, but can also supply sediment to the side channel (Toonen et al., 2012; Riquier et al., 2017). Whether degradation or aggradation occurs depends on the bed shear stress in the side channel (Riquier et al., 2017) and can change with increasing bed level (Chapter 4). More detailed measurements of the bed level changes during and immediately after peak flow in combination with a better understanding of the sediment supply during such discharges can improve the predictability of the aggradation rate as a function of the hydrodynamic conditions in the river.

BETTER ESTIMATION OF THE DEVELOPMENT OF FLOODPLAIN CHANNELS

Side channels are constructed in various ways. Side channels that are connected to the main channel at one or neither of its extremities were not explicitly discussed in this thesis. Floodplain processes, such as the deposition of fines and vegetation, are important for the bed level changes in such side channels. A limited amount of measurements is available. More insight into the development of such channels can be given by existing floodplain aggradation models (e.g., Middelkoop and Van der Perk, 1998; Asselman and Van Wijngaarden, 2002) or possibly using more complex models in which the deposited fines can also erode (Braat et al., 2017; Kleinhans et al., 2018).

INFLUENCES OF NAVIGATION

There are several indications that navigational induced currents can have a large effect on the development of a side channel (Section 6.3.2). Flow velocity and sediment transport measurements can give insight into the forcing of the navigational currents in the side channels. In addition, bed level measurements during base flow conditions can be used to estimate the import or export of sediment from the side channel.

THE ECOLOGICAL VALUE OF SIDE CHANNELS

One of the common objectives to construct side channels is to increase the ecological value of the river (e.g., Schiemer et al., 1999; Buijse et al., 2002; Riquier et al., 2015). An optimal side channel from a morphological point of view might not meet ecological objectives. In addition, the ecosystem elements, such as vegetation (Section 6.4.2), can affect the morphodynamic development of a side channel. Combining both the morphodynamic and the ecological objectives could lead to a more generally applicable guide for side channel design.

CAN WE AFFECT THE PARTITIONING USING STRUCTURES?

Structures such as groynes seem to affect the sediment supply to the side channel. Other types interventions could be constructed to control the sediment supply to the side channel. Bottom vanes are an example of such an intervention (e.g., Odgaard and Wang, 1991; Barkdoll et al., 1999). Bottom vanes can direct sediment that is transported near the bed away from the side channel entrance reducing its sediment supply. Such interventions seem to be mainly effective for bed load supplied side channels because bed load sediment transport is largest near the bed and the bed load sediment partitioning is not assumed the same as the discharge partitioning. Therefore, the effectiveness of such interventions depends on the category of side channels (Chapter 5).

7.2.2 RIVER MANAGERS

KEEP MONITORING

Side channels change after construction and monitoring is needed to verify that the side channels meets its requirements or objectives. In addition, the bed level changes can be used to predict the development of side channels more accurately. Just after construction, the bed level change in the side channel can be large (for the East channel at Gameren 0.18 m/yr), but after this initial change the bed level changes are much smaller (at the East channel at Gameren on average 0.05 m/yr). To estimate the development of the side channel, regular measurements are needed. The largest changes in the aggradation rate are expected during peak flow events and therefore, measurements just before and after peak flow events can give insight into the time scale of the side channel development. In addition, grain size samples should be taken such that the side channel category can be determined. The frequency of these measurements can be smaller than the bed level measurements. A large change in grain size over time can suggest a transition to a different side channel category.

ADJUST THE SIDE CHANNEL DESIGN BASED ON THE EXPECTED MORPHODYNAMIC CHANGES

Side channels are designed based on their discharge conveyance such that they reduce the water level during peak flow conditions. In the design of such a channel a large initial bed level change should be expected. The model as proposed in Chapter 5 can be used to get a first estimate of this initial bed level change. If we do not take into account such an initial bed level change, the side channel might not meet its requirements shortly after its construction. The initial bed level can be chosen such that after the initial bed level change occurred that the channel still meets its objectives. In addition, the effect of the initial bed level change can be reduced by changing, for example, the slope or width/depth ratio of the channel, but because the future discharge conditions of the river are unknown, the initial bed level change will always occur.

AN AGGRADING SIDE CHANNEL IS NOT A DUTCH ISSUE

Side channel construction is a common intervention in many managed rivers and these side channels are generally aggrading. We can learn from the experiences of abroad on both natural and artificial side channels. The proposed characterization of side channels can aid river managers to determine whether the observed changes or mechanisms in other rivers are applicable to their side channel systems. Using data and experiences from abroad can improve the prediction of side channel development and thereby, the overall design of side channels.

Photo: Ralph Schielen

References

Akkerman, G. J., 1993: Zandverdeling bij splitsingspunten: Literatuurinventarisatie voor inlaten van nevengeulen. Technical Report Q1573, WL Delft Hydraulics, Delft, The Netherlands.

Amoros, C., A. Elger, S. Dufour, L. Grospretre, H. Piégay, and C. Henri, 2003: Flood scouring and groundwater supply in rehabilitated side-channels of the Rhone River, France: sedimentation and aquatic vegetation responses. *Large Rivers,* 15, 147-167, doi:10.1127/lr/15/2003/147.

Ashida, K., and M. Michiue, 1972: Study on hydraulic resistance and bedload transport rate in alluvial streams. *Transactions Japanese Society of Civil Engineers,* 206, 59-69.

Asselman, N. E. M., and M. Van Wijngaarden, 2002: Development and application of a 1D floodplain sedimentation model for the River Rhine in The Netherlands. *Journal of Hydrology,* 268, 127-142, doi:10.1016/S0022-1694(02)00162-2.

Augustijn, D. C. M., S. J. M. H. Hulscher, and R. M. J. Schielen, 2018: RiverCare: Researching measures to prepare multi-functional rivers for the next century. *5th IAHR Europe Congress - New Challenges in Hydraulic Research and Engineering,* Trento, Italy, A. Armanini, and E. Nucci, Eds., 473-474, doi:10.3850/978-981-11-2731-1_224-cd.

Baar, A. W., S. A. H. Weisscher, W. S. J. Uijttewaal, and M. G. Kleinhans, 2017: Sediment transport processes on transverse bed slopes. *NCR days 2017*, Wageningen, The Netherlands, A. J. F. Hoitink, et al., Eds., 50-51.

Baar, A. W., J. de Smit, W. S. J. Uijttewaal, and M. G. Kleinhans, 2018: Sediment transport of fine sand to fine gravel on transverse bed slopes in rotating annular flume experiments. *Water Resources Research*, 54, 19-45, doi:10.1002/2017WR020604.

Baptist, M. J., and E. Mosselman, 2002: Biogeomorphological modelling of secondary channels in the Waal River. *Riverflow 2002, Louvain-la-Neuve, Belgium, D. Bousmar, and Y. Zech, Eds., 773-782.*

Baptist, M. J., V. Babovic, J. Rodríguez Uthurburu, M. Keijzer, R. E. Uittenbogaard, A. Mynett, and A. Verwey, 2007: On inducing equations for vegetation resistance. *Journal of Hydraulic Research*, 45, 435-450, doi:10.1080/00221686.2007.9521778.

Barkdoll, B. D., R. Ettema, and A. J. Odgaard, 1999: Sediment control at lateral diversions: Limits and enhancements to vane use. *Journal of Hydraulic Engineering,* 125, 862-870, doi:10.1061/(ASCE)0733-9429(1999)125:8(862).

Becker, A., 2015: Rijn-modellen 5de generatie Modelopzet, kalibratie en verificatie WAQUA. Technical Report 1205994-002, Deltares, Delft, The Netherlands.

Becker, A., M. Scholten, D. Kerhoven, and A. Spruyt, Year: Das behördliche Modellinstrumentarium der Niederlande. *Dresdner Wasserbauliche Mitteilungen 50, Dresden, Germany, 539-548.*

Berends, K. D., J. J. Warmink, and S. J. M. H. Hulscher, 2018: Efficient uncertainty quantification for impact analysis of human interventions in rivers. *Environmental Modelling & Software*, 107, 50-58, doi:10.1016/j.envsoft.2018.05.021.

Berger, S. A., and L. D. Jou, 2000: Flows in stenotic vessels. *Annual Review of Fluid Mechanics,* 32, 347-382, doi:10.1146/annurev.fluid.32.1.347.

Bertoldi, W., and M. Tubino, 2007: River bifurcations: Experimental observations on equilibrium configurations. *Water Resources Research,* 43, doi:10.1029/2007WR005907.

Bertoldi, W., L. Zanoni, S. Miori, R. Repetto, and M. Tubino, 2009: Interaction between migrating bars and bifurcations in gravel bed rivers. *Water Resources Research,* 45, doi:10.1029/2008wr007086.

Blanckaert, K., and H. J. De Vriend, 2004: Secondary flow in sharp open-channel bends. *Journal of Fluid Mechanics,* 198, 353-380, doi:10.1017/S0022112003006979.

Blom, A., 2008: Different approaches to handling vertical and streamwise sorting in modeling river morphodynamics. *Water Resources Research,* 44, doi:10.1029/2006WR005474.

Blom, A., E. Viparelli, and V. Chavarrías, 2016: The graded alluvial river: Profile concavity and downstream fining. *Geophysical Research Letters,* 43, 6285-6293, doi:10.1002/2016GL068898.

Blom, A., L. Arkesteijn, V. Chavarrías, and E. Viparelli, 2017: The equilibrium alluvial river under variable flow and its channel-forming discharge. *Journal of Geophysical Research-Earth Surface,* 122, 1924-1948, doi:10.1002/2017jf004213.

Bolla Pittaluga, M., R. Repetto, and M. Tubino, 2003: Channel bifurcation in braided rivers: Equilibrium configurations and stability. *Water Resources Research,* 39, doi:10.1029/2001wr001112.

Bolla Pittaluga, M., G. Coco, and M. G. Kleinhans, 2015: A unified framework for stability of channel bifurcations in gravel and sand fluvial systems. *Geophysical Research Letters,* 42, 7521-7536, doi:10.1002/2015gl065175.

Braat, L., T. van Kessel, J. R. F. W. Leuven, and M. G. Kleinhans, 2017: Effects of mud supply on large-scale estuary morphology and development over centuries to millennia. *Earth Surface Dynamics,* 5, 617-652, doi:10.5194/esurf-5-617-2017.

Braat, L., J. R. F. W. Leuven, I. R. Lokhorst, and M. G. Kleinhans, 2019: Effects of estuarine mudflat formation on tidal prism and large-scale morphology in experiments. *Earth Surface Processes and Landforms, doi:10.1002/esp.4504.*

Bravard, J. P., 1986: La basse vallée de l'Ain – Dynamique fluviale appliquée à l'écologie. Technical Report, SOGREAH.

Bridge, J. S., 2003: *Rivers and floodplains: forms, processes, and sedimentary.* Wiley-Blackwell.

Buijse, A. D., H. Coops, M. Staras, L. H. Jans, G. J. Van Geest, R. E. Grift, B. W. Ibelings, W. Oosterberg, and F. C. J. M. Roozen, 2002: Restoration strategies for river floodplains along large lowland rivers in Europe. *Freshwater Biology*, 47, 889-907, doi:DOI 10.1046/j.1365-2427.2002.00915.x.

Bulle, H., 1926: *Untersuchungen über die Geschiebeableitung bei der Spaltung von Wasserläufen.* VDIVerlag.

Burge, L. M., 2006: Stability, morphology and surface grain size patterns of channel bifurcation in gravel-cobble bedded anabranching rivers. *Earth Surface Processes and Landforms*, 31, 1211-1226, doi:10.1002/esp.1325.

Buschman, F. A., M. van der Vegt, A. J. F. Hoitink, and P. Hoekstra, 2013: Water and suspended sediment division at a stratified tidal junction. *Journal of Geophysical Research-Oceans,* 118, 1459-1472, doi:10.1002/jgrc.20124.

Busnelli, M. M., 2001: Numerical simulation of free surface flows with steep gradients. PhD thesis, Delft University of Technology.

Candel, J. H. J., M. G. Kleinhans, B. Makaske, W. Z. Hoek, C. Quik, and J. Wallinga, 2018: Late Holocene channel pattern change from laterally stable to meandering - a palaeohydrological reconstruction. *Earth Surface Dynamics,* 6, 723-741, doi:10.5194/esurf-6-723-2018.

Chaichana, T., Z. Sun, and J. Jewkes, 2011: Computation of hemodynamics in the left coronary artery with variable angulations. *Journal of Biomechanics,* 44, 1869-1878, doi:10.1016/j.jbiomech.2011.04.033.

Chavarrías, V., G. Stecca, and A. Blom, 2018: Ill-posedness in modeling mixed sediment river morphodynamics. *Advances in Water Resources,* 114, 219-235, doi:10.1016/j.advwatres.2018.02.011.

Church, M., 2006: Bed material transport and the morphology of alluvial river channels. *Annual Review of Earth and Planetary Sciences,* 34, 325-354, doi:10.1146/annurev.earth.33.092203.122721.

Citterio, A., and H. Piégay, 2009: Overbank sedimentation rates in former channel lakes: characterization and control factors. *Sedimentology,* 56, 461-482, doi:10.1111/j.1365-3091.2008.00979.x.

Collas, F. P. L., A. D. Buijse, L. van den Heuvel, N. van Kessel, M. M. Schoor, H. Eerden, and R. S. E. W. Leuven, 2018: Longitudinal training dams mitigate effects of shipping on environmental conditions and fish density in the littoral zones of the river Rhine. *Science of The Total Environment,* 619-620, 1183-1193, doi:10.1016/j.scitotenv.2017.10.299.

Constantine, J. A., T. Dunne, H. Piégay, and G. M. Kondolf, 2010: Controls on the alluviation of oxbow lakes by bed-material load along the Sacramento River, California. *Sedimentology,* 57, 389-407, doi:10.1111/j.1365-3091.2009.01084.x.

Cortes Arevalo, V. J., L. N. H. Verbrugge, R. J. den Haan, F. Baart, M. C. van der Voort, and S. J. M. H. Hulscher, 2018: Users' perspectives about the potential usefulness of online storylines to communicate river research to a multi-disciplinary audience. *Environmental Communication*, 1-17, doi:10.1080/17524032.2018.1504098.

Dargahi, B., 2004: Three-dimensional flow modelling and sediment transport in the River Klarälven. *Earth Surface Processes and Landforms*, 29, 821-852, doi:10.1002/esp.1071.

De Heer, A., and E. Mosselman, 2004: Flow structure and bedload distribution at alluvial diversions. *River flow 2004,* Napoli, Italy, M. Greco, A. Carravetta, and R. Della Morte, Eds.

De Ruijsscher, T., S. Naqshband, and T. Hoitink, 2018: Flow bifurcation at a longitudinal training dam: Effects on local morphology. *River Flow 2018 - Ninth International Conference on Fluvial Hydraulics*, Lyon-Villeurbanne, France, A. Paquier, and R. N., Eds., doi:10.1051/e3sconf/20184005020

De Vries, M., 1971: Aspecten van zandtransport in open waterlopen. Technical Report, Delft University of Technology, Delft, The Netherlands.

Den Haan, R. J., J. M. Fliervoet, M. C. van der Voort, V. J. Cortes Arevalo, and S. J. M. H. Hulscher, 2018: Understanding actor perspectives regarding challenges for integrated river basin management. *International Journal of River Basin Management*, 1-14, doi:10.1080/15715124.2018.1503186.

Dépret, T., J. Riquier, and H. Piégay, 2017: Evolution of abandoned channels: Insights on controlling factors in a multi-pressure river system. *Geomorphology,* 294, 99-118, doi:10.1016/j.geomorph.2017.01.036.

Dieras, P. L., J. A. Constantine, T. C. Hales, H. Piégay, and J. Riquier, 2013: The role of oxbow lakes in the off-channel storage of bed material along the Ain River, France. *Geomorphology,* 188, 110-119, doi:DOI 10.1016/j.geomorph.2012.12.024.

Dietrich, W. E., and J. D. Smith, 1984: Bed load transport in a river meander. *Water Resources Research,* 20, 1355-1380, doi:10.1029/WR020i010p01355.

Duel, H., M. J. Baptist, G. J. Geerling, A. J. M. Smits, and J. S. L. Van Alphen, Year: Cyclic floodplain rejuvenation as a strategy for both flood protection and enhancement of the biodiversity of the river Rhine. *Conference Proceedings of the Fourth International Ecohydraulics Symposium,* Cape Town, South Africa.

Duró, G., A. Crosato, and P. Tassi, 2016: Numerical study on river bar response to spatial variations of channel width. *Advances in Water Resources*, 93, 21-38, doi:10.1016/j.advwatres.2015.10.003.

Duró, G., A. Crosato, M. G. Kleinhans, and W. S. Uijttewaal, 2018a: Bank erosion processes measured with UAV-SfM along complex banklines of a straight mid-sized river reach. *Earth Surface Dynamics,* 6, 933-953, doi:10.5194/esurf-6-933-2018.

Duró, G., A. Crosato, M. G. Kleinhans, and W. S. J. Uijttewaal, Year: On the morphological evolution of restored banks: Case study of the Meuse river. *River Flow 2018 - Ninth International Conference on Fluvial Hydraulics*, Lyon-Villeurbanne, France, 02021, doi:10.1051/e3sconf/20184002021.

Dutta, S., and M. H. García, 2018: Nonlinear distribution of sediment at river diversions: Brief history of the Bulle Effect and its implications. *Journal of Hydraulic Engineering*, 144, doi:10.1061/(ASCE)HY.1943-7900.0001449.

Dutta, S., D. Wang, P. Tassi, and M. H. García, 2017: Three-dimensional numerical modeling of the Bulle effect: the nonlinear distribution of near-bed sediment at fluvial diversions. *Earth Surface Processes and Landforms,* 42, 2322-2337, doi:10.1002/esp.4186.

Edmonds, D. A., and R. L. Slingerland, 2008: Stability of delta distributary networks and their bifurcations. *Water Resources Research,* 44, doi:10.1029/2008wr006992.

Engelund, F., and E. Hansen, 1967: A monograph on sediment transport in alluvial streams. Technical Report, Tekniskforlag, Copenhagen.

Federici, B., and C. Paola, 2003: Dynamics of channel bifurcations in noncohesive sediments. *Water Resources Research,* 39, doi:10.1029/2002wr001434.

Fernandez Luque, R., and R. Van Beek, 1976: Erosion and transport of bed-load sediment. *Journal of Hydraulic Research,* 14, 127-144, doi:10.1080/00221687609499677.

Fernández, R., M. H. García, and G. Parker, 2018: Upper Mississippi River flow and sediment characteristics and their effect on a harbor siltation case. *Journal of Hydraulic Engineering,* 144, doi:10.1061/(ASCE)HY.1943-7900.0001507.

Formann, E., H. M. Habersack, and S. Schober, 2007: Morphodynamic river processes and techniques for assessment of channel evolution in Alpine gravel bed rivers. *Geomorphology,* 90, 340-355, doi:10.1016/j.geomorph.2006.10.029.

Frings, R. M., 2007: From gravel to sand. PhD Thesis, University of Utrecht.

Frings, R. M., and M. G. Kleinhans, 2008: Complex variations in sediment transport at three large river bifurcations during discharge waves in the river Rhine. *Sedimentology,* 55, 1145-1171,doi:10.1111/j.1365-3091.2007.00940.x.

Frings, R. M., K. Banhold, and I. Evers, 2015: Sedimentbilanz des Oberen Rheindeltas. Technical Report, Lehrstuhl und Institut für Wasserbau und Wasserwirtschaft, RWTH Aachen University.

García, M., and G. Parker, 1991: Entrainment of bed sediment into suspension. *Journal of Hydraulic Engineering,* 117, 414-435, doi:10.1061/(ASCE)0733-9429(1991)117:4(414).

Gaweesh, A., and E. Meselhe, 2016: Evaluation of sediment diversion design attributes and their impact on the capture efficiency. *Journal of Hydraulic Engineering,* 142, doi:10.1061/(asce)hy.1943-7900.0001114.

Goodman, S. N., 2001: Of P-values and Bayes: a modest proposal. *Epidemiology,* 12, 295-297, doi:10.1097/00001648-200105000-00006.

Gupta, N., M. G. Kleinhans, E. A. Addink, P. M. Atkinson, and P. A. Carling, 2014: One-dimensional modeling of a recent Ganga avulsion: Assessing the potential effect of tectonic subsidence on a large river. *Geomorphology,* 213, 24-37, doi:DOI 10.1016/j.geomorph.2013.12.038.

Habermaas, F., 1935: Geschiebeeinwanderung in Werkkanäle und deren Verhinderung. *Wasserkraft und Wirtschaft,* 30, 97-103.

Hardy, R. J., S. N. Lane, and D. Yu, 2011: Flow structures at an idealized bifurcation: a numerical experiment. *Earth Surface Processes and Landforms,* 36, 2083-2096, doi:10.1002/esp.2235.

Harmar, O. P., 2004: Morphological and process dynamics of the Lower Mississippi River. PhD Thesis, University of Nottingham.

Hegnauer, M., J. J. Beersma, H. F. P. Van den Boogaard, T. A. Buishand, and R. H. Passchier, 2014: Generator of Rainfall and Discharge Extremes (GRADE) for the Rhine and Meuse basins. Technical Report, Deltares, Delft, The Netherlands.

Helfield, J. M., J. Engstrom, J. T. Michel, C. Nilsson, and R. Jansson, 2012: Effects of river restoration on riparian biodiversity in secondary channels of the Pite River, Sweden. *Environmental Management,* 49, 130-141, doi:10.1007/s00267-011-9773-6.

Henry, C. P., C. Amoros, and Y. Giuliani, 1995: Restoration ecology of riverine wetlands: II. An example in a former channel of the Rhône River. *Environmental Management,* 19, 903-913, doi:10.1007/bf02471941.

Hirano, M., 1972: Studies on variation and equilibrium state of a river bed composed of non-uniform material. *Transactions Japanese Society of Civil Engineers,* 4, 128-129.

Hohensinner, S., M. Jungwirth, S. Muhar, and S. Schmutz, 2014: Importance of multi-dimensional morphodynamics for habitat evolution: Danube River 1715–2006. *Geomorphology,* 215, 3-19, doi:10.1016/j.geomorph.2013.08.001.

Hoitink, A. J. F., Z. B. Wang, B. Vermeulen, Y. Huismans, and K. Kastner, 2017: Tidal controls on river delta morphology. *Nature Geoscience,* 10, 637-645, doi:10.1038/Ngeo3000.

Hulscher, S. J. M. H., R. M. J. Schielen, D. C. M. Augustijn, J. J. Warmink, M. C. Van der Voort, H. Middelkoop, M. G. Kleinhans, R. S. E. W. Leuven, H. J. R. Lenders, A. J. M. Smits, J. M. Fliervoet, W. S. J. Uijttewaal, A. Blom, J. Wallinga, A. J. F. Hoitink, A. D. Buijsse, G. W. Geerling, and B. Makaske, 2014: RiverCare: towards self-sustaining multifunctional rivers. *NCR-Days 2014, Book of Abstracts,* Enschede, the Netherlands, D. C. M. Augustijn, and J. J. Warmink, Eds., 13-14.

Jans, L., 2004: Evaluatie nevengeulen Gamerensche Waard 1996-2002. Technical Report, Rijkswaterstaat.

Jansen, P. P., L. Van Bendegom, J. Van den Berg, M. De Vries, and A. Zanen, 1979: *Principles of river engineering: The non-tidal alluvial river.* Delftse Uitgevers Maatschappij.

Johannesson, H., and G. Parker, 1989: Linear theory of river meanders. *River meandering*, S. Ikeda, and G. Parker, Eds., American Geophysical Union, 181-213.

Kästner, K., A. J. F. Hoitink, B. Vermeulen, T. J. Geertsema, and N. S. Ningsih, 2017: Distributary channels in the fluvial to tidal transition zone. *Journal of Geophysical Research-Earth Surface,* 122, 696-710, doi:10.1002/2016jf004075.

Kernkamp, H. W. J., A. Van Dam, G. S. Stelling, and E. D. De Goede, 2011: Efficient scheme for the shallow water equations on unstructured grids with application to the continental shelf. *Ocean Dynamics,* 61, 1175-1188, doi:10.1007/s10236-011-0423-6.

Kleinhans, M. G., H. R. A. Jagers, E. Mosselman, and C. J. Sloff, 2008: Bifurcation dynamics and avulsion duration in meandering rivers by one-dimensional and three-dimensional models. *Water Resources Research,* 44, doi:10.1029/2007wr005912.

Kleinhans, M. G., K. M. Cohen, J. Hoekstra, and J. M. IJmker, 2011: Evolution of a bifurcation in a meandering river with adjustable channel widths, Rhine delta apex, The Netherlands. *Earth Surface Processes and Landforms,* 36, 2011-2027, doi:10.1002/esp.2222.

Kleinhans, M. G., T. de Haas, E. Lavooi, and B. Makaske, 2012: Evaluating competing hypotheses for the origin and dynamics of river anastomosis. *Earth Surface Processes and Landforms,* 37, 1337-1351, doi:10.1002/esp.3282.

Kleinhans, M. G., R. I. Ferguson, S. N. Lane, and R. J. Hardy, 2013: Splitting rivers at their seams: bifurcations and avulsion. *Earth Surface Processes and Landforms,* 38, 47-61, doi:10.1002/esp.3268.

Kleinhans, M. G., B. de Vries, L. Braat, and M. van Oorschot, 2018: Living landscapes: Muddy and vegetated floodplain effects on fluvial pattern in an incised river. *Earth Surface Processes and Landforms,* 43, 2948-2963, doi:10.1002/esp.4437.

Klop, E. R., 2015: Morfologische ontwikkeling hoofd- en vaargeul na kribverlaging op basis van multibeamgegevens in periode 2009-2012. Technical Report, Arcadis, Amersfoort, The Netherlands.

Klop, E. R., and B. Dongen, 2015: Morfologische dynamiek in kribvakken na kribverlaging. Technical Report, Arcadis, Amersfoort, The Netherlands.

Koch, F. G., and C. Flokstra, Year: Bed level computations for curved alluvial channels. *Proceedings of the 19th Congress of the IAHR,* New Delhi, India, 357.

Konsoer, K. M., 2014: Influence of riparian vegetation on near-bank flow structure and rates of erosion on a large meandering river. PhD Thesis, University of Illinois.

Ku, D. N., 1997: Blood flow in arteries. *Annual Review of Fluid Mechanics*, 29, 399-434, doi:10.1146/annurev.fluid.29.1.399.

Lane, E. W., 1955: The importance of fluvial morphology in hydraulic engineering. *Proceedings American Society of Civil Engineers,* 81, 1-17.

Lane, S. N., K. F. Bradbrook, K. S. Richards, P. A. Biron, and A. G. Roy, 1999: The application of computational fluid dynamics to natural river channels: three-dimensional versus two-dimensional approaches. *Geomorphology,* 29, 1-20, doi:10.1016/S0169-555x(99)00003-3.

Lauchlan, C., 2004: Experimental investigation of bed-load and suspended-load transport over weirs. *Journal of Hydraulic Research,* 42, 549-555, doi:10.1080/00221686.2004.9641224.

Le Coz, J., M. Michalková, A. Hauet, M.Čomaj, G. Dramais, K. Holubová, H. Piégay, and A. Paquier, 2010: Morphodynamics of the exit of a cutoff meander: experimental findings from field and laboratory studies. *Earth Surface Processes and Landforms,* 35, 249-261, doi:10.1002/esp.1896.

Le, T. B., A. Crosato, and W. S. J. Uijttewaal, 2018a: Long-term morphological developments of river channels separated by a longitudinal training wall. *Advances in Water Resources,* 113, 73-85, doi:10.1016/j.advwatres.2018.01.007.

Le, T. B., A. Crosato, E. Mosselman, and W. S. J. Uijttewaal, 2018b: On the stability of river bifurcations created by longitudinal training walls. Numerical investigation. *Advances in Water Resources,* 113, 112-125, doi:10.1016/j.advwatres.2018.01.012.

Lesser, G. R., J. A. Roelvink, J. A. T. M. Kester, and G. S. Stelling, 2004: Development and validation of a three-dimensional morphological model. *Coastal Engineering,* 51, 883-951, doi:10.1016/j.coastaleng.2004.07.014.

Makaske, B., D. G. Smith, and H. J. A. Berendsen, 2002: Avulsions, channel evolution and floodplain sedimentation rates of the anastomosing upper Columbia River, British Columbia, Canada. *Sedimentology,* 49, 1049-1071, doi:10.1046/j.1365-3091.2002.00489.x.

Mendoza, A., J. D. Abad, C. E. Frias, C. Ortals, J. Paredes, H. Montoro, J. Vizcarra, C. Simon, and G. Soto-Cortes, 2016: Planform dynamics of the Iquitos anabranching structure in the Peruvian Upper Amazon River. *Earth Surface Processes and Landforms,* 41, 961-970, doi:10.1002/esp.3911.

Meyer-Peter, E., and R. Müller, 1948: Formulas for bed-load transport. *Proceedings of the 2nd Congress IAHR,* Stockholm, Sweden, 39-64.

Middelkoop, H., and N. E. M. Asselman, 1998: Spatial variability of floodplain sedimentation at the event scale in the Rhine-Meuse delta, the Netherlands. *Earth Surface Processes and Landforms*, 23, 561-573, doi:10.1002/(Sici)1096-9837(199806)23:6<561::Aid-Esp870>3.3.Co;2-X.

Middelkoop, H., and M. Van der Perk, 1998: Modelling spatial patterns of overbank sedimentation on embanked floodplains. *Geografiska Annaler: Series A, Physical Geography,* 80, 95-109, doi:10.1111/j.0435-3676.1998.00029.x.

Miori, S., R. Repetto, and M. Tubino, 2006: A one-dimensional model of bifurcations in gravel bed channels with erodible banks. *Water Resources Research,* 42, doi:10.1029/2006wr004863.

Mosselman, E., 2001: Morphological development of side channels. Technical Report, WL | Delft Hydraulics.

Mosselman, E., 2017: Theoretical bifurcation stability for rivers with adjusting widths. *RCEM 2017 - Back to Italy,* Trento-Padova, Italy, S. Lanzoni, M. Redolfi, and G. Zolezzi, Eds., 227.

Mosselman, E., M. Huisink, E. Koomen, and A. C. Seymonsbergen, 1995: Morphological changes in a large braided sand-bed river. *River Geomorphology*, E. J. Hickin, Ed., Wiley, 235-247.

Mosselman, E., B. Jagers, F. Suryadi, and S. Van Schijndel, 2004: Optimalisatie inlaat nevengeulen. Technical Report, WL Delft hydraulics.

Nabet, F., 2014: Etude du réajustement du lit actif en Loire moyenne, bilan géomorphologique et diagnostic du fonctionnement des chenaux secondaires en vue d'une gestion raisonnée. PhD Thesis, Geography, Université Panthéon-Sorbonne - Paris I.

Nesshöver, C., T. Assmuth, K. N. Irvine, G. M. Rusch, K. A. Waylen, B. Delbaere, D. Haase, L. Jones-Walters, H. Keune, E. Kovacs, K. Krauze, M. Külvik, F. Rey, J. Van Dijk, O. I. Vistad, M. E. Wilkinson, and H. Wittmer, 2017: The science, policy and practice of nature-based solutions: An interdisciplinary perspective. *Science of The Total Environment,* 579, 1215-1227, doi:10.1016/j.scitotenv.2016.11.106.

Nienhuis, P. H., A. D. Buijse, R. S. E. W. Leuven, A. J. M. Smits, R. J. W. De Nooij, and E. M. Samborska, 2002: Ecological rehabilitation of the lowland basin of the river Rhine (NW Europe). *Hydrobiologia,* 478, 53-72, doi:10.1023/A:1021070428566.

Nittrouer, J. A., M. A. Allison, and R. Campanella, 2008: Bedform transport rates for the lowermost Mississippi River. *Journal of Geophysical Research: Earth Surface,* 113, doi:10.1029/2007JF000795.

Nuzzo, R., 2014: Scientific method: statistical errors. *Nature,* 506, 150-152, doi:10.1038/506150a.

Odgaard, A. J., and Y. Wang, 1991: Sediment Management with Submerged Vanes. I: Theory. *Journal of Hydraulic Engineering,* 117, 267-267, doi:10.1061/(asce)0733-9429(1991)117:3(267).

Olivier, J. M., M. J. Dole-Olivier, C. Amoros, G. Carrel, F. Malard, N. Lamouroux, and J. P. Bravard, 2009: The Rhone River Basin. *Rivers of Europe, K. Tockner, U. Uehlinger, and C. T. Robinson, Eds., Academic Press,* 247-295.

Ottevanger, W., 2013: Modelling and parameterizing the hydro- and morphodynamics of curved open channels. PhD thesis, Delft University of Technology.

Paola, C., 2001: Modelling stream braiding over a range of scales. *Gravel-bed Rivers V, M. P. Mosley, Ed., New Zealand Hydrological Society,* 11-46.

Parker, G., 2004: 1D sediment transport morphodynamics with applications to rivers and turbidity currents. E-book, http://hydrolab.illinois.edu/people/parkerg/morphodynamics_e-book.htm.

Parker, G., and E. D. Andrews, 1985: Sorting of Bed Load Sediment by Flow in Meander Bends. *Water Resources Research,* 21, 1361-1373, doi:10.1029/WR021i009p01361.

Piégay, H., G. Bornette, and P. Grante, 2002: Assesment of silting-up dynamics of eleven cut-off channel plugs on a free meandering river (Ain River, France). *Applied geomorphology: theory and practice,* R. J. Allison, Ed., John Wiley & Sons, 227-247.

Raymond, C. M., N. Frantzeskaki, N. Kabisch, P. Berry, M. Breil, M. R. Nita, D. Geneletti, and C. Calfapietra, 2017: A framework for assessing and implementing the co-benefits of nature-based solutions in urban areas. *Environmental Science & Policy,* 77, 15-24, doi:10.1016/j.envsci.2017.07.008.

Riad, K., 1961: Analytical and experimental study of bed load distribution at alluvial diversions. PhD Thesis, Delft University of Technology.

Ribberink, J. S., 1987: Mathematical modelling of one-dimensional morphological changes in rivers with non-uniform sediment. PhD Thesis, Delft University of Technology.

Riquier, J., H. Piégay, and M. S. Michalková, 2015: Hydromorphological conditions in eighteen restored floodplain channels of a large river: linking patterns to processes. *Freshwater Biology,* 60, 1085-1103, doi:10.1111/fwb.12411.

Riquier, J., H. Piégay, N. Lamouroux, and L. Vaudor, 2017: Are restored side channels sustainable aquatic habitat features? Predicting the potential persistence of side channels as aquatic habitats based on their fine sedimentation dynamics. *Geomorphology,* 295, 507-528, doi:10.1016/j.geomorph.2017.08.001.

Rodrigues, S., J. G. Bréhéret, J. J. Macaire, F. Moatar, D. Nistoran, and P. Jugé, 2006: Flow and sediment dynamics in the vegetated secondary channels of an anabranching river: The Loire River (France). *Sedimentary Geology,* 186, 89-109, doi:10.1016/j.sedgeo.2005.11.011.

Rollet, A. J., 2007: Étude et gestion de la dynamique sédimentaire d'un tronçon fluvial à l'aval d'un barrage : le cas de la basse vallée de l'Ain. PhD Thesis, L'Université Jean Moulin Lyon 3.

Schielen, R. M. J., and A. Blom, 2018: A reduced complexity model of a gravel-sand river bifurcation: Equilibrium states and their stability. *Advances in Water Resources,* 121, 9-21, doi:10.1016/j.advwatres.2018.07.010.

Schiemer, F., C. Baumgartner, and K. Tockner, 1999: Restoration of floodplain rivers: The 'Danube restoration project'. *Regulated Rivers: Research & Management,* 15, 231-244, doi:10.1002/(sici)1099-1646(199901/06)15:1/3<231::aid-rrr548>3.0.co;2-5.

Schuurman, F., W. A. Marra, and M. G. Kleinhans, 2013: Physics-based modeling of large braided sand-bed rivers: Bar pattern formation, dynamics, and sensitivity. *Journal of Geophysical Research-Earth Surface,* 118, 2509-2527, doi:Doi 10.1002/2013jf002896.

Sieben, J., 2009: Sediment management in the Dutch Rhine branches. *International Journal of River Basin Management,* 17, 43-53, doi:10.1080/15715124.2009.9635369.

Simon, A., and A. J. C. Collison, 2002: Quantifying the mechanical and hydrologic effects of riparian vegetation on streambank stability. *Earth Surface Processes and Landforms,* 27, 527-546, doi:10.1002/esp.325.

Simons, J. H. E. J., C. Bakker, M. H. I. Schropp, L. H. Jans, F. R. Kok, and R. E. Grift, 2001: Man-made secondary channels along the River Rhine (the Netherlands); results of post-project monitoring. *Regulated Rivers-Research & Management,* 17, 473-491, doi:DOI 10.1002/rrr.661.abs.

Singer, M. B., and T. Dunne, 2004: Modeling decadal bed material sediment flux based on stochastic hydrology. *Water Resources Research,* 40, doi:10.1029/2003WR002723.

Slingerland, R., and N. D. Smith, 1998: Necessary conditions for a meandering-river avulsion. *Geology,* 26, 435-438, doi:10.1130/0091-7613(1998)026<0435:Ncfamr>2.3.Co;2.

Slingerland, R., and N. D. Smith, 2004: River avulsions and their deposits. *Annual Review of Earth and Planetary Sciences,* 32, 257-285, doi:10.1146/annurev.earth.32.101802.120201.

Sloff, C. J., M. Bernabè, and T. Baur, 2003: On the stability of the Pannerdensche Kop river bifurcation. *IAHR Symposium River, Coastal and Estuarine Morphodynamics,* Madrid, Spain, A. Sánchez-Arcilla, and A. Bateman, Eds., 1001-1011.

Sloff, C. J., H. R. A. Jagers, Y. Kitamura, and P. Kitamura, 2001: 2D morphodynamic modelling with graded sediment. *2nd IAHR Symposium of River, Coastal and Estuarine Morphodynamics*, Obihiro, Japan, S. Ikeda, Ed., 535-544.

Sloff, K., and E. Mosselman, 2012: Bifurcation modelling in a meandering gravel-sand bed river. *Earth Surface Processes and Landforms*, 37, 1556-1566, doi:10.1002/esp.3305.

Sorber, A. M., 1997: Oeversedimentatie tijdens de hoogwaters van 1993/1994 en 1995. Technical Report RIZA rapport 97.015, Rijkswaterstaat.

Stecca, G., A. Siviglia, and A. Blom, 2014: Mathematical analysis of the Saint-Venant-Hirano model for mixed-sediment morphodynamics. *Water Resources Research,* 50, doi:10.1002/2014WR015251.

Struiksma, N., and A. Crosato, 1989: Analysis of a 2-D bed topography model for rivers. *River meandering,* S. Ikeda, and G. Parker, Eds., American Geophysical Union, 153-180.

Struiksma, N., K. W. Olesen, C. Flokstra, and H. J. De Vriend, 1985: Bed deformation in curved alluvial channels. *Journal of Hydraulic Research,* 23, 57-79, doi:10.1080/00221688509499377.

Sukhodolov, A., W. S. J. Uijttewaal, and C. Engelhardt, 2002: On the correspondence between morphological and hydrodynamical patterns of groyne fields. *Earth Surface Processes and Landforms,* 27, 289-305, doi:10.1002/esp.319.

Talmon, A. M., N. Struiksma, and M. C. L. M. Van Mierlo, 1995: Laboratory measurements of the direction of sediment transport on transverse alluvial-bed slopes. *Journal of Hydraulic Research,* 33, 495-517, doi:10.1080/00221689509498657.

Ten Brinke, W. B. M., 1997: De bodemsamenstelling van Waal en Ijssel in de jaren 1966, 1976, 1984 en 1995. Technical Report RIZA rapport 97.009, Rijkswaterstaat.

Ten Brinke, W. B. M., F. H. Schulze, and P. Van der Veer, 2004: Sand exchange between groyne-field beaches and the navigation channel of the Dutch Rhine: the impact of navigation versus river flow. *River Research and Applications,* 20, 899-928, doi:10.1002/rra.809.

Ten Brinke, W. B. M., M. M. Schoor, A. M. Sorber, and H. J. A. Berendsen, 1998: Overbank sand deposition in relation to transport volumes during large-magnitude floods in the Dutch sand-bed Rhine river system. *Earth Surface Processes and Landforms,* 23, 809-824, doi:10.1002/(sici)1096-9837(199809)23:9<809::aid-esp890>3.0.co;2-1.

Thomas, R. E., D. R. Parsons, S. D. Sandbach, G. M. Keevil, W. A. Marra, R. J. Hardy, J. L. Best, S. N. Lane, and J. A. Ross, 2011: An experimental study of discharge partitioning and flow structure at symmetrical bifurcations. *Earth Surface Processes and Landforms,* 36, 2069-2082, doi:10.1002/esp.2231.

Tockner, K., F. Schiemer, and J. V. Ward, 1998: Conservation by restoration: The management concept for a river-floodplain system on the Danube River in Austria. *Aquatic Conservation-Marine and Freshwater Ecosystems,* 8, 71-86, doi:10.1002/(SICI)1099-0755(199801/02)8:1<71::AID-AQC265>3.0.CO;2-D.

Toonen, W. H. J., M. G. Kleinhans, and K. M. Cohen, 2012: Sedimentary architecture of abandoned channel fills. *Earth Surface Processes and Landforms,* 37, 459-472, doi:10.1002/esp.3189.

Van den Berg, J. H., 1995: Prediction of alluvial channel pattern of perennial rivers. *Geomorphology,* 12, 259-279, doi:10.1016/0169-555x(95)00014-v.

Van Denderen, R. P., R. M. J. Schielen, and S. J. M. H. Hulscher: Numerical modelling of morphodynamic changes in side channel systems.

Van Denderen, R. P., R. M. J. Schielen, A. Blom, S. J. M. H. Hulscher, and M. G. Kleinhans, 2018: Morphodynamic assessment of side channel systems using a simple one-dimensional bifurcation model and a comparison with aerial images. *Earth Surface Processes and Landforms,* 43, 1169-1182, doi:10.1002/esp.4267.

Van Denderen, R. P., R. M. J. Schielen, S. G. Westerhof, S. Quartel, and S. J. M. H. Hulscher, 2018b: Replication dataset: Explaining artificial side channel dynamics using data analysis and model calculations. 4TU.Centre for Research Data, doi:10.4121/uuid:2704f813-d23b-43b5-b837-fdb02ceef261.

Van Denderen, R. P., R. M. J. Schielen, S. G. Westerhof, S. Quartel, and S. J. M. H. Hulscher, 2019: Explaining artificial side channel dynamics using data analysis and model calculations. *Geomorphology,* 327, 93-110, doi:10.1016/j.geomorph.2018.10.016.

Van der Mark, C. F., and E. Mosselman, 2013: Effects of helical flow in one-dimensional modelling of sediment distribution at river bifurcations. *Earth Surface Processes and Landforms,* 38, 502-511, doi:10.1002/esp.3335.

Van Dijk, W. M., R. Teske, W. I. van de Lageweg, and M. G. Kleinhans, 2013: Effects of vegetation distribution on experimental river channel dynamics. *Water Resources Research,* 49, 7558-7574, doi:10.1002/2013wr013574.

Van Dijk, W. M., F. Schuurman, W. I. van de Lageweg, and M. G. Kleinhans, 2014: Bifurcation instability and chute cutoff development in meandering gravel-bed rivers. *Geomorphology,* 213, 277-291, doi:10.1016/j.geomorph.2014.01.018.

Van Dyke, C., 2016: Nature's complex flume - Using a diagnostic state-and-transition framework to understand post-restoration channel adjustment of the Clark Fork River, Montana. *Geomorphology,* 254, 1-15, doi:10.1016/j.geomorph.2015.11.007.

Van Oorschot, M., M. Kleinhans, G. Geerling, and H. Middelkoop, 2016: Distinct patterns of interaction between vegetation and morphodynamics. *Earth Surface Processes and Landforms,* 41, 791-808, doi:10.1002/esp.3864.

Van Rijn, L. C., 1984a: Sediment transport, Part I: Bed load transport. *Journal of Hydraulic Engineering,* 110, 1431-1456, doi:10.1061/(asce)0733-9429(1984)110:10(1431).

Van Rijn, L. C., 1984b: Sediment transport, Part II: Suspended load transport. *Journal of Hydraulic Engineering,* 110, 1613-1641, doi:10.1061/(ASCE)0733-9429(1984)110:11(1613).

Van Rijn, L. C., 1984c: Sediment transport, Part III: Bed forms and alluvial roughness. *Journal of Hydraulic Engineering,* 110, 1733-1754, doi:10.1061/(ASCE)0733-9429(1984)110:12(1733).

Van Rijn, L. C., 1993: *Principles of sediment transport in rivers, estuaries and coastal seas*. Aqua publications Amsterdam.

Van Stokkom, H. T. C., A. J. M. Smits, and R. E. S. W. Leuven, 2005: Flood defense in the Netherlands. *Water International*, 30, 76-87, doi:10.1080/02508060508691839.

Wang, Z. B., R. J. Fokkink, M. De Vries, and A. Langerak, 1995: Stability of river bifurcations in 1D morphodynamic models. *Journal of Hydraulic Research,* 33, 739-750, doi:10.1080/00221689509498549.

Warmink, J. J., M. W. Straatsma, F. Huthoff, M. J. Booij, and S. J. M. H. Hulscher, 2013: Uncertainty of design water levels due to combined bed form and vegetation roughness in the Dutch River Waal. *Journal of Flood Risk Management,* 6, 302-318, doi:10.1111/jfr3.12014.

Wright, S., and G. Parker, 2004: Flow resistance and suspended load in sand-bed rivers: Simplified stratification model. *Journal of Hydraulic Engineering,* 130, 163-170, doi:10.1061/(ASCE)0733-9429(2004)130:8(796).

Yossef, M. F. M., 2005: Morphodynamics of rivers with groynes. PhD thesis, Delft University of Technology.

Yossef, M. F. M., H. R. A. Jagers, S. Van Vuren, and A. Sieben, Year: Innovative techniques in modelling large-scale river morphology. *Riverflow 2008, Proceedings of the International Conference on Fluvial Hydraulics,* Çesme, Izmir, Turkey, 1065-1074.

Zinger, J. A., 2016: From meander bend to oxbow lake: morphodynamics and sedimentology of chute cutoffs, University of Illinois.

Zinger, J. A., B. L. Rhoads, and J. L. Best, 2011: Extreme sediment pulses generated by bend cutoffs along a large meandering river. *Nature Geoscience,* 4, 675-678, doi:Doi 10.1038/Ngeo1260.

Zinger, J. A., B. L. Rhoads, J. L. Best, and K. K. Johnson, 2013: Flow structure and channel morphodynamics of meander bend chute cutoffs: A case study of the Wabash River, USA. *Journal of Geophysical Research-Earth Surface,* 118, 2468-2487, doi:10.1002/jgrf.20155.

About the author

Pepijn van Denderen was born on the 7th of February in 1991 in Heemstede, the Netherlands. After graduating from the Kennemer Lyceum in Overveen in 2009, he started the bachelor of Civil Engineering at Delft University of Technology. In 2012, Pepijn started the master Civil Engineering with the Hydraulic Engineering track in Delft. During his internship at Deltares, he studied the effect of the calibration method for a hydrodynamic river model on the water level during extreme discharge conditions. His graduation project focused on measured and computed bed level changes in the river Waal during floods. Pepijn received his MSc degree in 2014. After his graduation, Pepijn moved to Enschede to start his PhD at the Water Engineering and Management department of the University of Twente.

List of publications

PEER-REVIEWED JOURNAL PAPERS

Van Denderen, R. P., R. M. J. Schielen, A. Blom, S. J. M. H. Hulscher, and M. G. Kleinhans, 2018: Morphodynamic assessment of side channel systems using a simple one-dimensional bifurcation model and a comparison with aerial images. *Earth Surface Processes and Landforms*, 43, 1169-1182, doi:10.1002/esp.4267.

Van Denderen, R. P., R. M. J. Schielen, S. G. Westerhof, S. Quartel, and S. J. M. H. Hulscher, 2019: Explaining artificial side channel dynamics using data analysis and model calculations. *Geomorphology*, 327, 93-110, doi:10.1016/j.geomorph.2018.10.016.

Van Denderen, R. P., R. M. J. Schielen, and S. J. M. H. Hulscher, subm.: Numerical modelling of morphodynamic changes in side channel systems.

Van Denderen, R. P., R. M. J. Schielen, M. W. Straatsma, M. G. Kleinhans and S. J. M. H. Hulscher, subm.: A characterization of side channel development.

CONFERENCE PAPERS AND ABSTRACTS

Van Denderen, R. P., R. M. J. Schielen, and S. J. M. H. Hulscher, 2015: Observed evolution of side channels. 73-76. *Abstract from NCR-Days 2015*, Nijmegen, Netherlands.

Van Denderen, R. P., R. M. J. Schielen, A. Blom, M. G. Kleinhans, and S. J. M. H. Hulscher, 2016: Characteristics of side channels in the River Ain, France. In G. Constantinescu, M. García, & D. Hanes (Eds.), *Proceedings of the international conference on fluvial hydraulics (River Flow 2016)*, St. Louis, USA, 220-228.

Van Denderen, R. P., R. M. J. Schielen, and S. J. M. H. Hulscher, 2017: Sediment sorting at a side channel system. In A. J. F. Hoitink et al. (Eds.), *Abstract from NCR days 2017*, Wageningen, Netherlands.

Van Denderen, R. P., R. M. J. Schielen, and S. J. M. H. Hulscher, 2017: Mechanisms for sediment fining in a side channel system. In S. Lanzoni, M. Redolfi, & G. Zolezzi (Eds.), *RCEM2017 - Back to Italy*, Trento-Padova, Italy, 252.

Cortes Arevalo, V. J., Sools, A. M., Verbrugge, L. N. H., Brugnach, M. F., **Van Denderen, R. P.**, Candel, J. H. J., Van Gemert-Pijnen, J. E. W. C. & Hulscher, S. J. M. H., 2018: Usefulness of storylines to increase the accessibility and transparency of RiverCare knowledge. In Y. Huismans, K. D. Berends, I. Niesten, E. Mosselman (Eds.), *NCR Days 2018*, Delft, Netherlands, 64-65

Van Denderen, R. P., Hulscher, S. J. M. H., & Schielen, R. M. J., 2018: A simple estimation of side channel development. In A. Armanini, & E. Nucci (Eds.), *New Challenges in Hydraulic Research and Engineering: Proceedings of the 5th IAHR Europe Congress*, Trento, Italy, 471-472. doi:10.3850/978-981-11-2731-1_106-cd.

Van Denderen, R. P., R. M. J. Schielen, and S. J. M. H. Hulscher, 2019: Measuring and modeling the development of side channels. In E. Stouthamer et al. (Eds.), *Land of Rivers: NCR Days 2019 Proceedings*, Utrecht, The Netherlands, 44-45.

OTHERS

Van Denderen, R. P., Schielen, R. M. J., & Hulscher, S. J. M. H., 2016: B1: On the dynamics of side channels as restoration measure: linking theory and practice. In S. J. M. H. Hulscher, R. M. J. Schielen & D. C. M. Augustijn (Eds.) *RiverCare Knowledge Dissemination Days* October 31 - November 2016, Rijkswaterstaat, Utrecht, The Netherlands.

Van Denderen, R. P., Morphodynamic modelling of side channel development. *J.M. Burgers Symposium 2018*, Lunteren, Netherlands.

Van Denderen, R. P., Cortes Arevalo, V. J., Verbrugge, L. & Schielen, R. M. J., 2018: How do side channels develop? *RiverCare knowledge base*: https://kbase.ncr-web.org/wp-content/storyline-app/index.html?appid=be6408b2aa304dd7948cf087454e6492.

Van Denderen, R. P., R. M. J. Schielen, and S. J. M. H. Hulscher, 2019: Aggrading side channels: The filling in of secondary channels in the river Rhine. *Conceptueel*, 28, 24-27.

Photo: Rijkswaterstaat